Wigner functionals and ghost imaging

by

Akshay Durgapersadh

Submitted in partial fulfilment of the academic requirements of
Master of Science in Physics

UNIVERSITY OF
KWAZULU-NATAL

School of Chemistry and Physics
College of Agriculture, Engineering and Science
University of KwaZulu-Natal
Westville
South Africa

November 2023

Preface

The research discussed in this dissertation was carried out in the College of Agriculture, Engineering, and Science of the University of Kwa-Zulu Natal, Durban, from January 2021 until November 2023 by Akshay Durgapersadh under the supervision of Prof Thomas Konrad and co-supervised by Filippus Stefanus Roux.

As the candidate's supervisor, I, Thomas Konrad, agree to the submission of this dissertation.

Signed:
Date:

As the candidate's co-supervisor, I, Filippus Stefanus Roux, agree to the submission of this dissertation.

Signed:
Date:

I, Akshay Durgapersadh, hereby declare that all the material incorporated in this dissertation are my own original work, except where acknowledgment is made by name or in the form of a reference. The work contained herein has not been submitted in any form for any degree or diploma to any other institution.

Signed:
Date:

DECLARATION 1: PLAGIARISM

I, Akshay Durgapersadh, declare that:

(i) the research reported in this dissertation, except where otherwise indicated or acknowledged, is my original work;

(ii) this dissertation has not been submitted in full or in part for any degree or examination to any other university;

(iii) this dissertation does not contain other persons' data, pictures, graphs or other information, unless specifically acknowledged as being sourced from other persons;

(iv) this dissertation does not contain other persons' writing, unless specifically acknowledged as being sourced from other researchers. Where other written sources have been quoted, then:

  a) their words have been re-written but the general information attributed to them has been referenced;

  b) where their exact words have been used, their writing has been placed inside quotation marks, and referenced;

(v) where I have used material for which publications followed, I have indicated in detail my role in the work;

(vi) this dissertation is primarily a collection of material, prepared by myself, published as journal articles or presented as a poster and oral presentations at conferences. In some cases, additional material has been included;

(vii) this dissertation does not contain text, graphics or tables copied and pasted from the Internet, unless specifically acknowledged, and the source being detailed in the dissertation and in the References sections.

Signed:
Date:

Abstract

This dissertation discusses Wigner functionals and an application, namely ghost imaging. Wigner functionals aim to provide more accurate measurement results due to the inclusion of all the degrees of freedom of light. The main concepts discussed are spontaneous parametric down-conversion (SPDC), the evolution equation for light through the SPDC crystal, the probability distribution for the ghost image, conditional probability distribution, and the point spread function. The ghost imaging calculation is done for the rational thin crystal and extreme thin crystal limits.

It is shown that the probability distribution produced is the same for the rational thin crystal and extreme thin crystal limits, and consequently, the point spread function, and conditional probability distributions are the same.

Acknowledgements

I would like to thank my supervisor, Prof Thomas Konrad, for many meetings, discussions, and revisions for my masters dissertation. I was able to see the formalism in a different perspective due to our discussions.
A special thanks goes to my co-supervisor, Filippus Stefanus Roux, who has helped me with countless meetings, discussions, and notes. My co-supervisor had worked tirelessly to help me with this dissertation and I greatly appreciate his efforts to provide me with an understanding of such a new formalism.
I would also like to thank Tsepo Sekhoasha for proof reading my thesis.

Contents

List of Figures

Chapter 1

Introduction

For thousands of years, humanity has attempted to capture images, be it in the form of parietal art or photography. Images produced by famous painters such as Pablo Ruiz Picasso, Leonardo Da Vinci, or Vincent Van Gogh, to name a few, are valued immensely for various reasons e.g. the abstract meaning or detailed accuracy. Recent technological advances allow for high-resolution images to be captured within split seconds. Such a convenience enables anyone with a smartphone to capture memories that could last a lifetime.

The science behind using quantum optics to produce an image via a process called ghost imaging is written in terms of Wigner functionals. The modeling of ghost imaging with Wigner functionals has not been done before.

Quantum optics deals with the quanta of light called photons and how it interacts with atoms and molecules, entanglement can be generated as a result. It describes many interesting phenomena, such as teleportation, black-body radiation, ghost imaging, quantum communication, quantum cryptography, and metrology [4, 2]. There are quantum optical effects that give rise to macroscopic phenomena.

Entanglement is a phenomenon arising due to specifically preparing particles. The preparation requires the impossibility of describing the particles independently, irrespective of the distances between them, i.e. the state describing the quantum system must not be factorizable. Entanglement can be generated in quantum optics by spontaneous parametric down-conversion (SPDC) and can be ingrained in various degrees of freedom, such as frequency, spatial, spin, polarization, and particle number. Entanglement is an interesting yet counter-intuitive phenomenon with various applications in

physics, such as cryptography, quantum computing, and statistical physics, to name a few.

In recent years, a Wigner functional formalism of quantum optics has been invented [15, 18, 17, 19] which includes all the degrees of freedom of light and results from the introduction of a complete and orthogonal basis, for comprising all degrees of freedom of light, i.e. its spatiotemporal, polarization, and the photon number degree of freedom [15]. The quadrature basis is used for such a purpose, and consists of eigenstates of the momentum dependent, or fixed-momentum, quadrature operator [15].

Incorporating all the degrees of freedom allows for more accurate measurements over conventional methods [15]. It is possible to produce entanglement in all degrees of freedom. However, how one proceeds to harvest the entanglement is out of the scope of this project. Wigner functionals allow quantum optics to be rewritten on functional phase space rather than using the operator and state vector approach. The normalization factors in the state vector approach for particular states with more than one photon has been shown not to work very well, as it is not possible to normalize [15].

The Wigner functional formalism will be introduced and applied to ghost imaging to calculate the conditional probability distribution for detection of image photons and the resolution of ghost imaging. The modeling of ghost imaging with Wigner functionals has not been done previously and is thus unique to this project. Ghost imaging is based on generating entangled photons by means of SPDC. The signal beam is then sent to the object, and the idler beam is sent to the CCD (charge-coupled device) array or scanning detector. A picture should then be produced by the idler beam even though it has not interacted with the object. However, the transverse momentum degree of freedom is used when modeling the ghost image. One of the advantages of ghost imaging is the possibility to interact with the object with photons in the infrared spectrum, but detect their entangled partners in the visible spectrum where the detection efficiency is higher than in the infrared spectrum. Basically, this amounts to a change of frequency between optical object and image. Another advantage is that the ghost image is transferred without physical carrier between the object and image, this is of use if the light cannot directly be sent from the object to the image.

The structure of this dissertation is as follows. The main goal is to introduce the formalism of Wigner functionals and describe its application to ghost imaging. One of the basic ingredients of ghost imaging is a pair of entangled photons, which can be obtained from spontaneous parametric

down-conversion (SPDC). Chapter 2 describes SPDC in nonlinear crystals and derives the nonlinear Helmholtz equation, which governs the propagation of light in the nonlinear medium. Chapter 2 provides the infinitesimal propagation operator for the state of light in the nonlinear medium.
Chapter 3 introduces Wigner functionals and shows how to calculate Wigner functionals of operators, and products of operators. Moreover, it is shown how to calculate probabilities, such as the detection probability.
Chapter 4 discusses Wigner functionals in SPDC, and an equation is derived for Wigner functionals that describes the evolution of light propagating through a nonlinear crystal. The derivation is not original but follows the literature [15, 18, 17, 19] and privately communicated notes by my co-supervisor, FS Roux.
The concepts from chapter 4 are then used in chapter 5 to calculate the ghost image of an aperture in the near field.

Chapter 2

Spontaneous parametric down-conversion

Spontaneous parametric down-conversion (SPDC) has various uses such as for the generation of entangled photons, and the preparation of squeezed states. It is also employed in quantum cryptography, quantum simulation, quantum metrology, etc [2]. SPDC involves a pump beam incident on a nonlinear crystal, typically the beta barium borate crystal [23], and is usually assumed to be paraxial, i.e. it propagates with small divergence along a particular direction. The incident pump beam then produce down-converted photon pairs. Due to energy conservation, the sum of the frequency of the down-converted photons must equal to the frequency of the pump photon. A similar rule holds for the momentum phase matching condition, whereby the sum of the wave vectors for the down-converted photons must equal to the wave vector of the pump photon.

There are two types of SPDC, namely type I and type II. An illustration of the down-conversion process is shown in figure 2.1. A pump beam of angular frequency ω_p, and wave vector $\tilde{\mathbf{k}}_p$, is incident on a nonlinear crystal and produces a signal and idler beam with angular frequency ω_s, and ω_i respectively. The three-dimensional wave vectors for the signal and idler beams are $\tilde{\mathbf{k}}_s$, and $\tilde{\mathbf{k}}_i$, respectively. The angular frequencies and transverse wave vectors abides by the phase matching conditions and is explained in greater detail in the sections below. The underlying reason why SPDC occurs is due to the second order polarization term. The response of a dielectric medium to the incident light beam is to form electric dipoles with a certain density. The polarization, or electric dipole density, of the medium can be

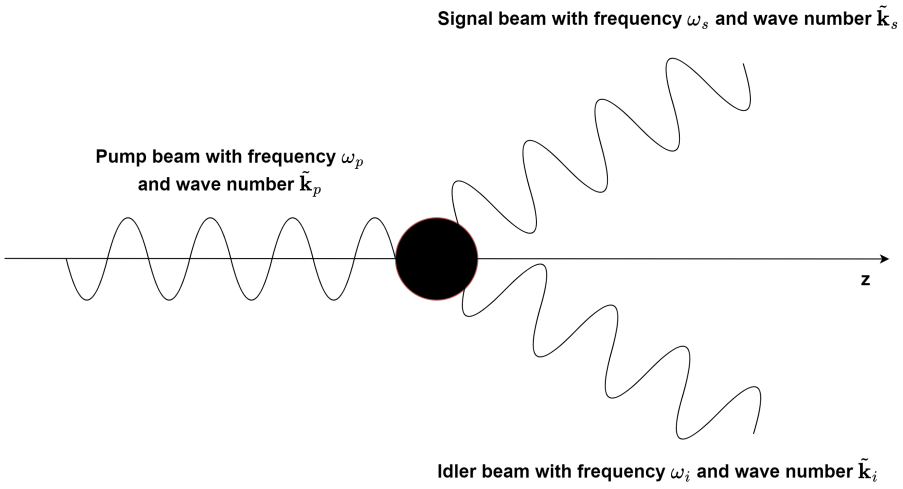

Figure 2.1: *An illustration of SPDC which shows the pump beam producing the signal and idler beams with time propagating in the z direction. The interaction between the crystal and pump beam is shown as a dot in the center of the diagram.*

expressed as a power series of the electric field [1]

$$P_i(E_a) = \epsilon_0 \chi^{(1)}_{ib} E_b + \epsilon_0 \chi^{(2)}_{ibc} E_b E_c + \epsilon_0 \chi^{(3)}_{ibcd} E_b E_c E_d + ..., \tag{2.1}$$

where the coefficient χ^n of the expansion above is called the n-th order electric susceptibility, and ϵ_0 is the permittivity of free space. Here tensor notation is used, and the summation is over repeated indices. The assumption is $\chi^{(1)}_{ab} = \chi^{(1)}\delta_{ab}$ is made, where δ_{ab} is the Kronecker delta. Note that $\chi^{(1)}$ is the first order electric susceptibility, and is a constant. The polarization function simplifies to

$$P_i(E_a) = \epsilon_0 \chi^{(1)} E_i + \epsilon_0 \chi^{(2)}_{ibc} E_b E_c + \epsilon_0 \chi^{(3)}_{ibcd} E_b E_c E_d + ..., \tag{2.2}$$

and the displacement field can be written as

$$D_i = \epsilon_0 \left(1 + \chi^{(1)}\right) E_i + \epsilon_0 \chi^{(2)}_{ibc} E_b E_c + \epsilon_0 \chi^{(3)}_{ibcd} E_b E_c E_d + ..., \tag{2.3}$$

where tensor notation has been assumed on b, c and d. The expression $\epsilon_0 \left(1 + \chi^{(1)}\right)$ is a constant. Equation (2.2) can be converted to vector form

by considering all the components of the polarization

$$\mathbf{P} = \epsilon_0 \chi^{(1)} \mathbf{E} + \epsilon_0 \boldsymbol{\chi}^{(2)} : \mathbf{E}^2 + \epsilon_0 \boldsymbol{\chi}^{(3)} \vdots \mathbf{E}^3 + ..., \tag{2.4}$$

where $\boldsymbol{\chi}^{(k)}$ is a rank $k+1$ tensor which is contracted with k dot products with the electric field vector, these dot products are depicted by the vertical dots between the electric field and the nonlinear susceptibility tensor. For SPDC, only the first and second order polarization terms will be considered. The polarization for SPDC reduces to

$$\mathbf{P} = \epsilon_0 \chi^{(1)} \mathbf{E} + \epsilon_0 \mathbf{E} \cdot \boldsymbol{\chi}^{(2)} \cdot \mathbf{E}. \tag{2.5}$$

Eq. (2.5) is combined with $\mathbf{D} = \epsilon_0 \mathbf{E} + \mathbf{P}$ to give

$$\mathbf{D} = \epsilon \mathbf{E} + \epsilon_0 \mathbf{E} \cdot \boldsymbol{\chi}^{(2)} \cdot \mathbf{E}, \tag{2.6}$$

where $\epsilon = \epsilon_0 \left(1 + \chi^{(1)}\right)$. SPDC requires a nonlinear anisotropic crystal which possesses birefringence. Anisotropy is defined as having physical properties which depend on the incident angle of the pump beam, and birefringence is the property of a crystal to have two refractive indices, i.e. double refraction [6].

2.1 Type I SPDC

Only two types of SPDC will be mentioned, namely, type I and type II. In type I SPDC, the signal and idler beams have an identical polarization, whilst the pump beam has an orthogonal polarization to the signal and idler beams [6]. All the possible paths of the signal beams for a fixed frequency form a cone which can be seen in figure 2.2, and applies to the trajectories of the idler beams as well. Each of these cones have a particular frequency, and therefore appear to be a different colour, with the innermost cone having the highest frequency.

2.2 Type II SPDC

In type II SPDC, the signal and idler photons have an orthogonal polarization to each other whilst the pump beam can have any polarization [6]. All the possible trajectories of the signal and idler beams in type II SPDC produces

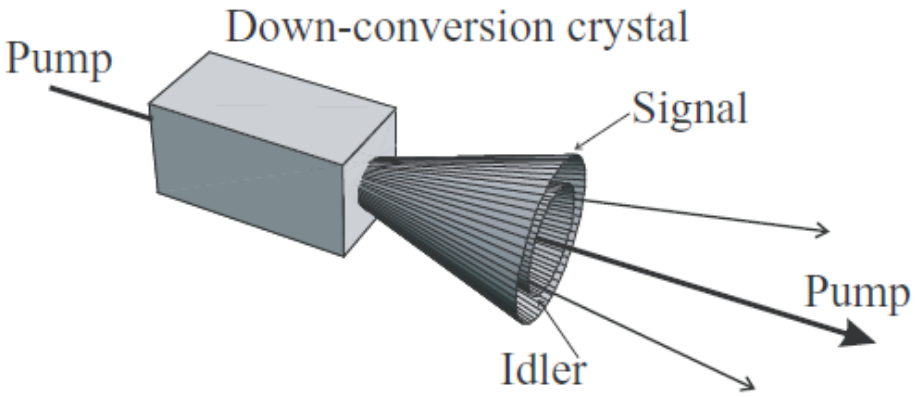

Figure 2.2: *A Diagram showing type I SPDC with the cones representing all the possible trajectories of the signal and idler beams [6].*

two cones that intersects each other which is shown in figure 2.3. Each cone is now characterized by the type of polarization. The intersection of cones can be produced by changing the orientation of the nonlinear crystal [8]. Type II SPDC can be used to entangle photons at the intersection of these cones. Entanglement will then be engrained in the polarization degree of freedom.

2.3 Phase matching conditions

SPDC has to satisfy the conservation of energy and momentum for efficiency. The simultaneous satisfaction of these two conditions are referred to as the phase matching condition [2, 6, 14]. The conservation of energy requires

$$\hbar\omega_p = \hbar\omega_i + \hbar\omega_s, \tag{2.7}$$

where ω_p, ω_i, and ω_s are the angular frequencies of the pump, idler, and signal beams respectively. The following condition holds for the wave numbers, which is called the phase mismatch

$$\Delta k = k_p - k_s - k_i, \tag{2.8}$$

where k_p, k_i, and k_s are the wave numbers of the pump, idler, and signal beams respectively. The pump beam is not efficiently converted into the

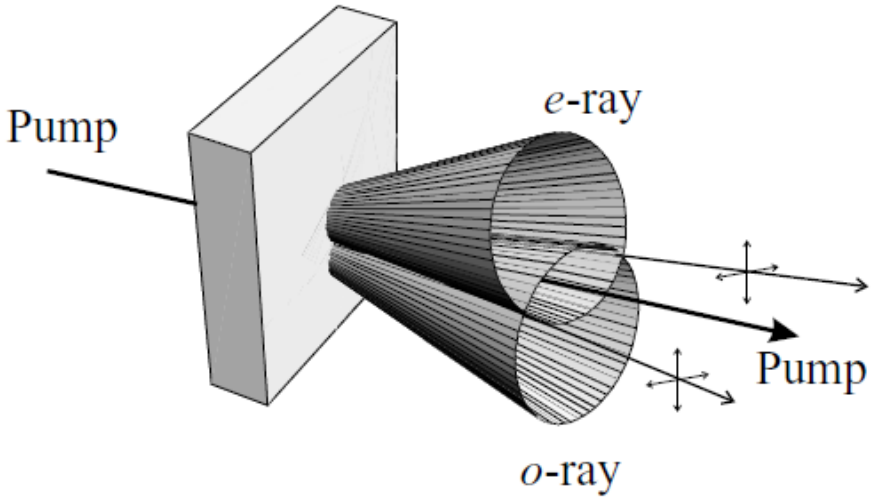

Figure 2.3: *A Diagram showing type II SPDC with the cones representing all the possible trajectories of the signal and idler beams. The diagram also shows the type of polarization of the down-converted beams. These are the extraordinary polarization (e-ray) and ordinary polarization (o-ray) [6].*

down-converted beams. The pump beam has a higher momentum than the sum of the momenta from the signal and idler beams. If $\Delta k = 0$, then it implies that the pump beam is efficiently converted into its down-converted beams [1].

Critical phase matching is considered, and is dependent on the down-conversion angle. The down-conversion angle is the angle between the down-converted beams and the optical axis, which is taken to be the z direction and coincides with the propagation direction of the pump beam.

There are two types of phase mismatch, namely collinear and noncollinear. Collinear phase mismatch is when the pump, signal and idler beams propagate in the same direction, i.e. the down-conversion angle, which is measured between the propagation direction of the down-converted beam and the optical axis, is $0°$. As explained before, these are paraxial beams. Noncollinear phase mismatching means that the pump beam produces signal and idler beams that have a nonzero angle with respect to the optical axis, resulting

in obtaining a phase mismatch which is dependent on the down-conversion angle.

As mentioned before, the phase mismatch is in the z component of the wave vector which arises due to maximal entanglement and includes a small crystal length. As a result, the discussion of the z wave vector component of a beam is of interest. The three-dimensional wave vector, which will be depicted by a tilde[1], is given as

$$\tilde{\mathbf{k}} = k_x\hat{\mathbf{x}} + k_y\hat{\mathbf{y}} + k_z\hat{\mathbf{z}}. \tag{2.9}$$

The wave number is then given by

$$\left|\tilde{\mathbf{k}}\right| = \sqrt{k_x^2 + k_y^2 + k_z^2} = \frac{2\pi}{\lambda} = \frac{\omega}{v}, \tag{2.10}$$

where λ, ω and v are the wavelength, angular frequency and velocity of the light beam respectively. Rearranging the above equation yields

$$k_z(\mathbf{k},\omega) = \sqrt{\frac{\omega^2}{v^2} - |\mathbf{k}|^2}, \tag{2.11}$$

where $\mathbf{k} = k_x\hat{\mathbf{x}} + k_y\hat{\mathbf{y}}$. The term $k_z(\mathbf{k},\omega)$ depends on the transverse wave vector components given by $\mathbf{k}$ and the frequency. It will be shown in the next section that the calculations reduce to a phase mismatch with the z momentum component in the section below, i.e. $\Delta k_z \neq 0$. It arises due to the finite length of the nonlinear medium.

It is beneficial to look at a few quantities such as the angular frequency and the ratio of the crystal length (L) with the Rayleigh range. The ratio is defined as $\mathcal{P}$, which is given in Eq. (2.13), and is required to be very small in order to maximize entanglement [19, 9]. The case where $\mathcal{P} \ll 1$ is called the thin crystal limit and will have two cases, these are the extreme and rational thin crystal limits which are explored in the ghost imaging calculation in chapter 5. The conservation of transverse components of the wave vectors is also desired for better entanglement [9, 24].

The angular frequency is discussed first where type I SPDC and degeneracy[2] are assumed. It is assumed that the wavelength for one of the down-converted beams, say the signal beam, is $\lambda_d = 200 \times 10^{-6}$ m. The wavelength can be used to calculate the angular frequency, which can then be used to in $\mathcal{P}$

[1]The three dimensional wave vector is written with a tilde since it does not appear much throughout this dissertation in comparison to the transverse wave vectors.

[2]Degeneracy is when the down-converted photons have the same frequency.

and is done by using the equation $\omega_d = 2\pi f_d = \frac{2\pi v_d}{\lambda_d} = \frac{2\pi c}{n_0 \lambda_d}$ that produces $\omega_d = 5.7 \times 10^{14}$ Hz, where Sellmeier's equation was used to calculate the refractive index [23]

$$n_0^2 = 1 + \frac{0.90291\lambda^2}{\lambda^2 - 0.003926} + \frac{0.83155\lambda^2}{\lambda^2 - 0.018786} + \frac{0.76536\lambda^2}{\lambda^2 - 60.01}, \tag{2.12}$$

which produces $n_0 = 1.63$. The collinear case is considered here, i.e. $\theta_d \approx 0$. Assuming $w_p = 0.001$ m and $L = 0.001$ m, all of the required variables are obtained in order to calculate $\mathcal{P}$. The order of $\mathcal{P}$ is

$$\begin{aligned} \mathcal{P} &= \frac{L}{2w_p^2 k_z(\omega_d)} \\ &= \frac{Lv_d}{2w_p^2 \omega_d} \\ &= \frac{cL}{2n_0 w_p^2 \omega_d} \\ &\sim 10^{-4}. \end{aligned} \tag{2.13}$$

The above quantity, $\mathcal{P}$, is small and dimensionless, during the calculation of the probability distribution for the rational thin crystal limit in chapter 5, $\mathcal{P}$ will be used as a Taylor expansion parameter.

2.4 The nonlinear Helmholtz equation

The nonlinear Helmholtz equation is calculated here and is based on frequent discussions and notes written by my co-supervisor, FS Roux.
In order to obtain the nonlinear Helmholtz equation, consider the set of Maxwell's equations with no free charges

$$\begin{aligned} \nabla \times \mathbf{E} &= -\frac{\partial \mathbf{B}}{\partial t}, \\ \nabla \times \mathbf{H} &= \frac{\partial \mathbf{D}}{\partial t}, \\ \nabla \cdot \mathbf{D} &= 0, \\ \nabla \cdot \mathbf{B} &= 0, \end{aligned} \tag{2.14}$$

where $\mathbf{E}$ is the electric field vector, $\mathbf{B} = \mu_0 \mathbf{H}$ is the magnetic field, $\mathbf{H}$ is the magnetic field strength, and $\mathbf{D}$ is the displacement field which is given in Eq.

(2.6)

$$\mathbf{D} = \epsilon\mathbf{E} + \epsilon_0\mathbf{E}\cdot\boldsymbol{\chi}^{(2)}\cdot\mathbf{E}. \tag{2.15}$$

Calculation of the second of Maxwell's equations

$$\begin{aligned}\nabla\times\mathbf{H} &= \frac{\partial\mathbf{D}}{\partial t}\\ &= \epsilon\frac{\partial\mathbf{E}}{\partial t} + \epsilon_0\frac{\partial\mathbf{E}}{\partial t}\cdot\boldsymbol{\chi}^{(2)}\cdot\mathbf{E} + \epsilon_0\mathbf{E}\cdot\boldsymbol{\chi}^{(2)}\cdot\frac{\partial\mathbf{E}}{\partial t}\\ &= \epsilon\frac{\partial\mathbf{E}}{\partial t} + 2\epsilon_0\mathbf{E}\cdot\boldsymbol{\chi}^{(2)}\cdot\frac{\partial\mathbf{E}}{\partial t}.\end{aligned} \tag{2.16}$$

Now the third of Maxwell's equations is evaluated to

$$\begin{aligned}&\nabla\cdot\mathbf{D} = 0\\ \implies\ &\epsilon\nabla\cdot\mathbf{E} + \nabla\cdot\left(\epsilon_0\mathbf{E}\cdot\boldsymbol{\chi}^{(2)}\cdot\mathbf{E}\right) = 0.\end{aligned} \tag{2.17}$$

The last term is written in terms of tensor notation. Note that the ith component is given by $\epsilon_0\chi^{(2)}_{ibc}E_bE_c$, which can be seen in Eq. (2.3). Therefore,

$$\begin{aligned}&\epsilon_0\nabla\cdot\left(\mathbf{E}\cdot\boldsymbol{\chi}^{(2)}\cdot\mathbf{E}\right)\\ &= \epsilon_0\begin{pmatrix}\frac{\partial}{\partial x_1} & \frac{\partial}{\partial x_2} & \frac{\partial}{\partial x_3}\end{pmatrix}\begin{pmatrix}\chi^{(2)}_{1bc}E_bE_c\\ \chi^{(2)}_{2bc}E_bE_c\\ \chi^{(2)}_{3bc}E_bE_c\end{pmatrix}\\ &= 2\epsilon_0\left(\chi^{(2)}_{1bc}E_b\frac{\partial E_c}{\partial x_1} + \chi^{(2)}_{2bc}E_b\frac{\partial E_c}{\partial x_2} + \chi^{(2)}_{3bc}E_b\frac{\partial E_c}{\partial x_3}\right)\\ &= 2\epsilon_0\sum_i\chi^{(2)}_{ibc}E_b\frac{\partial E_c}{\partial x_i}\\ &= 2\epsilon_0\chi^{(2)}_{abc}E_b\frac{\partial E_c}{\partial x_a},\end{aligned} \tag{2.18}$$

where i is the summation index, a, b and c are tensor notation indices, and x_i are spatial variables. Therefore Eq. (2.17) becomes

$$\nabla\cdot\mathbf{D} = \epsilon\nabla\cdot\mathbf{E} + 2\epsilon_0\chi^{(2)}_{abc}E_b\frac{\partial E_c}{\partial x_a} = 0. \tag{2.19}$$

2.4.1 Time dependence removal

An expression for the electric field in Eq. (2.19) is now considered. The idea is to remove the time dependence, and thus the electric field written in terms of the inverse Fourier transform of a complex valued field called the phasor field, $\mathbf{E}'$, is considered,

$$\mathbf{E}(\mathbf{x},t) = \frac{1}{2\pi}\int \mathbf{E}'(\mathbf{x},\omega)\exp(i\omega t)\,d\omega. \tag{2.20}$$

The real part of $\mathbf{E}(\mathbf{x},t)$ represents the physical electrical field, and the phasor field, $\mathbf{E}'$, within the definition of $\mathbf{E}(\mathbf{x},t)$ does not depend on time, which is one of the properties of a phasor field. The same operation is performed on the magnetic field

$$\mathbf{H}(\mathbf{x},t) = \frac{1}{2\pi}\int \mathbf{H}'(\mathbf{x},\omega)\exp(i\omega t)\,d\omega. \tag{2.21}$$

The phasor field for the magnetic field is $\mathbf{H}'$. The expressions for the electric and magnetic fields are substituted into the first of Maxwell's equations giving

$$\begin{aligned}
&\nabla\times\mathbf{E} = -\frac{\partial\mathbf{B}}{\partial t} = -\mu_0\frac{\partial\mathbf{H}}{\partial t}\\
\implies &\nabla\times\int \mathbf{E}'(\mathbf{x},\omega)\exp(i\omega t)\,d\omega = -\mu_0\frac{\partial}{\partial t}\int \mathbf{H}'(\mathbf{x},\omega)\exp(i\omega t)\,d\omega\\
\implies &\int \nabla\times\mathbf{E}'(\mathbf{x},\omega)\exp(i\omega t)\,d\omega = -i\mu_0\int \omega\mathbf{H}'(\mathbf{x},\omega)\exp(i\omega t)\,d\omega.
\end{aligned} \tag{2.22}$$

A Fourier transform is performed with respect to time in order to remove the time dependence

$$\begin{aligned}
&\int \nabla\times\mathbf{E}'(\mathbf{x},\omega)\exp(i(\omega-\omega')t)\,d\omega dt\\
&= -i\mu_0\int \omega\mathbf{H}'(\mathbf{x},\omega)\exp(i(\omega-\omega')t)\,d\omega dt.
\end{aligned} \tag{2.23}$$

The integral over angular frequency and time is removed since the integral over time produces a delta function,

$$\int \nabla\times\mathbf{E}'(\mathbf{x},\omega)\delta(\omega-\omega')\,d\omega = -i\mu_0\int \omega\mathbf{H}'(\mathbf{x},\omega)\delta(\omega-\omega')\,d\omega, \tag{2.24}$$

and we are left with

$$\nabla \times \mathbf{E}'(\mathbf{x}, \omega') = -i\mu_0 \omega' \mathbf{H}'(\mathbf{x}, \omega'). \tag{2.25}$$

The electric and magnetic fields are substituted into Eq. (2.16) and a Fourier transform is performed with respect to time

$$\begin{aligned}
&\nabla \times \mathbf{H} = \epsilon \frac{\partial \mathbf{E}}{\partial t} + 2\epsilon_0 \mathbf{E} \cdot \boldsymbol{\chi}^{(2)} \cdot \frac{\partial \mathbf{E}}{\partial t} \\
\implies &\int \nabla \times \mathbf{H}'(\mathbf{x}, \omega) \exp(i\omega t)\, d\omega \\
&= \epsilon \frac{\partial}{\partial t} \int \mathbf{E}'(\mathbf{x}, \omega) \exp(i\omega t)\, d\omega \\
&+ \frac{2\epsilon_0}{2\pi} \int \mathbf{E}'(\mathbf{x}, \omega') \exp(i\omega' t) \cdot \boldsymbol{\chi}^{(2)} \cdot \frac{\partial}{\partial t} \mathbf{E}'(\mathbf{x}, \omega) \exp(i\omega t)\, d\omega' d\omega \\
\implies &\int \nabla \times \mathbf{H}'(\mathbf{x}, \omega) \exp(i\omega t)\, d\omega \\
&= i\epsilon \int \omega \mathbf{E}'(\mathbf{x}, \omega) \exp(i\omega t)\, d\omega \\
&+ \frac{2i\epsilon_0}{2\pi} \int \omega \mathbf{E}'(\mathbf{x}, \tilde{\omega}) \cdot \boldsymbol{\chi}^{(2)} \cdot \mathbf{E}'(\mathbf{x}, \omega) \exp(i\omega t + i\tilde{\omega} t)\, d\tilde{\omega} d\omega.
\end{aligned} \tag{2.26}$$

Performing the Fourier transform with respect to time, we obtain

$$\begin{aligned}
&\nabla \times \mathbf{H}'(\mathbf{x}, \omega') \\
&= i\omega' \epsilon \mathbf{E}'(\mathbf{x}, \omega') \\
&+ \frac{2i\epsilon_0}{(2\pi)^2} \int \omega \mathbf{E}'(\mathbf{x}, \tilde{\omega}) \cdot \boldsymbol{\chi}^{(2)} \cdot \mathbf{E}'(\mathbf{x}, \omega) \exp(it(\omega + \tilde{\omega} - \omega'))\, d\tilde{\omega} d\omega dt.
\end{aligned} \tag{2.27}$$

Focusing on the last term

$$\begin{aligned}
&\frac{2i\epsilon_0}{(2\pi)^2} \int \omega \mathbf{E}'(\mathbf{x}, \tilde{\omega}) \cdot \boldsymbol{\chi}^{(2)} \cdot \mathbf{E}'(\mathbf{x}, \omega) \exp(it(\omega + \tilde{\omega} - \omega'))\, d\tilde{\omega} d\omega dt \\
&= \frac{i\epsilon_0}{\pi} \int \omega \mathbf{E}'(\mathbf{x}, \tilde{\omega}) \cdot \boldsymbol{\chi}^{(2)} \cdot \mathbf{E}'(\mathbf{x}, \omega) \delta(\omega + \tilde{\omega} - \omega')\, d\tilde{\omega} d\omega \\
&= \frac{i\epsilon_0}{\pi} \int \omega \mathbf{E}'(\mathbf{x}, \omega' - \omega) \cdot \boldsymbol{\chi}^{(2)} \cdot \mathbf{E}'(\mathbf{x}, \omega) d\omega.
\end{aligned} \tag{2.28}$$

The result is

$$\begin{aligned}
&\nabla \times \mathbf{H}'(\mathbf{x}, \omega') \\
&= i\omega' \epsilon \mathbf{E}'(\mathbf{x}, \omega') + \frac{i\epsilon_0}{\pi} \int \omega \mathbf{E}'(\mathbf{x}, \omega' - \omega) \cdot \boldsymbol{\chi}^{(2)} \cdot \mathbf{E}'(\mathbf{x}, \omega) d\omega.
\end{aligned} \tag{2.29}$$

Considering $\nabla \cdot \mathbf{D}$ in Eq. (2.19)

$$\begin{aligned} &\epsilon \nabla \cdot \int \mathbf{E}'(\mathbf{x}, \omega) \exp(i\omega t)\, d\omega \\ &+ \frac{\epsilon_0 \chi^{(2)}_{abc}}{\pi} \int E'_b(\mathbf{x}, \tilde{\omega}) \frac{\partial}{\partial x_a} E'_c(\mathbf{x}, \omega) \exp(i\omega t + i\tilde{\omega} t)\, d\tilde{\omega} d\omega = 0. \end{aligned} \tag{2.30}$$

Taking the Fourier transform with respect to time

$$\begin{aligned} &\epsilon \nabla \cdot \mathbf{E}'(\mathbf{x}, \omega') \\ &+ \frac{\epsilon_0 \chi^{(2)}_{abc}}{\pi} \int E'_b(\mathbf{x}, \tilde{\omega}) \frac{\partial}{\partial x_a} E'_c(\mathbf{x}, \omega) \delta(\omega + \tilde{\omega} - \omega')\, d\tilde{\omega} d\omega = 0 \\ \implies \epsilon \nabla \cdot \mathbf{E}'(\mathbf{x}, \omega') &= -\frac{\epsilon_0 \chi^{(2)}_{abc}}{\pi} \int E'_b(\mathbf{x}, \tilde{\omega}) \frac{\partial}{\partial x_a} E'_c(\mathbf{x}, \omega' - \tilde{\omega}) d\tilde{\omega}. \end{aligned} \tag{2.31}$$

And similarly, the following can be shown

$$\nabla \cdot \mathbf{H}' = 0. \tag{2.32}$$

2.4.2 The nonlinear Helmholtz equation

The Maxwell's equations in terms of phasor fields are obtained. The goal is to derive the nonlinear Helmholtz equation with the assistance of the following identity

$$\nabla \times \nabla \times \mathbf{E} = \nabla(\nabla \cdot \mathbf{E}) - \nabla^2 \mathbf{E}. \tag{2.33}$$

The left-hand side of the equation, when substituting Eq. (2.25) along with Eq. (2.29) yields

$$\begin{aligned} &\nabla \times \nabla \times \mathbf{E} = -i\mu_0 \omega' \nabla \times \mathbf{H}'(\mathbf{x}, \omega') \\ &= \mu_0 \omega'^2 \epsilon \mathbf{E}'(\mathbf{x}, \omega') + \frac{\mu_0 \omega' \epsilon_0}{\pi} \int \omega \mathbf{E}'(\mathbf{x}, \omega' - \omega) \cdot \boldsymbol{\chi}^{(2)} \cdot \mathbf{E}'(\mathbf{x}, \omega) d\omega. \end{aligned} \tag{2.34}$$

Using Eq. (2.31), the right-hand side of Eq. (2.36) becomes

$$\begin{aligned} &\nabla(\nabla \cdot \mathbf{E}) - \nabla^2 \mathbf{E} \\ &= -\frac{\epsilon_0 \chi^{(2)}_{abc}}{\epsilon \pi} \nabla \int E'_b(\mathbf{x}, \omega) \frac{\partial}{\partial x_a} E'_c(\mathbf{x}, \omega' - \omega) d\omega - \nabla^2 \mathbf{E}'(\mathbf{x}, \omega'). \end{aligned} \tag{2.35}$$

Putting these terms together, we obtain

$$\begin{aligned} &\nabla \times \nabla \times \mathbf{E} = \nabla(\nabla \cdot \mathbf{E}) - \nabla^2 \mathbf{E} \\ \implies &\mu_0 \omega'^2 \epsilon \mathbf{E}'(\mathbf{x}, \omega') + \frac{\mu_0 \omega' \epsilon_0}{\pi} \int \omega \mathbf{E}'(\mathbf{x}, \omega' - \omega) \cdot \boldsymbol{\chi}^{(2)} \cdot \mathbf{E}'(\mathbf{x}, \omega) d\omega \\ &= -\frac{\epsilon_0 \chi^{(2)}_{abc}}{\epsilon \pi} \nabla \int E'_b(\mathbf{x}, \omega) \frac{\partial}{\partial x_a} E'_c(\mathbf{x}, \omega' - \omega) d\omega - \nabla^2 \mathbf{E}'(\mathbf{x}, \omega'). \end{aligned} \tag{2.36}$$

Rearranging the equation yields the following result by making the substitution $k_0 = \omega' \sqrt{\mu_0 \epsilon_0}$ and $k = \omega' \sqrt{\mu_0 \epsilon}$,

$$\begin{aligned} &\nabla^2 \mathbf{E}'(\mathbf{x}, \omega') + k^2 \mathbf{E}'(\mathbf{x}, \omega') \\ &= -\frac{\epsilon_0 \chi^{(2)}_{abc}}{\epsilon \pi} \nabla \int E'_b(\mathbf{x}, \omega) \frac{\partial}{\partial x_a} E'_c(\mathbf{x}, \omega' - \omega) d\omega \\ &- \frac{k_0^2}{\omega' \pi} \int \omega \mathbf{E}'(\mathbf{x}, \omega' - \omega) \cdot \boldsymbol{\chi}^{(2)} \cdot \mathbf{E}'(\mathbf{x}, \omega) d\omega, \end{aligned} \tag{2.37}$$

which is called the nonlinear Helmholtz equation. The terms on the right-hand side contains the second order electric susceptibility, which means that they are the nonlinear part of the Helmholtz equation.
It is possible to make a paraxial approximation to the nonlinear Helmholtz equation. A phasor of the following form is chosen

$$\begin{aligned} \mathbf{E}'(\mathbf{x}, \omega') &= \tilde{\mathbf{E}}(\mathbf{x}, \omega') \exp(-ikz) \\ &= \tilde{\mathbf{E}}(\mathbf{x}, \omega') \exp\left(-\frac{i\omega' z}{v}\right). \end{aligned} \tag{2.38}$$

According to the paraxial approximation, it is assumed that $\tilde{\mathbf{E}}(\mathbf{x}, \omega')$ varies slowly in the propagation direction, which means that $\frac{\partial \tilde{\mathbf{E}}(\mathbf{x}, \omega')}{\partial z} \gg \frac{\partial^2 \tilde{\mathbf{E}}(\mathbf{x}, \omega')}{\partial z^2}$, it is then possible to neglect the second order derivative. Note that equation (2.38) shows that $\tilde{\mathbf{E}}$ depends on the angular frequency, and so does the phase factor. For a different frequency, a different wave number will be obtained. Substituting Eq. (2.38) into the left-hand side of the Helmholtz equation produces

$$\begin{aligned} &\nabla^2 \mathbf{E}'(\mathbf{x}, \omega') + k^2 \mathbf{E}'(\mathbf{x}, \omega') \\ &= \nabla^2 \left(\tilde{\mathbf{E}}(\mathbf{x}, \omega') \exp(-ikz) \right) + k^2 \tilde{\mathbf{E}}(\mathbf{x}, \omega') \exp(-ikz). \end{aligned} \tag{2.39}$$

Acting with the z derivatives on the left-hand side only, and separating the transversal gradient from the second derivative with respect to the propagation length, z, we define $\tilde{\nabla}^2 = \nabla^2 - \frac{\partial^2}{\partial z^2}$. The expression above becomes

$$\begin{aligned}
&\nabla^2\mathbf{E}'(\mathbf{x},\omega') + k^2\mathbf{E}'(\mathbf{x},\omega') \\
&= \tilde{\nabla}^2\tilde{\mathbf{E}}(\mathbf{x},\omega')\exp(-ikz) + \frac{\partial^2}{\partial z^2}\left(\tilde{\mathbf{E}}(\mathbf{x},\omega')\exp(-ikz)\right) \\
&+ k^2\tilde{\mathbf{E}}(\mathbf{x},\omega')\exp(-ikz) \\
&= \tilde{\nabla}^2\tilde{\mathbf{E}}(\mathbf{x},\omega')\exp(-ikz) + k^2\tilde{\mathbf{E}}(\mathbf{x},\omega')\exp(-ikz) \\
&+ \frac{\partial}{\partial z}\left(\frac{\partial}{\partial z}\tilde{\mathbf{E}}(\mathbf{x},\omega')\exp(-ikz) + \tilde{\mathbf{E}}(\mathbf{x},\omega')\frac{\partial}{\partial z}\exp(-ikz)\right) \\
&= \tilde{\nabla}^2\tilde{\mathbf{E}}(\mathbf{x},\omega')\exp(-ikz) + k^2\tilde{\mathbf{E}}(\mathbf{x},\omega')\exp(-ikz) \\
&+ \frac{\partial^2}{\partial z^2}\tilde{\mathbf{E}}(\mathbf{x},\omega')\exp(-ikz) - ik\frac{\partial}{\partial z}\tilde{\mathbf{E}}(\mathbf{x},\omega')\exp(-ikz) \\
&- ik\frac{\partial}{\partial z}\tilde{\mathbf{E}}(\mathbf{x},\omega')\exp(-ikz) - k^2\tilde{\mathbf{E}}(\mathbf{x},\omega')\exp(-ikz)\,.
\end{aligned} \tag{2.40}$$

According the to paraxial approximation, the second derivative with respect to z can be neglected if the first derivative with respect to z is kept

$$\begin{aligned}
&\nabla^2\mathbf{E}'(\mathbf{x},\omega') + k^2\mathbf{E}'(\mathbf{x},\omega') \\
&= \tilde{\nabla}^2\tilde{\mathbf{E}}(\mathbf{x},\omega')\exp(-ikz) - i2k\frac{\partial}{\partial z}\tilde{\mathbf{E}}(\mathbf{x},\omega')\exp(-ikz)\,.
\end{aligned} \tag{2.41}$$

It is assumed that the phasor field approximates a plane wave [5]. It is then possible to neglect the following term since $\nabla\cdot\mathbf{E}'(\mathbf{x},\omega') \approx 0$,

$$\frac{\epsilon_0\chi^{(2)}_{abc}}{\epsilon\pi}\nabla\int E'_b(\mathbf{x},\omega)\frac{\partial}{\partial x_a}E'_c(\mathbf{x},\omega'-\omega)d\omega = \nabla(\nabla\cdot\mathbf{E}'(\mathbf{x},\omega')) \approx 0. \tag{2.42}$$

The right-hand side of the nonlinear Helmholtz equation with the paraxial approximation becomes

$$\begin{aligned}
&-\frac{k_0^2}{\omega'\pi}\int\omega\tilde{\mathbf{E}}(\mathbf{x},\omega'-\omega)\exp(-ik_1z)\cdot\boldsymbol{\chi}^{(2)}\cdot\tilde{\mathbf{E}}(\mathbf{x},\omega)\exp(-ik_2z)\,d\omega \\
&= -\frac{k_0^2}{\omega'\pi}\int\omega\tilde{\mathbf{E}}(\mathbf{x},\omega'-\omega)\cdot\boldsymbol{\chi}^{(2)}\cdot\tilde{\mathbf{E}}(\mathbf{x},\omega)\exp(-ik_1z-ik_2z)\,d\omega,
\end{aligned} \tag{2.43}$$

where k_1 and k_2 are the wave numbers associated with different frequencies[3]. Hence, the nonlinear Helmholtz equation under the paraxial approximation produces the nonlinear paraxial Helmholtz equation

$$\begin{aligned}
&\tilde{\nabla}^2\tilde{\mathbf{E}}(\mathbf{x},\omega')\exp(-ikz) - i2k\frac{\partial}{\partial z}\tilde{\mathbf{E}}(\mathbf{x},\omega')\exp(-ikz) \\
&\quad = -\frac{k_0^2}{\omega'\pi}\int \omega\tilde{\mathbf{E}}(\mathbf{x},\omega'-\omega)\cdot\boldsymbol{\chi}^{(2)}\cdot\tilde{\mathbf{E}}(\mathbf{x},\omega)\exp(-ik_1z - ik_2z)\,d\omega \\
\implies &\tilde{\nabla}^2\tilde{\mathbf{E}}(\mathbf{x},\omega') - i2k\frac{\partial}{\partial z}\tilde{\mathbf{E}}(\mathbf{x},\omega') \\
&\quad = -\frac{k_0^2}{\omega'\pi}\int \omega\tilde{\mathbf{E}}(\mathbf{x},\omega'-\omega)\cdot\boldsymbol{\chi}^{(2)}\cdot\tilde{\mathbf{E}}(\mathbf{x},\omega)\exp(i\Delta kz)\,d\omega,
\end{aligned} \tag{2.44}$$

where $\Delta k = k - k_1 - k_2$ is the phase mismatch and will be reduced to just the z components. It is desirable to have the above equation written in terms of wave vector and angular frequency dependencies, therefore the paraxial nonlinear Helmholtz equation is rewritten in terms of its angular spectra of the phasor field. The two-dimensional inverse Fourier transform will be used to obtain the angular spectrum

$$\tilde{\mathbf{E}}(\mathbf{x},\omega') = \int \mathbf{E}(\mathbf{k},z,\omega')\exp(i\mathbf{k}\cdot\mathbf{X})\,\frac{d^2\mathbf{k}}{(2\pi)^2}, \tag{2.45}$$

where $\mathbf{X}$ in $\mathbb{R}^2$ is the transverse spatial vector and $d^2\mathbf{k}$ is the integral measure representing the transverse components of the wave vector, $\mathbf{k}$. Eq. (2.44) becomes

$$\begin{aligned}
&\int\left(-|\mathbf{k}|^2\mathbf{E}(\mathbf{k},z,\omega') - i2k\frac{\partial}{\partial z}\mathbf{E}(\mathbf{k},z,\omega')\right)\exp(i\mathbf{k}\cdot\mathbf{X})\,\frac{d^2\mathbf{k}}{(2\pi)^2} \\
&= -\frac{k_0^2}{\omega'\pi}\int \omega\mathbf{E}(\mathbf{k}_1,z,\omega'-\omega)\cdot\boldsymbol{\chi}^{(2)}\cdot\mathbf{E}(\mathbf{k}_2,z,\omega) \\
&\times\exp(i(\mathbf{k}_1+\mathbf{k}_2)\cdot\mathbf{X})\exp(i\Delta kz)\,\frac{d^2k_1}{(2\pi)^2}\frac{d^2k_2}{(2\pi)^2}d\omega.
\end{aligned} \tag{2.46}$$

In order to remove the integrals over the transverse wave vector components, the Fourier transform with respect to $\mathbf{X}$ over the entire equation is taken,

[3]Unless the degenerate case is considered.

resulting in two-dimensional Dirac delta functions

$$\begin{aligned}
&\int \left(-|\mathbf{k}|^2\mathbf{E}(\mathbf{k},z,\omega') - i2k\frac{\partial}{\partial z}\mathbf{E}(\mathbf{k},z,\omega')\right)\delta\left(\mathbf{k}'-\mathbf{k}\right)\frac{d^2\mathbf{k}}{(2\pi)^2} \\
&= -\frac{k_0^2}{\omega'\pi}\int \omega\mathbf{E}(\mathbf{k}_1,z,\omega'-\omega)\cdot\boldsymbol{\chi}^{(2)}\cdot\mathbf{E}(\mathbf{k}_2,z,\omega) \\
&\times\delta\left(\mathbf{k}'-\mathbf{k}_1-\mathbf{k}_2\right)\exp\left(i\Delta kz\right)\frac{d^2\mathbf{k}_1}{(2\pi)^2}\frac{d^2\mathbf{k}_2}{(2\pi)^2}d\omega \\
\implies &|\mathbf{k}'|^2\mathbf{E}(\mathbf{k}',z,\omega') + i2k\frac{\partial}{\partial z}\mathbf{E}(\mathbf{k}',z,\omega') \\
&= \frac{k_0^2}{\omega'\pi}\int \omega\mathbf{E}(\mathbf{k}'-\mathbf{k}_2,z,\omega'-\omega)\cdot\boldsymbol{\chi}^{(2)}\cdot\mathbf{E}(\mathbf{k}_2,z,\omega) \\
&\times\exp\left(i\Delta kz\right)\frac{d^2\mathbf{k}_2}{(2\pi)^2}d\omega.
\end{aligned} \tag{2.47}$$

The left-hand side of the above equation is part of the linear Helmholtz equation, whereas the right-hand side contains the nonlinear part. A light beam with transverse wave vector $\mathbf{k}'$ is sent through the nonlinear crystal for the purpose of SPDC. The medium couples the output electric fields with these wave vectors. The result is a superposition of a pair of light fields with such transversal wave vector components involving different transversal $\mathbf{k}_2$ wave vectors. This superposition corresponds to beams with entangled wave vectors. A similar result holds for the frequency. In other words, the phase matching conditions apply. There is also a phase mismatch expression which will be simplified and will be reduced to the z components of the three-dimensional wave vectors.

2.4.3 The co-propagating frame

The next goal is to obtain an expression for an operator called the infinitesimal propagation operator, $\hat{P}_\Delta$ [17]. The IPO is analogous to a Hamiltonian, and contains operators for the pump field, down-converted fields, and the phase mismatch. An expression of the IPO will be provided at the end of the section. A preliminary step in acquiring the IPO is to first convert our equations to the co-propagating frame and is accomplished below.
Equation (2.47) is defined in terms of phasor fields which are vector fields.

The phasor field is split into its polarization vector, $\boldsymbol{\eta}$, along with a scalar field, E

$$\mathbf{E}(\mathbf{k}, z, \omega) = \boldsymbol{\eta} E(\mathbf{k}, z, \omega). \tag{2.48}$$

The electric fields left-hand side and right-hand side Eq. (2.47) represent the pump beam and down-converted beams, respectively. For type I SPDC, the pump has extraordinary polarization $\boldsymbol{\eta}^e$, whilst the down-converted beams will have ordinary polarizations $\boldsymbol{\eta}^o$. The down-converted beams have the same polarizations since type I SPDC is considered. Performing the substitution produces

$$\begin{aligned} &|\mathbf{k}'|^2 \boldsymbol{\eta}^e E(\mathbf{k}', z, \omega') + i2k \frac{\partial}{\partial z} \boldsymbol{\eta}^e E(\mathbf{k}', z, \omega') \\ &= \frac{k_0^2}{\omega' \pi} \int \omega E(\mathbf{k}' - \mathbf{k}_2, z, \omega' - \omega) \boldsymbol{\eta}^o \cdot \boldsymbol{\chi}^{(2)} \cdot \boldsymbol{\eta}^o E(\mathbf{k}_2, z, \omega) \\ &\times \exp\left(i \Delta k z\right) \frac{d^2 \mathbf{k}_2}{(2\pi)^2} d\omega. \end{aligned} \tag{2.49}$$

A dot product with the complex conjugate of the extraordinary polarization vector leads to

$$\begin{aligned} &|\mathbf{k}'|^2 E(\mathbf{k}', z, \omega') + i2k \frac{\partial}{\partial z} E(\mathbf{k}', z, \omega') \\ &= \frac{k_0^2 d_{ooe}}{\epsilon_0 \omega'} \int \omega E(\mathbf{k}' - \mathbf{k}_2, z, \omega' - \omega) E(\mathbf{k}_2, z, \omega) \exp\left(i \Delta k z\right) đ\mathbf{k}_2 \end{aligned} \tag{2.50}$$

where

$$d_{ooe} = 2\epsilon_0 \chi^{(2)}_{abc} \eta^o_a \eta^o_b \eta^{e*}_c, \tag{2.51}$$

and

$$đ\mathbf{k} = \frac{d^2 \mathbf{k}}{(2\pi)^3} d\omega. \tag{2.52}$$

The polarization vector components are represented by η. The scalar field is modeled in a co-propagating frame which removes the free space propagation terms. For the co-propagating frame to come into play, the following expression is considered

$$E(\mathbf{k}, z, \omega) = G(\mathbf{k}, z, \omega) \exp\left(\frac{iz}{2k} |\mathbf{k}|^2\right). \tag{2.53}$$

Substitution of the above expression produces

$$
\begin{aligned}
&|\mathbf{k}'|^2 G(\mathbf{k}', z, \omega') \exp\left(\frac{iz}{2k}|\mathbf{k}'|^2\right) + i2k\frac{\partial}{\partial z}\left(G(\mathbf{k}', z, \omega') \exp\left(\frac{iz}{2k}|\mathbf{k}'|^2\right)\right) \\
&= \frac{k_0^2 d_{ooe}}{\epsilon_0 \omega'} \int \omega G(\mathbf{k}' - \mathbf{k}_2, z, \omega' - \omega) \exp\left(\frac{iz}{2k_1}|\mathbf{k}' - \mathbf{k}_2|^2\right) G(\mathbf{k}_2, z, \omega) \\
&\times \exp\left(\frac{iz}{2k_2}|\mathbf{k}_2|^2\right) \exp\left(i\Delta k z\right) đ\mathbf{k}_2 \\
\implies\ & i2k\frac{\partial}{\partial z}\left(G(\mathbf{k}', z, \omega')\right) \exp\left(\frac{iz}{2k}|\mathbf{k}'|^2\right) \\
&= \frac{k_0^2 d_{ooe}}{\epsilon_0 \omega'} \int \omega G(\mathbf{k}' - \mathbf{k}_2, z, \omega' - \omega) G(\mathbf{k}_2, z, \omega) \\
&\times \exp\left(\frac{iz}{2k_1}|\mathbf{k}' - \mathbf{k}_2|^2 + \frac{iz}{2k_2}|\mathbf{k}_2|^2\right) \exp\left(i\Delta k z\right) đ\mathbf{k}_2.
\end{aligned}
\tag{2.54}
$$

Multiplying the complex conjugate of the exponential on the left-hand side and gathering all the terms in the exponents results in the following expression for the co-propagating frame:

$$
\begin{aligned}
&i2k\frac{\partial}{\partial z} G(\mathbf{k}', z, \omega') \\
&= \frac{k_0^2 d_{ooe}}{\epsilon_0 \omega'} \int \omega G(\mathbf{k}' - \mathbf{k}_2, z, \omega' - \omega) G(\mathbf{k}_2, z, \omega) \\
&\times \exp\left(\frac{iz}{2k_1}|\mathbf{k}' - \mathbf{k}_2|^2 + \frac{iz}{2k_2}|\mathbf{k}_2|^2 - \frac{iz}{2k}|\mathbf{k}'|^2 + i\Delta k z\right) đ\mathbf{k}_2.
\end{aligned}
\tag{2.55}
$$

It is possible to simplify the phase mismatch by considering the following three-dimensional wave vector as defined in Eq. (2.9)

$$
\begin{aligned}
\tilde{\mathbf{k}} &= k_x \hat{\mathbf{x}} + k_y \hat{\mathbf{y}} + k_z \hat{\mathbf{z}} \\
\implies k_z(\mathbf{k}, \omega) &= \sqrt{\frac{\omega^2}{v^2} - |\mathbf{k}|^2} \\
&= \sqrt{k^2 - |\mathbf{k}|^2}.
\end{aligned}
\tag{2.56}
$$

The square root is approximated using either the Taylor expansion or the binomial expansion. Due to the paraxial expansion, only the first two terms

are taken

$$\begin{aligned} k_z(\mathbf{k},\omega) &\approx k - \frac{|\mathbf{k}|^2}{2k} \\ \implies k &\approx \frac{|\mathbf{k}|^2}{2k} + k_z. \end{aligned} \tag{2.57}$$

According to Eq. (2.55), the pump beam has the transverse wave vector $\mathbf{k}'$, and the down-converted beams have the transverse wave vectors $\mathbf{k}' - \mathbf{k}_2$, and $\mathbf{k}_2$. Substituting the approximated expression into the phase mismatch

$$\begin{aligned} \Delta k &= k - k_1 - k_2 \\ &\approx \frac{|\mathbf{k}'|^2}{2k} + k_z - \frac{|\mathbf{k}' - \mathbf{k}_2|^2}{2k_1} - k_{z1} - \frac{|\mathbf{k}_2|^2}{2k_2} - k_{z2} \\ &= \frac{|\mathbf{k}'|^2}{2k} - \frac{|\mathbf{k}' - \mathbf{k}_2|^2}{2k_1} - \frac{|\mathbf{k}_2|^2}{2k_2} + \Delta k_z, \end{aligned} \tag{2.58}$$

where $\Delta k_z = k_z - k_{z1} - k_{z2}$. The expression is substituted into the exponent in Eq. (2.55)

$$\begin{aligned} &\frac{iz}{2k_1}|\mathbf{k}' - \mathbf{k}_2|^2 + \frac{iz}{2k_2}|\mathbf{k}_2|^2 - \frac{iz}{2k}|\mathbf{k}'|^2 + i\Delta kz \\ &\approx i\Delta k_z z. \end{aligned} \tag{2.59}$$

It is now possible to obtain a more convenient expression of Eq. (2.55) using the approximations above

$$\begin{aligned} &i2k\frac{\partial}{\partial z}G(\mathbf{k}', z, \omega') \\ &= \frac{k_0^2 d_{ooe}}{\epsilon_0 \omega'} \int \omega G(\mathbf{k}' - \mathbf{k}_2, z, \omega' - \omega) G(\mathbf{k}_2, z, \omega) \exp\left(i\Delta k_z z\right) đ\mathbf{k}_2. \end{aligned} \tag{2.60}$$

2.4.4 The infinitesimal propagation operator

The remaining objective is to obtain the infinitesimal propagation operator (IPO), $\hat{P}_\Delta$. The IPO is a Hamiltonian analogue depending on the propagation direction. The starting point is to quantize the equation above and considering $G(\mathbf{k}', z, \omega')$ as an operator similar to the annihilation operator for photons in quantum optics [17]. The operators for the pump and down-converted fields are separated. The annihilation operator for down converted photons satisfies an eigenvalue equation for coherent states $|\alpha\rangle$ [17]

$$\hat{G}_d(\mathbf{k}, \omega, z)\,|\alpha\rangle = |\alpha\rangle\, N'(\omega)\alpha(\mathbf{k}, \omega), \tag{2.61}$$

represents operator for the down-converted beams. Likewise, the operator representing the pump beam is represented by [17]

$$\hat{G}_p(\mathbf{k},\omega,z)\,|\beta\rangle = |\beta\rangle\, N'(\omega)\beta(\mathbf{k},\omega). \tag{2.62}$$

The eigenfunctions, $\alpha(\mathbf{k},\omega)$ and $\beta(\mathbf{k},\omega)$, represent the complex-valued spectral functions of the transversal fields at a fixed distance, z, of the down-converted field and the pump field respectively[17]. The norm square of $\alpha(\mathbf{k},\omega,z)$ be the average number of photons with transversal wave vector $\mathbf{k}$ and frequency omega at z. The remaining term is

$$N'(\omega) = \sqrt{\frac{\hbar k}{2\epsilon}}. \tag{2.63}$$

The creation and annihilation operators satisfy the usual commutation relation [17]

$$[\hat{G}(\mathbf{k},\omega,z), \hat{G}^{\dagger}(\mathbf{k}',\omega',z)] = \frac{n\hbar}{2\epsilon_0}(2\pi)^3 k_z \delta\left(\mathbf{k}-\mathbf{k}'\right)\delta\left(\omega-\omega'\right). \tag{2.64}$$

The quantized operators are substituted into the infinitesimal propagation equation (IPE). The IPE is given as [17]

$$i\hbar\frac{\mathrm{d}}{\mathrm{d}z}\hat{\rho}(z) = \left[\hat{P}_{\Delta}, \hat{\rho}(z)\right]. \tag{2.65}$$

The density operator representing the state of the paraxial electromagnetic field at propagation distance, z, is given as $\hat{\rho}(z)$. For example, for a coherent state including a mode function with transversal spectral function, $\alpha(\mathbf{k},\omega,z)$, the density operator reads $\hat{\rho} = |\alpha\rangle\langle\alpha|$. The propagation of $\hat{\rho}(z)$ along the z axis can be described by a unitary transformation with generator $\hat{P}_{\Delta}$ [17], or equivalently by the IPE shown in Eq. (2.65). It takes the form of a master equation in the Schrödinger picture, where the time derivative is replaced by the z derivative.
By comparison with the paraxial wave equation for the quantized operators in the co-propagating frame, the IPO can be shown as [17]

$$\hat{P}_{\Delta} = \int V(\mathbf{k},\mathbf{k}_1,\mathbf{k}_2,\omega,\omega_1,\omega_2)\hat{G}_p^{\dagger}(\mathbf{k},\omega,z)\hat{G}_d(\mathbf{k}_1,\omega_1,z)\hat{G}_d(\mathbf{k}_2,\omega_2,z)đ\mathbf{k}đ\mathbf{k}_1đ\mathbf{k}_2 + h.c., \tag{2.66}$$

where $h.c.$ is the Hermitian conjugate, and [17]

$$V(\mathbf{k}, \mathbf{k}_1, \mathbf{k}_2) = \frac{(2\pi)^3}{2} d_{ooe} \exp\left(i\Delta k_z z\right) \delta\left(\mathbf{k} - \mathbf{k}_1 - \mathbf{k}_2\right) \delta\left(\omega - \omega_1 - \omega_2\right). \tag{2.67}$$

$V(\mathbf{k}, \mathbf{k}_1, \mathbf{k}_2)$ is called a vertex kernel which depends on three transverse wave vectors and represents the interaction between the nonlinear crystal and the beams involved [17]. The IPE and IPO will come in handy when deriving the Wigner functional version for the IPE in order to obtain the evolution equation which will be done in chapter 4.

Chapter 3

Wigner functionals

Quantum mechanics can be formulated on phase space [3]. A density matrix can be transformed into a quasi-probability distribution on phase space. One such distribution is the Wigner function. For certain cases, the distribution could be negative or even singular, hence the name, quasi-probability distribution. The Wigner function written in position basis is given by [6]

$$W(q,p) = \frac{1}{2\pi\hbar}\int_{-\infty}^{\infty} \left\langle q + \frac{1}{2}q' \right| \hat{\rho} \left| q - \frac{1}{2}q' \right\rangle e^{ipq'/\hbar} dq', \tag{3.1}$$

where $\hat{\rho}$ is an arbitrary density matrix, and q' and p are the position and momentum eigenvalues of the position and momentum operators. A set of operators with the eigenvectors and eigenvalues are given below

$$\begin{aligned} \hat{q}\,|q\rangle &= q\,|q\rangle\,, \\ \hat{p}\,|p\rangle &= p\,|p\rangle\,. \end{aligned} \tag{3.2}$$

The Wigner function contains an integral over all possible position values, q'.
A similar set of operators are now presented, which will be called the fixed-momentum quadrature operators, with its eigenvectors and eigenvalues depending on $\mathbf{k}$ [15]

$$\begin{aligned} \hat{q}(\mathbf{k})\,|q\rangle &= q(\mathbf{k})\,|q\rangle\,, \\ \hat{p}(\mathbf{k})\,|p\rangle &= p(\mathbf{k})\,|p\rangle\,. \end{aligned} \tag{3.3}$$

The eigenvalues of $\hat{q}(\mathbf{k})$ and $\hat{p}(\mathbf{k})$ will be referred to as eigenfunctions. The fixed-momentum quadrature operators are given in terms of the creation and

annihilation operators of a photon with wave vector $\mathbf{k}$ [21]

$$\begin{aligned}\hat{q} &= \frac{1}{\sqrt{2}}\left(\hat{a}(\mathbf{k}) + \hat{a}^{\dagger}(\mathbf{k})\right), \\ \hat{p} &= -\frac{i}{\sqrt{2}}\left(\hat{a}(\mathbf{k}) - \hat{a}^{\dagger}(\mathbf{k})\right),\end{aligned} \tag{3.4}$$

where the spin indices are neglected. The eigenvectors are defined in terms of quadrature creation operators [21, 15] as

$$\begin{aligned}|q\rangle &= \hat{a}_q^{\dagger}|vac\rangle, \\ |p\rangle &= \hat{a}_p^{\dagger}|vac\rangle.\end{aligned} \tag{3.5}$$

where the creation operators are given by [21, 15]

$$\begin{aligned}\hat{a}_q^{\dagger} &= \pi^{-\Omega/4}\exp\left(-\frac{1}{2}\|q(\mathbf{k})\|^2 + \hat{a}_Q^{\dagger} - \hat{a}_R^{\dagger}\right), \\ \hat{a}_p^{\dagger} &= 2^{\Omega/2}\pi^{\Omega/4}\exp\left(-\frac{1}{2}\|p(\mathbf{k})\|^2 + i\hat{a}_P^{\dagger} + \hat{a}_R^{\dagger}\right),\end{aligned} \tag{3.6}$$

and

$$\begin{aligned}\hat{a}_Q^{\dagger} &= \sqrt{2}\int \hat{a}^{\dagger}(\mathbf{k})q(\mathbf{k})đ\mathbf{k}, \\ \hat{a}_P^{\dagger} &= \sqrt{2}\int \hat{a}^{\dagger}(\mathbf{k})p(\mathbf{k})đ\mathbf{k}, \\ \hat{a}_R^{\dagger} &= \frac{1}{2}\int \hat{a}^{\dagger}(\mathbf{k})\hat{a}^{\dagger}(\mathbf{k})đ\mathbf{k},\end{aligned} \tag{3.7}$$

where the integral measure is given as

$$đ\mathbf{k} = \frac{d^2\mathbf{k}d\omega}{(2\pi)^3}. \tag{3.8}$$

Using all real-valued square integrable eigenfunctions $q(\mathbf{k})$ and $p(\mathbf{k})$, we obtain an orthonormal basis $|q\rangle$ and $|p\rangle$, respectively, for the complete Hilbert space of the quantised electromagnetic fields [21, 15]. Consider a Wigner function written in terms of the position basis using Eq. (3.3). The following expression is obtained which is called a Wigner functional [21, 15]

$$W_{\hat{A}}[p,q] = \int \left\langle q + \frac{1}{2}q' \middle| \hat{A} \middle| q - \frac{1}{2}q' \right\rangle \exp\left(-ip \diamond q'\right) \mathcal{D}[q'], \tag{3.9}$$

where $\mathcal{D}[q] = d^{\Omega}q$, $\Omega = \mathrm{tr}\,(\mathbb{1})$, and $\hat{A}$ is an arbitrary operator. The explicit dependence of p and q on $\mathbf{k}$ is dropped, only the eigenfunctions will be considered from this point onward. Eq. (3.9) is called a functional because it is integrated over all possible functions of $q(\mathbf{k})$. There are other functional quasi-probability distributions such as the functional Weyl transform and the characteristic functional [21]. The notation $\diamond$ represents an integral over $\mathbf{k}$ and will be explained in greater detail in section 3.1. In terms of complex fields, the Wigner functional is [21]

$$\begin{aligned} W_{\hat{A}}[\alpha] = N_0 \int \exp\Bigg(&-2\|\alpha\|^2 + 2\alpha^* \diamond \alpha_1 + 2\alpha_2^* \diamond \alpha - \frac{1}{2}\|\alpha_1\|^2 \\ &-\frac{1}{2}\|\alpha_2\|^2 - \alpha_2^* \diamond \alpha_1\Bigg) \langle \alpha_1 |\, \hat{A}\, | \alpha_2 \rangle\, \mathcal{D}^{\circ}[\alpha_1, \alpha_2], \end{aligned} \tag{3.10}$$

where $N_0 = 2^{\Omega}$, $\mathcal{D}^{\circ}[\alpha_1, \alpha_2] = \mathcal{D}^{\circ}[\alpha_1]\mathcal{D}^{\circ}[\alpha_2]$, and $\mathcal{D}^{\circ}[\alpha] = \frac{1}{(2\pi)^{\Omega}}\mathcal{D}[p]\mathcal{D}[q]$. The circle in the superscript of the integral measure implies a factor of $\frac{1}{(2\pi)^{\Omega}}$. The integral also integrates over the complex conjugate of the complex field. The state vector approach diverges when attempting to include the spatiotemporal, particle number, and spin degrees of freedom [15], therefore, the Wigner functional approach is used.

Combining Wigner functionals is now tackled. If there are two operators, $\hat{A}$ and $\hat{B}$, and the respective Wigner functionals are $W_{\hat{A}}$ and $W_{\hat{B}}$, the Wigner functional for a product of these operators is $W_{\hat{A}\hat{B}}$. A star product is used to represent $W_{\hat{A}\hat{B}}$ in terms of $W_{\hat{A}}$ and $W_{\hat{B}}$ which follows the Moyal formalism [12], and is defined as [21]

$$\begin{aligned} W_{\hat{A}\hat{B}}[p, q] = W_{\hat{A}} \star W_{\hat{B}} = N_0^2 \int W_{\hat{A}}[q - q_1, p - p_1] W_{\hat{B}}[q - q_2, p - p_2] \\ \exp\left(2i\left(q_1 \diamond p_2 - q_2 \diamond p_1\right)\right) \mathcal{D}[q_1, q_2]\mathcal{D}^{\circ}[p_1, p_2], \end{aligned} \tag{3.11}$$

which is written for two operators and is in terms of p and q. Rewriting this in terms of complex fields

$$\begin{aligned} &W_{\hat{A}\hat{B}}[\alpha] = W_{\hat{A}} \star W_{\hat{B}} \\ &= N_0^2 \int W_{\hat{A}}\left[\alpha - \alpha_1\right] W_{\hat{B}}\left[\alpha - \alpha_2\right] \exp\left(2\alpha_1^* \diamond \alpha_2 - 2\alpha_2^* \diamond \alpha_1\right) \mathcal{D}^{\circ}[\alpha_1]\mathcal{D}^{\circ}[\alpha_2], \end{aligned} \tag{3.12}$$

and is shown in appendix A. The equation above is obtained by simply rewriting the functional phase space variables in terms of the complex field

variables, which is done in appendix A. The star product of three operators is given by [21]

$$W_{\hat{A}\hat{B}\hat{C}}[\alpha] = \int W_{\hat{A}}\left[\frac{1}{2}\left(\alpha_a + \alpha_b + \alpha\right)\right] W_{\hat{B}}[\alpha_a] W_{\hat{C}}\left[\frac{1}{2}\left(\alpha_a - \alpha_b + \alpha\right)\right] \exp\left(\left(\alpha^* - \alpha_a^*\right) \diamond \alpha_b - \alpha_b^* \diamond \left(\alpha - \alpha_a\right)\right) \mathcal{D}^{\circ}[\alpha_a, \alpha_b]. \tag{3.13}$$

Note that the star product is associative since the order of integration does not influence the result. The case whereby the operator $\hat{A} = \hat{A}(\alpha_1, \alpha_2, \alpha_3, \alpha_4)$ is a bipartite system is of interest. The treatment of such a case would require that the Wigner functional, either Eq. (3.9) or Eq. (3.10), be applied to operator $\hat{A}$ twice. If the complex field approach is used, we have

$$\begin{aligned} W_{\hat{A}}[\alpha, \beta] = N_0^2 \int \exp\Bigg(& -2\|\alpha\|^2 + 2\alpha^* \diamond \alpha_1 + 2\alpha_2^* \diamond \alpha - \frac{1}{2}\|\alpha_1\|^2 \\ & - \frac{1}{2}\|\alpha_2\|^2 - \alpha_2^* \diamond \alpha_1 - 2\|\beta\|^2 + 2\beta^* \diamond \alpha_3 + 2\alpha_4^* \diamond \beta - \frac{1}{2}\|\alpha_3\|^2 \\ & - \frac{1}{2}\|\alpha_4\|^2 - \alpha_4^* \diamond \alpha_3 \Bigg) \left\langle \alpha_1, \alpha_3 \right| \hat{A} \left| \alpha_2, \alpha_4 \right\rangle \mathcal{D}^{\circ}[\alpha_1, \alpha_2, \alpha_3, \alpha_4]. \end{aligned} \tag{3.14}$$

Consider another operator, $\hat{B}$, which is also a bipartite system and has a Wigner functional $W_{\hat{B}}$. The Wigner functional for their product is obtained by using the star product twice

$$W_{\hat{A}\hat{B}}[\alpha, \beta] = W_{\hat{A}}[\alpha, \beta] \star \star W_{\hat{B}}[\alpha, \beta]. \tag{3.15}$$

We consider a special case whereby the operator $\hat{A}$ is not entangled i.e $\hat{A} = \hat{A}'(\alpha_1, \alpha_2) \otimes \tilde{\hat{A}}(\alpha_3, \alpha_4)$. The Wigner functional above simplifies to

$$W_{\hat{A}}[\alpha, \beta] = W_{\hat{A}'}[\alpha] W_{\tilde{\hat{A}}}[\beta]. \tag{3.16}$$

The star product reduces to a regular product for the case of a separable operator. Eq. (3.16) depicts a system which is not entangled in the Wigner functional formalism, and is due to

$$\begin{aligned} & \left\langle \alpha_1, \alpha_3 \right| \hat{A} \left| \alpha_2, \alpha_4 \right\rangle \\ & = \left\langle \alpha_1 \right| \hat{A}' \left| \alpha_2 \right\rangle \left\langle \alpha_3 \right| \tilde{\hat{A}} \left| \alpha_4 \right\rangle. \end{aligned} \tag{3.17}$$

3.1 Functional theory

The reader is provided with an intuitive idea of how to interpret functionals. A functional is a function of functions. Functional derivatives and functional integrals cannot be treated as conventional derivatives and integrals. A basic understanding of functionals and how to perform basic operations is provided here.
A few paragraphs are presented below describing kernels. Consider the matrix equation

$$\tilde{F}_j^T = \sum_{m=1}^{N} F_m^T K_{mj}, \tag{3.18}$$

where $\mathbf{F}$ is a column vector with dimension N and $\mathbf{K}$ is an $N \times N$ matrix. Eq. (3.18) is a discrete equation, and essentially maps elements of vector $\mathbf{F}^T$ to elements of vector $\tilde{\mathbf{F}}^T$ by means of matrix $\mathbf{K}$. The equation below is a continuous analog of Eq. (3.18)

$$\tilde{f}(y) = \int_{-\infty}^{\infty} f(x)K(x,y)dx, \tag{3.19}$$

where the kernel is given by $K(x,y)$. An example of a kernel is the Fourier kernel, where $K(x,y) = e^{-2\pi ixy}$, which reduces Eq. (3.19) to the Fourier transform. In optics, a linear map of a spectral function, $f(\mathbf{k}_1) \to \tilde{f}(\mathbf{k}_2)$, can be expressed by an integral with a two-dimensional kernel [21, 17]

$$\begin{aligned} \tilde{f}(\mathbf{k}_2) &= \int_{-\infty}^{\infty} f(\mathbf{k}_1)K(\mathbf{k}_1,\mathbf{k}_2)\frac{d^2\mathbf{k}_1 d\omega_1}{(2\pi)^3} \\ &= \int_{-\infty}^{\infty} f(\mathbf{k}_1)K(\mathbf{k}_1,\mathbf{k}_2)đ\mathbf{k}_1 \\ &= f \diamond K, \end{aligned} \tag{3.20}$$

where

$$đ\mathbf{k}_1 = \frac{d^2\mathbf{k}_1 d\omega_1}{(2\pi)^3}, \tag{3.21}$$

and $\diamond$ is called the diamond product (or diamond contraction) which represents an integral over the transverse wave vector, as well as ω. In other words, the diamond product, if calculated over $\mathbf{k}_1$, is an integral with the integral measure given above. It is possible to have cases in which kernels

are diamond contracted to each other. An example is if a kernel $K_1(\mathbf{k}_1, \mathbf{k}_2)$ is contracted to kernel $K_2(\mathbf{k}_3, \mathbf{k}_4)$. The variables of K_1 and K_2 are different, however by taking a diamond product of K_1 with K_2, it is implied that $\mathbf{k}_2 = \mathbf{k}_3$. The diamond product is shown below

$$\int K_1(\mathbf{k}_1, \mathbf{k}_2) K_2(\mathbf{k}_2, \mathbf{k}_4) đ\mathbf{k}_2 = K_1 \diamond K_2 = K'(\mathbf{k}_1, \mathbf{k}_4), \tag{3.22}$$

where K' is another kernel. A kernel is essentially a function of two or more transverse wave vectors. In the examples above, the kernels were functions of two transverse wave vectors. A kernel can depend on more than two transverse wave vectors, and represents an interaction. An example of such a kernel is the vertex kernel shown in Eq. (4.4). In most of the calculations involving diamond products, the transverse wave vector dependencies are dropped for simplicity since the expressions are quite lengthy. When a diamond product of two kernels is taken, it is implied that the second transverse wave vector of the first kernel will be contracted with the first transverse wave vector of the second kernel, as depicted in Eq. (3.22). The triple diamond product (containing three $\diamond$ symbols) of a kernel with three transverse wave vector dependencies become ambiguous since there can be different combinations of diamond products for such a kernel. Therefore, for calculations involving the triple diamond product, the integral form, along with the diamond product notation is written. The diamond product notation produces a neater expression and operators can be applied easier than with the integral notation.

In shift invariant systems, a matrix called the Toeplitz matrix can be defined which has a property that the diagonals have the same value [11]. For the purposes here, an analogous Toeplitz kernel is used which is also shift invariant and has the form

$$Y(\mathbf{k}, \mathbf{k}_1) = 2\pi\delta(\omega - \omega_1) \int a(\mathbf{X}) \exp\left(i\left(\mathbf{k} - \mathbf{k}_1\right) \cdot \mathbf{X}\right) d^2\mathbf{X}, \tag{3.23}$$

where $\mathbf{X}$ is a two-dimensional spatial vector, $a(\mathbf{X})$ is called an anchor, and $Y(\mathbf{k}, \mathbf{k}_1)$ is the Toeplitz kernel. The anchor is set to $a = 1$, then the identity kernel is obtained, $\mathbb{1}$ [17]

$$\begin{aligned} \mathbb{1} &= 2\pi\delta(\omega - \omega_1) \int \exp\left(i\left(\mathbf{k} - \mathbf{k}_1\right) \cdot \mathbf{X}\right) d^2\mathbf{X} \\ &= (2\pi)^3 \delta(\omega - \omega_1)\, \delta\left(\mathbf{k} - \mathbf{k}_1\right). \end{aligned} \tag{3.24}$$

The identity kernel is defined such that

$$K \diamond \mathbb{1} = K, \tag{3.25}$$

where K is a kernel. When Toeplitz kernels are diamond contracted with each other, they have a special property. Consider the diamond product of two kernels, from Eq. (3.22)

$$\begin{aligned}
&Y_1 \diamond Y_2 \\
&= (2\pi)^2 \int \delta(\omega - \omega_1)\, \delta(\omega_1 - \omega_2)\, a_1(\mathbf{X}) a_2(\mathbf{X'}) \\
&\exp\left(i(\mathbf{k} - \mathbf{k}_1) \cdot \mathbf{X} + i(\mathbf{k}_1 - \mathbf{k}_2) \cdot \mathbf{X}'\right) d^2\mathbf{X} d^2\mathbf{X}' đ\mathbf{k}_1 \\
&= (2\pi)^2 \int \delta(\omega - \omega_1)\, \delta(\omega_1 - \omega_2)\, a_1(\mathbf{X}) a_2(\mathbf{X'}) \\
&\exp\left(i\mathbf{k} \cdot \mathbf{X} - i\mathbf{k}_1 \cdot \mathbf{X} + i\mathbf{k}_1 \cdot \mathbf{X}' - i\mathbf{k}_2 \cdot \mathbf{X}'\right) d^2\mathbf{X} d^2\mathbf{X}' đ\mathbf{k}_1 \\
&= 2\pi\delta(\omega - \omega_2) \int a_1(\mathbf{X}) a_1(\mathbf{X}) \exp\left(i(\mathbf{k} - \mathbf{k}_2) \cdot \mathbf{X}\right) d^2\mathbf{X} \\
&= \tilde{Y}.
\end{aligned} \tag{3.26}$$

The anchors a_1 and a_2 belong to Y_1 and Y_2 respectively. The diamond product of Toeplitz kernels is equal to the Toeplitz kernel of the product of its anchors, $\tilde{Y}$.

Functional derivatives will now be defined. Consider a functional, $F[f_1, f_2](z)$ where f_1 and f_1 are functions depending on z and $\mathbf{k}$. The square bracket notation is used to distinguish functionals from functions. The full derivative of $F[f_1, f_2](z)$ with respect to z is considered, and will produce functional derivatives. The full derivative of a functional, $F[f_1, f_2](z)$, is defined as follows [17]

$$\begin{aligned}
&\frac{\mathrm{d}F[f_1, f_2](z)}{\mathrm{d}z} \\
&= \int \frac{\delta F[f_1, f_2](z)}{\delta f_1(z, \mathbf{k})} \frac{\partial f_1(z, \mathbf{k})}{\partial z} đ\mathbf{k} + \int \frac{\delta F[f_1, f_2](z)}{\delta f_2(z, \mathbf{k})} \frac{\partial f_2(z, \mathbf{k})}{\partial z} đ\mathbf{k} + \frac{\partial F[f_1, f_2](z)}{\partial z} \\
&= \frac{\delta F}{\delta f_1} \diamond \frac{\partial f_1}{\partial z} + \frac{\delta F}{\delta f_2} \diamond \frac{\partial f_2}{\partial z} + \frac{\partial F}{\partial z},
\end{aligned} \tag{3.27}$$

where the diamond product notation has been used to represent the integral over $\mathbf{k}$. The terms with δ, such as $\frac{\delta F}{\delta f_1}$, represents a functional derivative.

Note that in the diamond product notation all the variable dependencies have been dropped for convenience. The variables may sometimes be written, depending on the scenario of the calculation.
The full derivative of a functional was depicted, the functional derivative of a functional with respect to one of its functions is now looked at. Consider the following functional

$$\begin{aligned} & F \\ & = f \diamond K \diamond f \\ & = \int f(\mathbf{k}) K(\mathbf{k}, \mathbf{k}_1) f(\mathbf{k}_1) đ\mathbf{k} đ\mathbf{k}_1. \end{aligned} \tag{3.28}$$

The diamond product is associative. The functional derivative of the functional with respect to one of its functions, say $f = f(\tilde{\mathbf{k}})$, is defined as follows

$$\begin{aligned} \frac{\delta F}{\delta f} &= \frac{\delta \left(f \diamond K \diamond f \right)}{\delta f} \\ &= K \diamond f + f \diamond K \\ &= \int K(\tilde{\mathbf{k}}, \mathbf{k}_1) f(\mathbf{k}_1) đ\mathbf{k}_1 + \int f(\mathbf{k}) K(\mathbf{k}, \tilde{\mathbf{k}}) đ\mathbf{k}, \end{aligned} \tag{3.29}$$

where [21]

$$\frac{\delta f(\mathbf{k}')}{\delta f(\tilde{\mathbf{k}})} = \delta(\mathbf{k}' - \tilde{\mathbf{k}}). \tag{3.30}$$

It is possible to take another functional derivative with respect to $f = f(\mathbf{k}')$, and the transverse wave vector dependency is explicitly written

$$\frac{\delta^2 F}{\delta f(\mathbf{k}') \delta f(\tilde{\mathbf{k}})} = K(\tilde{\mathbf{k}}, \mathbf{k}') + K(\mathbf{k}', \tilde{\mathbf{k}}). \tag{3.31}$$

There is a problem with the above equation. The diamond product of Eq. (3.31) is taken with an arbitrary complex field variable, f', to the right, the following issue occurs

$$\frac{\delta^2 F}{\delta f \delta f} \diamond f' = \int K(\tilde{\mathbf{k}}, \mathbf{k}') f'(\tilde{\mathbf{k}}) đ\tilde{\mathbf{k}} + \int K(\mathbf{k}', \tilde{\mathbf{k}}) f'(\tilde{\mathbf{k}}) đ\tilde{\mathbf{k}}. \tag{3.32}$$

The first term on the right-hand side violates the definition of the diamond contraction in Eq. (3.20). When the diamond product of f' is taken to the

right, an integral over $\tilde{\mathbf{k}}$ is implied. The diamond contraction of a kernel and function/complex field variable should have matching transverse wave vectors on the diamond contracted transverse wave vector. The first term on the right-hand side is not in agreement. The correction would be

$$\frac{\delta^2 F}{\delta f \delta f} \diamond f' = \int K^T(\mathbf{k}', \tilde{\mathbf{k}}) f'(\tilde{\mathbf{k}}) đ\tilde{\mathbf{k}} + \int K(\mathbf{k}', \tilde{\mathbf{k}}) f'(\tilde{\mathbf{k}}) đ\tilde{\mathbf{k}}, \tag{3.33}$$

or

$$\frac{\delta^2 F}{\delta f \delta f} \diamond f' = K^T \diamond f' + K \diamond f', \tag{3.34}$$

where

$$K^T(\mathbf{k}', \tilde{\mathbf{k}}) = K(\tilde{\mathbf{k}}, \mathbf{k}'). \tag{3.35}$$

Therefore, the transverse wave vectors in Eq. (3.31) are separated by the use of a transpose

$$\frac{\delta^2 F}{\delta f(\mathbf{k}') \delta f(\tilde{\mathbf{k}})} = K^T(\mathbf{k}', \tilde{\mathbf{k}}) + K(\mathbf{k}', \tilde{\mathbf{k}}). \tag{3.36}$$

All the $\mathbf{k}'$ dependencies are on the left, and all the $\tilde{\mathbf{k}}$ dependencies are on the right. Eq. (3.36) is now ready for the diamond contraction process. As mentioned, the diamond product on the right-hand side yields

$$\frac{\delta^2 F}{\delta f(\mathbf{k}') \delta f(\tilde{\mathbf{k}})} \diamond f'(\tilde{\mathbf{k}}) = K^T(\mathbf{k}', \tilde{\mathbf{k}}) \diamond f'(\tilde{\mathbf{k}}) + K(\mathbf{k}', \tilde{\mathbf{k}}) \diamond f'(\tilde{\mathbf{k}}). \tag{3.37}$$

The diamond product can be taken on both sides with respect to $f'(\mathbf{k}')$, and produces

$$\begin{aligned} & f'(\mathbf{k}') \diamond \frac{\delta^2 F}{\delta f(\mathbf{k}') \delta f(\tilde{\mathbf{k}})} \diamond f'(\tilde{\mathbf{k}}) \\ &= f'(\mathbf{k}') \diamond K^T(\mathbf{k}', \tilde{\mathbf{k}}) \diamond f'(\tilde{\mathbf{k}}) + f'(\mathbf{k}') \diamond K(\mathbf{k}', \tilde{\mathbf{k}}) \diamond f'(\tilde{\mathbf{k}}) \\ &= f' \diamond K^T \diamond f' + f' \diamond K \diamond f'. \end{aligned} \tag{3.38}$$

Functional integrals are explained in the following. Consider the equation below, which is the integral for an isotropic Gaussian functional [21]

$$\begin{aligned} & \int \exp\left(-\mathrm{c}\alpha^* \diamond P \diamond \alpha - \alpha^* \diamond \beta - \beta' \diamond \alpha\right) \mathcal{D}^\circ[\alpha] \\ &= \frac{1}{c^\Omega \det[P]} \exp\left(\frac{1}{\mathrm{c}} \beta' \diamond P^{-1} \diamond \beta\right), \end{aligned} \tag{3.39}$$

where P is a kernel, c is a nonzero constant, α, β and β' are complex fields which depend on transverse wave vectors, $\Omega = \mathrm{tr}(\mathbb{1})$ is the cardinality of countable infinity [16], and $\mathcal{D}^\circ[\alpha] = \frac{1}{(2\pi)^\Omega}\mathcal{D}[p]\mathcal{D}[q]$ [21]. The integral measure for the momentum is $\mathcal{D}[p] = d^\Omega p$, and a similar definition applies for the position. The circle on the integral measure, $\mathcal{D}^\circ[\alpha]$, implies a factor of $\frac{1}{(2\pi)^\Omega}$ [21]. The proof for the discrete and finite case for Eq. (3.39) is shown in appendix B. The functional integral in Eq. (3.39) is performed over the complex field, α, and its complex conjugate.
The functional integral over a real field variable, q, is also considered

$$\begin{aligned} &\int \exp\left(-\mathrm{c}q \diamond P \diamond q - q \diamond \beta\right) \mathcal{D}[q] \\ &= \exp\left(\frac{\beta \diamond P^{-1} \diamond \beta}{4\mathrm{c}}\right) \frac{\pi^{\Omega/2}}{\mathrm{c}^{\Omega/2}\sqrt{\det\left(P\right)}}, \end{aligned} \tag{3.40}$$

where P is a kernel that does not need to be real-valued. The proof for the discrete and finite case for Eq. (3.40) is also shown in appendix B.

3.2 Examples of Wigner functionals

A few examples of Wigner functionals for certain operators are discussed here. A special Wigner functional called the detector Wigner functional is mentioned.
The Wigner functional for a fixed spectrum coherent state is studied. The fixed spectrum coherent state is given by [15]

$$|\alpha_F\rangle = \exp\left(-\frac{1}{2}|\alpha|^2\right) \sum_n \frac{\alpha^n}{\sqrt{n!}} |n_F\rangle\,, \tag{3.41}$$

and the fixed spectrum fock states are [15, 21]

$$|n_F\rangle = \frac{1}{\sqrt{n!}}(\hat{a}_F^\dagger)^n |\mathrm{vacuum}\rangle\,, \tag{3.42}$$

with the fixed-spectrum creation operator [15, 21]

$$\hat{a}_F^\dagger = \int \hat{a}^\dagger(\mathbf{k}) F(\mathbf{k}) đ\mathbf{k}. \tag{3.43}$$

The normalized spectrum is labeled as $F(\mathbf{k})$ which follows the following normalization condition

$$\int |F\mathbf{k}|^2 đ\mathbf{k}, \tag{3.44}$$

and the creation operator for momentum is $\hat{a}^\dagger(\mathbf{k})$. It is important to note that [21]

$$\hat{a}(\mathbf{k}) |\alpha_F\rangle = \alpha(\mathbf{k}) |\alpha_F\rangle . \tag{3.45}$$

The equation above implies that an eigenfunction of $\alpha(\mathbf{k})$ is calculated for a fixed spectrum coherent state, $|\alpha_F\rangle$ [21]. The eigenfunction, $\alpha(\mathbf{k})$, will sometimes be referred to as the spectral function [21, 17]. For a different fixed spectrum coherent state, a different eigenfunction will be obtained, i.e. $\hat{a}(\mathbf{k}) |\beta_F\rangle = \beta(\mathbf{k}) |\beta_F\rangle$. When referring to the fixed spectrum coherent state, the spectrum will be dropped for convenience. The Wigner functional for a fixed spectrum coherent state is calculated by starting with the following definition for the Wigner functional [15, 21]

$$W_{\hat{A}}[p,q] = \int \left\langle q + \frac{1}{2}q' \middle| \hat{A} \middle| q - \frac{1}{2}q' \right\rangle \exp\left(-ip \diamond q'\right) \mathcal{D}[q']. \tag{3.46}$$

The substitution of $\hat{A} = |\alpha_F\rangle \langle\alpha_F|$ gives

$$W_{|\alpha\rangle\langle\alpha|}[\alpha] = \int \left\langle q + \frac{1}{2}q' \middle| \alpha_F \right\rangle \left\langle \alpha_F \middle| q - \frac{1}{2}q' \right\rangle \exp\left(-ip \diamond q'\right) \mathcal{D}[q']. \tag{3.47}$$

The result is simplified by using the equation below [15]

$$\left\langle q + \frac{1}{2}q' \middle| \alpha_F \right\rangle = \pi^{-\frac{\Omega}{4}} \exp\left(-\frac{1}{2} \left\| q + \frac{1}{2}q' - q_0 \right\|^2 + ip_0 \diamond \left(q + \frac{1}{2}q' - \frac{1}{2}q_0 \right) \right), \tag{3.48}$$

where p_0 and q_0 are eigenfunctions which are evaluated at a point, and brings Eq. (3.47) to

$$\begin{aligned}
W_{|\alpha\rangle\langle\alpha|}[\alpha] &= \pi^{-\frac{\Omega}{2}} \int \exp\left(-\frac{1}{2}\left\|q+\frac{1}{2}q'-q_0\right\|^2 + ip_0 \diamond \left(q+\frac{1}{2}q'-\frac{1}{2}q_0\right)\right) \\
&\quad \exp\left(-\frac{1}{2}\left\|q-\frac{1}{2}q'-q_0\right\|^2 - ip_0 \diamond \left(q-\frac{1}{2}q'-\frac{1}{2}q_0\right)\right) \exp\left(-ip \diamond q'\right) \mathcal{D}[q'] \\
&= \pi^{-\frac{\Omega}{2}} \int \exp\left(-\frac{1}{2}\left\|q-q_0+\frac{1}{2}q'\right\|^2 + ip_0 \diamond q'\right) \\
&\quad \exp\left(-\frac{1}{2}\left\|q-q_0-\frac{1}{2}q'\right\|^2\right) \exp\left(-ip \diamond q'\right) \mathcal{D}[q'] \\
&= \pi^{-\frac{\Omega}{2}} \int \exp\left(-\frac{1}{2}\|q-q_0\|^2 - \frac{1}{2}(q-q_0)\diamond q' - \frac{1}{8}\|q'\|^2 + ip_0 \diamond q'\right) \\
&\quad \exp\left(-\frac{1}{2}\|q-q_0\|^2 + \frac{1}{2}(q-q_0)\diamond q' - \frac{1}{8}\|q'\|^2\right) \exp\left(-ip \diamond q'\right) \mathcal{D}[q'] \\
&= \pi^{-\frac{\Omega}{2}} \int \exp\left(-\|q-q_0\|^2 - \frac{1}{4}\|q'\|^2 + ip_0 \diamond q' - ip \diamond q'\right) \mathcal{D}[q'] \\
&= \pi^{-\frac{\Omega}{2}} \exp\left(-\|q\|^2 + 2q \diamond q_0 - \|q_0\|^2\right) \\
&\quad \times \int \exp\left(-\frac{1}{4}q' \diamond q' - (ip - ip_0) \diamond q'\right) \mathcal{D}[q'].
\end{aligned} \tag{3.49}$$

The result in Eq. (3.40) is used, where $\beta = ip - ip_0$, $P = \mathbb{1}$, and $\mathrm{c} = \frac{1}{4}$ [17, 21]

$$\begin{aligned}
W_{|\alpha\rangle\langle\alpha|}[\alpha] &= N_0 \exp\left(-\|q-q_0\|^2 - (p-p_0) \diamond (p-p_0)\right) \\
&= N_0 \exp\left(-\|q-q_0\|^2 - \|p-p_0\|^2\right) \\
&= N_0 \exp\left(-\|q-q_0+i\,(p-p_0)\|^2\right) \\
&= N_0 \exp\left(-2\left\|\frac{q+ip}{\sqrt{2}} - \frac{q_0+ip_0}{\sqrt{2}}\right\|^2\right) \\
&= N_0 \exp\left(-2\|\alpha-\alpha_0\|^2\right).
\end{aligned} \tag{3.50}$$

We consider the Wigner functional for the number operator, the proof of which is given in [21], however, the calculations are looked at here in slightly

more detail. The Wigner functional can be rewritten in terms of complex fields, for an arbitrary operator, $\hat{A}$, it is given by [21]

$$W_{\hat{A}}[\alpha] = N_0 \int \exp\left(-2\|\alpha\|^2 + 2\alpha^* \diamond \alpha_1 + 2\alpha_2^* \diamond \alpha - \frac{1}{2}\|\alpha_1\|^2 - \frac{1}{2}\|\alpha_2\|^2 - \alpha_2^* \diamond \alpha_1\right) \langle \alpha_1 | \hat{A} | \alpha_2 \rangle \mathcal{D}^\circ[\alpha_1, \alpha_2], \tag{3.51}$$

where $N_0 = 2^\Omega$. Eq. (3.51) will mostly be used in order to calculate Wigner functionals for operators, and will be referred to as the coherent-state assisted approach. The aim is to calculate the Wigner functional for the photon number operator, and is done by first calculating $\langle \alpha_1 | \hat{A} | \alpha_2 \rangle$, where $\hat{A}$ is replaced by the number operator $\hat{n}$. The number operator is given by [21]

$$\hat{n} = \int \hat{a}^\dagger(\mathbf{k}) \hat{a}(\mathbf{k}) đ\mathbf{k}. \tag{3.52}$$

Calculating the inner product by using Eq. (3.45) [21]

$$\langle \alpha_1 | \hat{n} | \alpha_2 \rangle = \alpha_1^* \diamond \alpha_2 \exp\left(-\frac{1}{2}\|\alpha_1\|^2 - \frac{1}{2}\|\alpha_2\|^2 + \alpha_1^* \diamond \alpha_2\right). \tag{3.53}$$

Observe that there is a factor of $\alpha_1^* \diamond \alpha_2$ above, and substitution of it into Eq. (3.51) will not produce a convenient Gaussian functional to integrate over, as defined in Eq. (3.40). A generating functional, $\mathcal{G}$, is defined in order to remedy the situation [21]

$$\mathcal{G} = \exp\left(-\frac{1}{2}\|\alpha_1\|^2 - \frac{1}{2}\|\alpha_2\|^2 + J\alpha_1^* \diamond \alpha_2\right), \tag{3.54}$$

where J is a generating parameter such that [21]

$$\left.\frac{\partial \mathcal{G}}{\partial J}\right|_{J=1} = \langle \alpha_1 | \hat{n} | \alpha_2 \rangle. \tag{3.55}$$

Instead of substituting Eq. (3.53) into the Wigner functional, the generating functional can be substituted instead to facilitate the calculation. A generating Wigner functional is then calculated. A derivative with respect to J of the expression is taken, and setting $J = 0$ in order to get the Wigner

functional for the number operator [21]. Generating Wigner functionals are written in calligraphy

$$\begin{aligned}\mathcal{W}_{\mathcal{G}}[\alpha] &= N_0 \int \mathcal{G} \exp\Bigg(-2\|\alpha\|^2 + 2\alpha^* \diamond \alpha_1 + 2\alpha_2^* \diamond \alpha - \frac{1}{2}\|\alpha_1\|^2 \\ &\quad -\frac{1}{2}\|\alpha_2\|^2 - \alpha_2^* \diamond \alpha_1\Bigg) \mathcal{D}^\circ[\alpha_1, \alpha_2] \\ &= N_0 \int \exp\Bigg(-2\|\alpha\|^2 + 2\alpha^* \diamond \alpha_1 + 2\alpha_2^* \diamond \alpha - \frac{1}{2}\|\alpha_1\|^2 \\ &\quad -\frac{1}{2}\|\alpha_2\|^2 - \alpha_2^* \diamond \alpha_1 - \frac{1}{2}\|\alpha_1\|^2 - \frac{1}{2}\|\alpha_2\|^2 + J\alpha_1^* \diamond \alpha_2\Bigg) \mathcal{D}^\circ[\alpha_1, \alpha_2] \\ &= N_0 \int \exp\left(-\|\alpha_1\|^2 + 2\alpha^* \diamond \alpha_1 - \alpha_2^* \diamond \alpha_1 + J\alpha_1^* \diamond \alpha_2\right. \\ &\quad \left. +2\alpha_2^* \diamond \alpha - \|\alpha_2\|^2 - 2\|\alpha\|^2\right) \mathcal{D}^\circ[\alpha_1, \alpha_2].\end{aligned} \tag{3.56}$$

The functional integral is performed. The generating Wigner functional is brought into the form of the isotropic Gaussian functional given in Eq. (3.39). The integral over the complex field variable, α_1, is performed first

$$\begin{aligned}\mathcal{W}_{\mathcal{G}}[\alpha] &= N_0 \int \exp\left(-\alpha_1^* \diamond \mathbb{1} \diamond \alpha_1 - (\alpha_2^* - 2\alpha^*) \diamond \alpha_1 - \alpha_1^* \diamond (-J\alpha_2)\right. \\ &\quad \left. +2\alpha_2^* \diamond \alpha - \|\alpha_2\|^2 - 2\|\alpha\|^2\right) \mathcal{D}^\circ[\alpha_1, \alpha_2] \\ &= \frac{N_0}{\det\{\mathbb{1}\}} \int \exp\left((\alpha_2^* - 2\alpha^*) \diamond \mathbb{1} \diamond (-J\alpha_2)\right. \\ &\quad \left. +2\alpha_2^* \diamond \alpha - \|\alpha_2\|^2 - 2\|\alpha\|^2\right) \mathcal{D}^\circ[\alpha_2] \\ &= N_0 \int \exp\left(-\|\alpha_2\|^2 - J\alpha_2^* \diamond \alpha_2 + 2J\alpha^* \diamond \alpha_2 + 2\alpha_2^* \diamond \alpha\right. \\ &\quad \left. -2\|\alpha\|^2\right) \mathcal{D}^\circ[\alpha_2],\end{aligned} \tag{3.57}$$

P is the identity kernel and $c = 1$. The functional integration over α_2 produces [21]

$$\begin{aligned}\mathcal{W}_{\mathcal{G}}[\alpha] &= N_0 \int \exp\left(-\left(1+J\right)\alpha_2^* \diamond \alpha_2 - \left(-2J\alpha^*\right) \diamond \alpha_2 - \alpha_2^* \diamond \left(-2\alpha\right)\right. \\ &\quad \left. -2\|\alpha\|^2\right) \mathcal{D}^{\circ}[\alpha_2] \\ &= \frac{N_0}{\left(1+J\right)^{\Omega} \det\{\mathbb{1}\}} \exp\left(\frac{1}{1+J}\left(-2J\alpha^*\right) \diamond \left(-2\alpha\right) - 2\|\alpha\|^2\right) \\ &= \frac{N_0}{\left(1+J\right)^{\Omega}} \exp\left(\frac{4J}{1+J}\alpha^* \diamond \alpha - 2\|\alpha\|^2\right) \\ &= \frac{N_0}{\left(1+J\right)^{\Omega}} \exp\left(-2\left(\frac{1-J}{1+J}\right)\alpha^* \diamond \alpha\right),\end{aligned} \tag{3.58}$$

where $c = 1 + J$, and the P is once again the identity kernel. The overall factor of $\left(1+J\right)^{\Omega}$ originates due to the constant, c, as seen in Eq. (3.39). It is important to note that the above equation is a generating Wigner functional and to obtain its Wigner function, a derivative with respect to its generating parameter needs to be taken. To calculate the Wigner functional for the number operator [21]

$$W_{\hat{n}}[\alpha] = \left.\frac{\partial \mathcal{W}_{\mathcal{G}}[\alpha]}{\partial J}\right|_{J=1} = \|\alpha\|^2 - \frac{\Omega}{2}, \tag{3.59}$$

where $\Omega = \mathrm{tr}(\mathbb{1})$. Another example for the Wigner functional of an operator, which will be used in the next section, is the Wigner functional for the projection operator for a fixed spectrum. The proof is also given in [21], the calculation for the Wigner functional for the projection operator for a fixed spectrum, M, is very similar to the calculation shown above. Therefore, only key points of the calculation will be made. The Wigner functional for the projection operator $|n_M\rangle\langle n_M|$ is calculated. Naturally, following the coherent-state assisted Wigner functional approach, the generating Wigner functional is calculated [21]

$$\begin{aligned}\mathcal{K} &= \sum_n J^n \langle \alpha_1 | n_M \rangle \langle n_M | \alpha_2 \rangle \\ &= \exp\left(-\frac{1}{2}\|\alpha_1\|^2 - \frac{1}{2}\|\alpha_2\|^2 + J\alpha_1^* \diamond MM^* \diamond \alpha_2\right),\end{aligned} \tag{3.60}$$

where J is a generating parameter. The generating Wigner functional is calculated, where K is the generating parameter, and amounts to [21]

$$\tilde{\mathcal{W}} = \frac{N_0}{1+J} \exp\left(-2\|\alpha\|^2 + \frac{4J}{1+J}\alpha^* \diamond MM^* \diamond \alpha\right). \tag{3.61}$$

If the following operation is performed [21]

$$\frac{1}{n!}\frac{\partial^n \tilde{\mathcal{W}}}{\partial J^n}\bigg|_{J=0} = W_{Pn}, \tag{3.62}$$

then the Wigner functional for the projection operator for n photons in spectrum M is produced. The Wigner functional is represented as W_{Pn}.

3.3 Using Wigner functionals to calculate probabilities

The calculation of probabilities using Wigner functionals is presented. The probability for measuring a single photon in the spatial mode with spectrum M depending on spatial frequencies, detecting a single photon, and a verification check is considered. The Wigner functional for the state considered for the first two cases is given in Eq. (3.50), and the verification will model the state as a single photon in a spatial mode to verify whether a bucket detector would detect the photon with unit probability. The process of functional integration for the purpose of probability calculation is described and the types of Wigner functionals used for the calculation in certain scenarios are discussed.
The following generating Wigner functional for spectrum M is focused on, which was already introduced in section 3.2 [21]

$$\tilde{\mathcal{W}} = \frac{N_0}{1+J} \exp\left(-2\|\alpha\|^2 + \frac{4J}{1+J}\alpha^* \diamond MM^* \diamond \alpha\right). \tag{3.63}$$

A few probabilities are calculated using $\tilde{\mathcal{W}}$. The case where Eq. (3.63) is treated as the generating Wigner functional of the projection operator for a

single photon with spectrum M, is considered

$$\begin{aligned} W_{P1} = &\left[-\frac{N_0}{(1+J)^2} \exp\left(-2\|\alpha\|^2 + \frac{4J}{1+J} \alpha^* \diamond MM^* \diamond \alpha \right) \right. \\ &\left. + \frac{N_0 \alpha^* \diamond MM^* \diamond \alpha}{1+J} \frac{\partial}{\partial J} \left(\frac{4J}{1+J} \right) \exp\left(-2\|\alpha\|^2 + \frac{4J}{1+J} \alpha^* \diamond MM^* \diamond \alpha \right) \right] \Bigg|_{J=0} \\ &= -N_0 \exp\left(-2\|\alpha\|^2 \right) + 4N_0 \alpha^* \diamond MM^* \diamond \alpha \exp\left(-2\|\alpha\|^2 \right). \end{aligned} \tag{3.64}$$

The probability of measuring one photon with spectrum, M, is found by taking the trace of the product of the Wigner functional of the projection operator with the Wigner functional of an appropriate density operator

$$p_1 = \mathrm{tr}\left(W_{P1} W_{\hat{\rho}} \right), \tag{3.65}$$

where the Wigner functional for the state, $W_{\hat{\rho}}$, is

$$W_{\hat{\rho}}[\alpha] = N_0 \exp\left(-2\|\alpha - \beta\|^2 \right), \tag{3.66}$$

which is the Wigner functional for the coherent state given by Eq. (3.50) in the previous section, and β is called a parameter function, which is a point in functional phase space. The probability becomes

$$\begin{aligned} p_1 = &N_0^2 \,\mathrm{tr}\left(-\exp\left(-4\|\alpha\|^2 + 2\alpha^* \diamond \beta + 2\alpha \diamond \beta^* - 2\|\beta\|^2 \right) \right. \\ &\left. + 4\alpha^* \diamond MM^* \diamond \alpha \exp\left(-4\|\alpha\|^2 + 2\alpha^* \diamond \beta + 2\alpha \diamond \beta^* - 2\|\beta\|^2 \right) \right) \\ &= -N_0^2 \int \left(\exp\left(-4\|\alpha\|^2 + 2\alpha^* \diamond \beta + 2\alpha \diamond \beta^* - 2\|\beta\|^2 \right) \right) \mathcal{D}^\circ[\alpha] \\ &+ N_0^2 \int \left(4\alpha^* \diamond MM^* \diamond \alpha \exp\left(-4\|\alpha\|^2 + 2\alpha^* \diamond \beta + 2\alpha \diamond \beta^* - 2\|\beta\|^2 \right) \right) \mathcal{D}^\circ[\alpha]. \end{aligned} \tag{3.67}$$

The integral obtained from the trace is separated into two integrals. The probability is defined as $p_1 = p_1' + \tilde{p}_1$ where p_1' is the first summand, and $\tilde{p}_1$ is the second summand in Eq. (3.67). The generating functional approach is used for the second functional summand, which is called $\tilde{p}_{1G}$, in order to

absorb the coefficient of the exponent in the exponent

$$\begin{aligned}\tilde{p}_{1G}(K) &= N_0^2 \int \exp\left(-4\|\alpha\|^2 + 2\alpha^* \diamond \beta + 2\alpha \diamond \beta^* - 2\|\beta\|^2\right. \\ &\quad \left. +4K\alpha^* \diamond MM^* \diamond \alpha\right) \mathcal{D}^\circ[\alpha] \\ &= N_0^2 \int \exp\left(-4\alpha^* \diamond (\mathbb{1} - KMM^*) \diamond \alpha - \alpha^* \diamond (-2\beta)\right. \\ &\quad \left. -(-2\beta^*) \diamond \alpha - 2\|\beta\|^2\right) \mathcal{D}^\circ[\alpha] \\ &= \frac{1}{\det[\mathbb{1} - KMM^*]} \exp\left(\beta^* \diamond (\mathbb{1} - KMM^*)^{-1} \diamond \beta - 2\|\beta\|^2\right),\end{aligned} \tag{3.68}$$

where K is the generating parameter and

$$\tilde{p}_1 = \left.\frac{\partial \tilde{p}_{1G}}{\partial K}\right|_{K=0}. \tag{3.69}$$

The simplification of the kernel $(\mathbb{1} - KMM^*)^{-1}$ will be examined. It is assumed that the kernel has an inverse of the form $\mathbb{1} - cKMM^*$ where c is a constant [21]. The implication is

$$\begin{aligned} & (\mathbb{1} - KMM^*)^{-1} \diamond (\mathbb{1} - KMM^*) = \mathbb{1} \\ \implies\ & (\mathbb{1} - cKMM^*) \diamond (\mathbb{1} - KMM^*) = \mathbb{1} \\ \implies\ & -KMM^* - cKMM^* + cK^2 MM^* \diamond MM^* = 0. \end{aligned} \tag{3.70}$$

Taking the diamond product of the above equation with M^* on the left, and M on the right and remembering that the modes are normalized, i.e., $M^* \diamond M = 1$

$$\begin{aligned} KM^* \diamond MM^* \diamond M + cKM^* \diamond MM^* \diamond M - cK^2 M^* \diamond MM^* \diamond MM^* \diamond M = 0 \\ \implies K + cK + cK^2 = 0 \\ \implies c = \frac{1}{K-1}. \end{aligned} \tag{3.71}$$

The kernel can now be written as

$$(\mathbb{1} - KMM^*)^{-1} = \mathbb{1} - \frac{KMM^*}{K-1}. \tag{3.72}$$

$\tilde{p}_{1G}(K)$ becomes

$$\begin{aligned}\tilde{p}_{1G}(K) &= \frac{1}{\det[\mathbb{1} - KMM^*]} \exp\left(\beta^* \diamond \left(\mathbb{1} - \frac{KMM^*}{K-1}\right) \diamond \beta - 2\|\beta\|^2\right) \\ &= \frac{1}{\det[\mathbb{1} - KMM^*]} \exp\left(-\frac{K\beta^* \diamond MM^* \diamond \beta}{K-1} - \|\beta\|^2\right).\end{aligned} \tag{3.73}$$

Simplifying the determinant

$$\det[\mathbb{1} - KMM^*] = \exp\left[\mathrm{tr}\left(\ln_\diamond\left(\mathbb{1} - KMM^*\right)\right)\right], \tag{3.74}$$

where the trace over kernels is defined as [21]

$$\mathrm{tr}\left(H(\mathbf{k}, \mathbf{k}_1)\right) = \int H(\mathbf{k}', \mathbf{k}')đ\mathbf{k}'. \tag{3.75}$$

The natural logarithm is Taylor expanded as a stepping stone towards simplifying the determinant

$$\begin{aligned}\ln_\diamond\left(\mathbb{1} - KMM^*\right) &= -\sum_{n=1}^{\infty} \frac{1}{n} \left(KMM^*\right)^{n_\diamond} \\ &= -KMM^* - \frac{1}{2}K^2 MM^* \diamond MM^* - \ldots,\end{aligned} \tag{3.76}$$

and applying the trace,

$$\begin{aligned}\mathrm{tr}\left(\ln_\diamond\left(\mathbb{1} - KMM^*\right)\right) &= \mathrm{tr}\left(-KMM^* - \frac{1}{2}K^2 MM^* \diamond MM^* - \ldots\right) \\ &= -KM \diamond M^* - \frac{1}{2}\left(KM^* \diamond M\right)^2 - \ldots \\ &= -K - \frac{1}{2}K^2 - \ldots \\ &= -\sum_{n=1}^{\infty} \frac{K^n}{n} \\ &= \ln\left(1 - K\right).\end{aligned} \tag{3.77}$$

Therefore,

$$\det[\mathbb{1} - KMM^*] = 1 - K. \tag{3.78}$$

The determinant simplifies to the following convenient expression

$$\tilde{p}_{1G}(K) = \frac{1}{(1-K)} \exp\left(-\frac{K\beta^* \diamond MM^* \diamond \beta}{K-1} - \|\beta\|^2\right). \tag{3.79}$$

The calculation of $\tilde{p}_1$ is as follows

$$\begin{aligned}
\tilde{p}_1 &= \left.\frac{\partial \tilde{p}_{1G}}{\partial K}\right|_{K=0} \\
&= \left[-\frac{1}{(1-K)^2} \exp\left(-\frac{K\beta^* \diamond MM^* \diamond \beta}{K-1} - \|\beta\|^2\right)\right. \\
&\quad \left.-\frac{\beta^* \diamond MM^* \diamond \beta}{(1-K)} \left(\frac{(K-1)-K}{(K-1)^2}\right) \exp\left(-\frac{K\beta^* \diamond MM^* \diamond \beta}{K-1} - \|\beta\|^2\right)\right]\Bigg|_{K=0} \\
&= -\exp\left(-\|\beta\|^2\right) + \beta^* \diamond MM^* \diamond \beta \exp\left(-\|\beta\|^2\right).
\end{aligned} \tag{3.80}$$

The second remaining piece of p_1 is p_1'. Recall that $p_1 = p_1' + \tilde{p}_1$, and p_1' is given as

$$\begin{aligned}
p_1' &= -N_0^2 \int \exp\left(-4\|\alpha\|^2 - \alpha^* \diamond (-2\beta) - \alpha \diamond (-2\beta^*) - 2\|\beta\|^2\right) \mathcal{D}^\circ[\alpha] \\
&= -\exp\left(-\|\beta\|^2\right).
\end{aligned} \tag{3.81}$$

Therefore,

$$\begin{aligned}
p_1 &= p_1' + \tilde{p}_1 \\
&= -\exp\left(-\|\beta\|^2\right) - \exp\left(-\|\beta\|^2\right) + \beta^* \diamond MM^* \diamond \beta \exp\left(-\|\beta\|^2\right) \\
&= -2\exp\left(-\|\beta\|^2\right) + \beta^* \diamond MM^* \diamond \beta \exp\left(-\|\beta\|^2\right).
\end{aligned} \tag{3.82}$$

This concludes the calculation of the probability of obtaining one photon with spectrum M.

3.3.1 Detectors

If a system is measured with a detector, possibly a position resolving or bucket detector, the Wigner functional for such detectors can be modeled as follows

$$\mathcal{W}_D = \left(\frac{2}{1+J}\right)^{\mathrm{tr}(D)} \exp\left(-2\left(\frac{1-J}{1+J}\right)\alpha^* \diamond D \diamond \alpha\right), \tag{3.83}$$

where J is the generating parameter and $D = MM^*$, with $D = \mathbb{1}$ for the bucket detector. Eq. (3.83) was obtained from discussions and notes by my co-supervisor, FS Roux, as well as Eqs. (3.84), (3.86), (3.87), and (3.88). The above equation contains experimental information about the detectors [17]. For example, consider the CCD array or scanning detector for which the function M is defined as

$$M(\mathbf{k}_1, \omega, \mathbf{X}_0) = N_M h(\omega - \omega_d, \delta_d) \exp\left(-\frac{1}{4} w_0^2 |\mathbf{k}_1|^2 + i\mathbf{X}_0 \cdot \mathbf{k}_1\right), \tag{3.84}$$

where w_0 is the width of the Gaussian and will be regarded as the pixel size, $\mathbf{X}_0$ is the pixel position, $\mathbf{X}$ is the location at the height of the Gaussian, and

$$N_M = \sqrt{2\pi} w_0. \tag{3.85}$$

where

$$M^*(\mathbf{k}_1, \omega, \mathbf{X}_0) \diamond M(\mathbf{k}_1, \omega, \mathbf{X}_0) = \mathrm{tr}\,(D) = 1, \tag{3.86}$$

and

$$h(\omega - \omega_p, \delta_p) = \sqrt{\frac{\sqrt{2}}{\sqrt{\pi}\delta_p}} \exp\left(-\frac{(\omega - \omega_p)^2}{\delta_p^2}\right) \tag{3.87}$$

is a narrow function with a width of δ_p that represents the angular frequency and has the following property [20]

$$\frac{1}{2\pi} \int h^2(\omega - \omega_p, \delta_p) d\omega = 1. \tag{3.88}$$

To understand Eq. (3.84) in terms of spatial vectors, the inverse Fourier transforms can be taken which produces

$$m = \frac{4\pi N_M}{(2\pi)^2 w_0^2} \mathcal{F}_\omega^{-1}\{h(\omega - \omega_d, \delta_d)\} \exp\left(-\frac{|\mathbf{X}_0 + \mathbf{X}|^2}{w_0^2}\right), \tag{3.89}$$

where $\mathcal{F}_\omega^{-1}\{h(\omega - \omega_d, \delta_d)\}$ is the inverse Fourier transform over the narrow spectral function

$$\begin{aligned} &\mathcal{F}_\omega^{-1}\{h(\omega - \omega_d, \delta_d)\} \\ &= \frac{\delta_d}{2\pi} \sqrt{\frac{\pi\sqrt{2}}{\sqrt{\pi}\delta_d}} \exp\left(-\delta_d^2 t^2\right) \left[\cos(\omega_d t) + i \sin(\omega_d t)\right]. \end{aligned} \tag{3.90}$$

The following normalization condition also applies

$$\int m^* m dt d\mathbf{X} = 1, \tag{3.91}$$

where

$$m^* m = \frac{2}{\pi w_0^2} \exp\left(-\frac{2|\mathbf{X}_0 + \mathbf{X}|^2}{w_0^2}\right). \tag{3.92}$$

The equation above is shown without the inverse Fourier transform over the narrow spectral function for simplicity. Eq. (3.92) is the pixel sensitivity function illustrating the probability of detecting a photon if it is incident at $-\mathbf{X}$ within a radius of the pixel size, w_0. For our purposes in ghost imaging, the maximum of the pixel sensitivity function is set at $-\mathbf{X}$ since there is momentum entanglement involved. The signal and idler beams will have opposite momenta resulting in opposite locations of the signal and idler photons, i.e. if the idler photon is at $\mathbf{X}$, then the signal photon is at $-\mathbf{X}$.
A graphical depiction of Eq. (3.92) is shown in figure 3.1. Technically speaking, since the pixel was modeled as a Gaussian, the pixel area should be circular, instead of using the square grids as shown in figure 3.1. The technicality is ignored, since the main purpose of figure 3.1 is to illustrate that the detector provides transverse spatial information. The bucket detector will be modeled as $D = \mathbb{1}$. The main purpose of the bucket detector is to detect photons without any spatial resolution. Such a detector can be imagined as a single large pixel. Since there is no spatial resolution, the pixel position, $\mathbf{X}_0$, is not present for the bucket detector. Eq. (3.83) will be referred to as the detector generating Wigner functional. The detector Wigner functional for the detection of n photons can be obtained from Eq. (3.83) by

$$\left.\frac{\partial^n \mathcal{W}_D}{\partial J^n}\right|_{J=0} = W_{Dn}. \tag{3.93}$$

The derivative of the detector generating Wigner functional is taken, and the generating parameter is then set to 0 to obtain the Wigner functional for the detection of a single photon at $\mathbf{X}_0$

$$\begin{aligned} W_{D1} &= \left.\frac{\partial \mathcal{W}_D}{\partial J}\right|_{J=0} \\ &= -\operatorname{tr}(D) 2^{\operatorname{tr}(D)} \exp\left(-2\alpha^* \diamond D \diamond \alpha\right) \\ &\quad + 2^{\operatorname{tr}(D)+2} \alpha^* \diamond D \diamond \alpha \exp\left(-2\alpha^* \diamond D \diamond \alpha\right). \end{aligned} \tag{3.94}$$

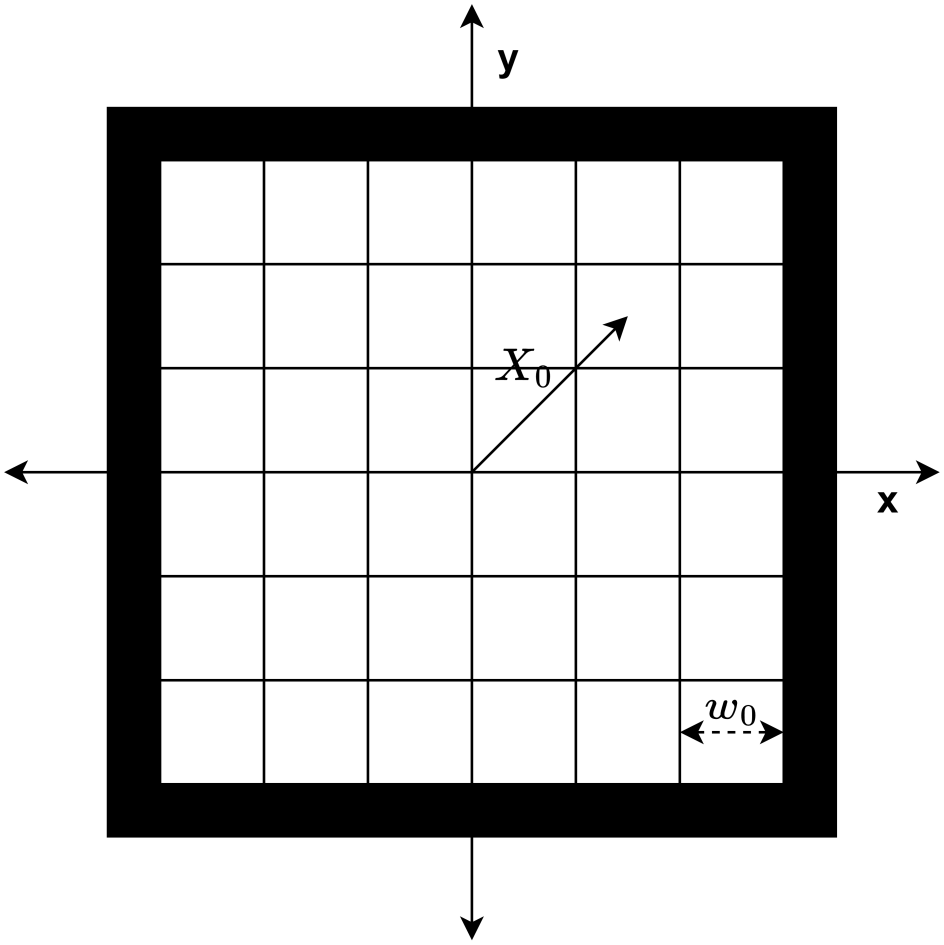

Figure 3.1: *An illustration of the CCD array with its pixels.*

Much like the case before, the trace over the product of W_{D1} with the Wigner functional of the state is performed in order to obtain the probability for detecting one photon, and is labeled as p_{D1}

$$\begin{aligned}
p_{D1} &= \operatorname{tr}\left(W_{D1}W_{\hat{\rho}}\right) \\
&= N_0 \operatorname{tr}\left[\left(-\operatorname{tr}(D)2^{\operatorname{tr}(D)}\exp\left(-2\alpha^*\diamond D\diamond\alpha\right)\right.\right. \\
&\left.\left.+2^{\operatorname{tr}(D)+2}\alpha^*\diamond D\diamond\alpha\exp\left(-2\alpha^*\diamond D\diamond\alpha\right)\right)\exp\left(-2\|\alpha-\beta\|^2\right)\right] \\
&= -\operatorname{tr}(D)2^{\operatorname{tr}(D)}N_0\int\exp\left(-2\alpha^*\diamond D\diamond\alpha-2\|\alpha\|^2+2\alpha^*\diamond\beta+2\alpha\diamond\beta^*\right. \\
&\left.-2\|\beta\|^2\right)\mathcal{D}^\circ[\alpha] \\
&+\int 4\alpha^*\diamond D\diamond\alpha\exp\left(-2\alpha^*\diamond D\diamond\alpha-2\|\alpha\|^2+2\alpha^*\diamond\beta+2\alpha\diamond\beta^*\right. \\
&\left.-2\|\beta\|^2\right)\mathcal{D}^\circ[\alpha].
\end{aligned} \tag{3.95}$$

The same strategy as before is used. Define $p_{D1} = p'_{D1} + \tilde{p}_{D1}$ where p'_{D1} is the first summand, and $\tilde{p}_{D1}$ is the second summand. Considering that the second summand uses the same generating functional approach, whereby

$$\tilde{p}_{D1} = \left.\frac{\partial\tilde{p}_{D1G}}{\partial J}\right|_{J=1}. \tag{3.96}$$

It follows that

$$\begin{aligned}
&\tilde{p}_{D1G} \\
&= -\int 2\exp\left(-2\alpha^*\diamond\left(JD+\mathbb{1}\right)\diamond\alpha-\alpha^*\diamond(-2\beta)-\alpha\diamond(-2\beta^*)\right. \\
&\left.-2\|\beta\|^2\right)\mathcal{D}^\circ[\alpha] \\
&= -\frac{2}{N_0\det\left[JD+\mathbb{1}\right]}\exp\left(2\beta^*\diamond\left(JD+\mathbb{1}\right)^{-1}\diamond\beta-2\|\beta\|^2\right).
\end{aligned} \tag{3.97}$$

Simplifying $(JD+\mathbb{1})^{-1}$ by assuming that $(JD+\mathbb{1})^{-1} = cJD+\mathbb{1}$, where c is a constant, it is possible to follow the same method as in Eq. (3.70) to obtain

$$\begin{aligned}
&(cJD+\mathbb{1})\diamond\left(JD+\mathbb{1}\right) = \mathbb{1} \\
\implies\ &D+cJD\diamond D+cD = 0.
\end{aligned} \tag{3.98}$$

The detector kernel, $D = MM^*$, is substituted, and considering the case where $M \diamond M^* = 1$

$$\begin{aligned} & (cJD + \mathbb{1}) \diamond (JD + \mathbb{1}) = \mathbb{1} \\ \implies & MM^* + cJMM^* + cMM^* = 0 \\ \implies & 1 + c(J+1) = 0 \\ \implies & c = -\frac{1}{J+1}. \end{aligned} \tag{3.99}$$

Therefore

$$(JD + \mathbb{1})^{-1} = \mathbb{1} - \frac{JD}{J+1}. \tag{3.100}$$

For the determinant, the same technique as for the previous calculation is applied, the result reads

$$\det[\mathbb{1} + JD] = 1 + J. \tag{3.101}$$

These results simplify $\tilde{p}_{D1G}$ to

$$\begin{aligned} & \tilde{p}_{D1G} \\ & = -\frac{2}{N_0 (1+J)} \exp\left(-\frac{2J}{J+1}\beta^* \diamond D \diamond \beta\right). \end{aligned} \tag{3.102}$$

Applying the derivative

$$\begin{aligned} \tilde{p}_{D1} &= \left.\frac{\partial \tilde{p}_{D1G}}{\partial J}\right|_{J=1} \\ &= \left[\frac{2}{N_0 (1+J)^2} \exp\left(-\frac{2J}{J+1}\beta^* \diamond D \diamond \beta\right)\right. \\ &\quad \left. + \frac{4\beta^* \diamond D \diamond \beta}{N_0 (1+J)} \left(\frac{2}{(J+1)^2}\right) \exp\left(-\frac{2J}{J+1}\beta^* \diamond D \diamond \beta\right)\right]\Bigg|_{J=1} \\ &= \frac{1}{2N_0} \exp\left(-\beta^* \diamond D \diamond \beta\right) + \frac{\beta^* \diamond D \diamond \beta}{N_0} \exp\left(-\beta^* \diamond D \diamond \beta\right). \end{aligned} \tag{3.103}$$

The calculation of p'_{D1} starts off as

$$\begin{aligned} p'_{D1} &= -\operatorname{tr}(D)2^{\operatorname{tr}(D)}N_0 \int \exp\left(-2\alpha^* \diamond D \diamond \alpha - 2\|\alpha\|^2 + 2\alpha^* \diamond \beta + 2\alpha \diamond \beta^* \right. \\ &\quad \left. -2\|\beta\|^2\right) \mathcal{D}^\circ[\alpha] \\ &= -\operatorname{tr}(D)2^{\operatorname{tr}(D)}N_0 \int \exp\left(-2\alpha^* \diamond (D+\mathbb{1}) \diamond \alpha - \alpha^* \diamond (-2\beta)\right. \\ &\quad \left. -\alpha \diamond (-2\beta^*) - 2\|\beta\|^2\right) \mathcal{D}^\circ[\alpha] \\ &= -\frac{\operatorname{tr}(D)2^{\operatorname{tr}(D)}}{\det\left[D+\mathbb{1}\right]} \exp\left(2\beta^* \diamond (D+\mathbb{1})^{-1} \diamond \beta - 2\|\beta\|^2\right), \end{aligned} \tag{3.104}$$

where $(D+\mathbb{1})^{-1}$ is simplified as

$$(D+\mathbb{1})^{-1} = \mathbb{1} - \frac{D}{2}, \tag{3.105}$$

the determinant reduces to

$$\det\left[D+\mathbb{1}\right] = 2. \tag{3.106}$$

The final result of p'_{D1} is calculated

$$\begin{aligned} p'_{D1} &= -\frac{\operatorname{tr}(D)2^{\operatorname{tr}(D)}}{2} \exp\left(2\beta^* \diamond \left(\mathbb{1} - \frac{D}{2}\right) \diamond \beta - 2\|\beta\|^2\right) \\ &= -\frac{\operatorname{tr}(D)2^{\operatorname{tr}(D)}}{2} \exp\left(-\beta^* \diamond D \diamond \beta\right). \end{aligned} \tag{3.107}$$

The case whereby Eq. (3.86) holds is considered. Finally, the probability of detecting one photon on the bucket detector is

$$\begin{aligned} p_{D1} &= p'_{D1} + \tilde{p}_{D1} \\ &= -\exp\left(-\beta^* \diamond D \diamond \beta\right) + \frac{1}{2N_0} \exp\left(-\beta^* \diamond D \diamond \beta\right) \\ &\quad + \frac{\beta^* \diamond D \diamond \beta}{N_0} \exp\left(-\beta^* \diamond D \diamond \beta\right). \end{aligned} \tag{3.108}$$

As a verification, the probability to detect a photon with density matrix $|n_M\rangle\langle n_M|$ for mode M is calculated, which should return 1. The starting

point is

$$
\begin{aligned}
p_s &= \operatorname{tr}\left(W_{D1}W_{\hat{\rho}}\right) \\
&= \operatorname{tr}\left(W_{D1}W_{P1}\right) \\
&= \operatorname{tr}\left[\left(-N_0\exp\left(-2\|\alpha\|^2\right)+4N_0\alpha^*\diamond D\diamond\alpha\exp\left(-2\|\alpha\|^2\right)\right)\right. \\
&\left.\left(-\operatorname{tr}(D)2^{\operatorname{tr}(D)}\exp\left(-2\alpha^*\diamond D\diamond\alpha\right)+2^{\operatorname{tr}(D)+2}\alpha^*\diamond D\diamond\alpha\exp\left(-2\alpha^*\diamond D\diamond\alpha\right)\right)\right] \\
&= \int\left[\operatorname{tr}(D)2^{\operatorname{tr}(D)}N_0\exp\left(-2\alpha^*\diamond D\diamond\alpha-2\|\alpha\|^2\right)\right. \\
&- 2^{\operatorname{tr}(D)+2}N_0\alpha^*\diamond D\diamond\alpha\exp\left(-2\alpha^*\diamond D\diamond\alpha-2\|\alpha\|^2\right) \\
&- \operatorname{tr}(D)2^{\operatorname{tr}(D)+2}N_0\alpha^*\diamond D\diamond\alpha\exp\left(-2\alpha^*\diamond D\diamond\alpha-2\|\alpha\|^2\right) \\
&\left.+2^{\operatorname{tr}(D)+4}N_0\left(\alpha^*\diamond D\diamond\alpha\right)^2\exp\left(-2\alpha^*\diamond D\diamond\alpha-2\|\alpha\|^2\right)\right]\mathcal{D}^\circ[\alpha].
\end{aligned}
\tag{3.109}
$$

The first few integrals are similar to the expression for p'_{D1} and $\tilde{p}_{D1}$ with $\beta = 0$. The expression can be rewritten as

$$
\begin{aligned}
p_s &= \operatorname{tr}(D)2^{\operatorname{tr}(D)-1}-(\operatorname{tr}(D)+1)2^{\operatorname{tr}(D)-1} \\
&+ 2^{\operatorname{tr}(D)+4}N_0\int\left(\alpha^*\diamond D\diamond\alpha\right)^2\exp\left(-2\alpha^*\diamond D\diamond\alpha-2\|\alpha\|^2\right)\mathcal{D}^\circ[\alpha].
\end{aligned}
\tag{3.110}
$$

For the remaining integral, observe the calculation for Eq. (3.111) whilst setting $\beta = 0$

$$
\begin{aligned}
&\tilde{p}_{D1G}(\beta=0) \\
&= -\int 2\exp\left(-2J\alpha^*\diamond D\diamond\alpha-2\alpha^*\diamond\alpha\right)\mathcal{D}^\circ[\alpha].
\end{aligned}
\tag{3.111}
$$

To obtain the integrand in Eq. (3.114), the following operation on Eq. (3.111) is performed

$$
-\frac{1}{8}\frac{\partial^2\tilde{p}_{D1G}(\beta=0)}{\partial J^2}\bigg|_{J=1}, \tag{3.112}
$$

which eases the calculation, since the first derivative of $\tilde{p}_{D1G}$ is already calculated, and is given in Eq. (3.103)

$$
\begin{aligned}
&\frac{\partial\tilde{p}_{D1G}(\beta=0)}{\partial J} = \frac{2}{N_0\left(1+J\right)^2} \\
\implies &\frac{\partial^2\tilde{p}_{D1G}(\beta=0)}{\partial J^2} = -\frac{4}{N_0\left(1+J\right)^3} \\
\implies &-\frac{1}{8}\frac{\partial^2\tilde{p}_{D1G}(\beta=0)}{\partial J^2}\bigg|_{J=1} = \frac{1}{16N_0}.
\end{aligned}
\tag{3.113}
$$

The probability, p_s, is reduced to

$$p_s = -2^{\mathrm{tr}(D)-1} + 2^{\mathrm{tr}(D)} = 2^{\mathrm{tr}(D)}(-2^{-1} + 1) = 2^{\mathrm{tr}(D)-1}. \tag{3.114}$$

Since the condition, $\mathrm{tr}(D) = 1$, has been acknowledged, it follows that $p_s = 1$. The verification works out as expected.

Chapter 4

SPDC in terms of Wigner functionals

The description of SPDC by means of Wigner functionals is based on an article entitled "Parametric down-conversion beyond the semiclassical approximation" [17]. In addition, the explanation and concepts in this chapter were pointed out to me by FS Roux in private, who had developed the Wigner functional formalism and applied it to SPDC.
The main goal is to obtain an equation describing the motion of light through the nonlinear SPDC (type I) crystal in the z direction, with a thickness of L. The infinitesimal propagation equation (IPE) is used, which was introduced in section 2.4. The IPE is defined in terms of the propagation distance, z. The Wigner functional version of the IPE is also introduced. After some simplifications, a functional differential equation will be produced, which depends on the Wigner functional for the state produced by SPDC, and will be called the evolution equation. The Wigner functional for the state produced by SPDC will be referred to as the Wigner functional for the SPDC state, and it will be solved by assuming an exponential functional as a solution, resulting in the Wigner functional for the SPDC state as a function of the propagation distance. Similar developments were made using the Moyal product to form an evolution equation [7] which allows a semi-classical expansion with the help of Planck's constant.
The IPE is given as [17]

$$i\hbar\frac{\mathrm{d}}{\mathrm{d}z}\hat{\rho}(z) = \left[\hat{P}_{\Delta}, \hat{\rho}(z)\right], \tag{4.1}$$

where $\hat{\rho}(z)$ is the state of light as a function of its propagation distance, the square brackets denote the commutator of the operators $\hat{P}_\Delta$, which is called the infinitesimal propagation operator (IPO) [17], and $\hat{\rho}(z)$. The IPO was introduced in section 2.4 and is repeated here for convenience. The IPO is given as [17]

$$\hat{P}_\Delta = \int V(\mathbf{k}, \mathbf{k}_1, \mathbf{k}_2, \omega, \omega_1, \omega_2)\hat{G}_p^\dagger(\mathbf{k}, \omega, z)\hat{G}_d(\mathbf{k}_1, \omega_1, z)\hat{G}_d(\mathbf{k}_2, \omega_2, z)đ\mathbf{k}đ\mathbf{k}_1đ\mathbf{k}_2 + h.c., \tag{4.2}$$

where $\mathbf{k}$ is a transverse wave vector, and

$$đ\mathbf{k} = \frac{d^2\mathbf{k}}{(2\pi)^3}d\omega. \tag{4.3}$$

The operators for the pump and down-converted fields are $\hat{G}_d(\mathbf{k}, \omega, z)$, and $\hat{G}_p(\mathbf{k}, \omega, z)$, respectively. The term *h.c.* stands for Hermitian conjugate, and $V(\mathbf{k}, \mathbf{k}_1, \mathbf{k}_2)$ is called a vertex kernel which depends on three transverse wave vectors and represents the interaction between the nonlinear crystal and the beams involved [17]

$$V(\mathbf{k}, \mathbf{k}_1, \mathbf{k}_2) = \frac{(2\pi)^3}{2}d_{ooe}\exp\left(i\Delta k_z z\right)\delta\left(\mathbf{k} - \mathbf{k}_1 - \mathbf{k}_2\right)\delta\left(\omega - \omega_1 - \omega_2\right), \tag{4.4}$$

where $d_{ooe} = 2\epsilon_0\chi^{(2)}_{abc}\eta^o_a\eta^o_b\eta^{e*}_c$ contains the polarization vectors and second order electric susceptibility, and Δk_z is the phase mismatch, which was provided in section 2.4. A simplified evolution equation is desired for a state of light written in terms of Wigner functionals. Such an equation is arrived at by simplifying the IPE in terms of Wigner functionals and substituting an exponential functional as an ansatz for a solution. Rewriting Eq. (4.1) with Wigner functionals yields

$$W_{i\hbar\frac{\mathrm{d}}{\mathrm{d}z}\hat{\rho}(z)}[\alpha, \beta](z) = W_{\left(\hat{P}_\Delta\hat{\rho}(z) - \hat{\rho}(z)\hat{P}_\Delta\right)}[\alpha, \beta]. \tag{4.5}$$

According to the definition of the coherent-state assisted Wigner functional provided in Eq. (3.51), it is possible to simplify the expression above

$$W_{i\hbar\frac{\mathrm{d}}{\mathrm{d}z}\hat{\rho}(z)}[\alpha, \beta](z) = i\hbar\frac{\mathrm{d}}{\mathrm{d}z}W_{\hat{\rho}(z)}[\alpha, \beta](z), \tag{4.6}$$

and

$$\begin{aligned} &W_{\left(\hat{P}_\Delta\hat{\rho}(z)-\hat{\rho}(z)\hat{P}_\Delta\right)}[\alpha,\beta] \\ &= W_{\hat{P}_\Delta\hat{\rho}(z)}[\alpha,\beta] - W_{\hat{\rho}(z)\hat{P}_\Delta}[\alpha,\beta] \\ &= W_{\hat{P}_\Delta}[\alpha,\beta] \star\star W_{\hat{\rho}}[\alpha,\beta](z) - W_{\hat{\rho}}[\alpha,\beta](z) \star\star W_{\hat{P}_\Delta}[\alpha,\beta], \end{aligned} \tag{4.7}$$

where $\star$ is an operation that combines Wigner functionals, called the star product, as explained in chapter 3. Recall that Eq. (3.15) is similar to the case above

$$W_{\hat{A}\hat{B}}[\alpha,\beta] = W_{\hat{A}}[\alpha,\beta] \star\star W_{\hat{B}}[\alpha,\beta], \tag{4.8}$$

where $\hat{A} = \hat{P}_\Delta$ and $\hat{B} = \hat{\rho}$. Due to the IPE, coherent-state assisted Wigner functional given in Eq. (3.51), and double star product, it was possible to obtain a Wigner functional version of the IPE [17]

$$\begin{aligned} &i\hbar\frac{\mathrm{d}}{\mathrm{d}z}W_{\hat{\rho}}[\alpha,\beta](z) \\ &= W_{\hat{P}_\Delta}[\alpha,\beta] \star\star W_{\hat{\rho}}[\alpha,\beta](z) - W_{\hat{\rho}}[\alpha,\beta](z) \star\star W_{\hat{P}_\Delta}[\alpha,\beta]. \end{aligned} \tag{4.9}$$

The functionals and fields involved are differentiable. The simplification of $W_{\hat{P}_\Delta}[\alpha,\beta]$ can get slightly complicated. Instead of evaluating the functional integrals directly, a generating functional is integrated over, and the appropriate derivatives are used. The advantage of the generating functional approach is so that the functional integral of the isotropic Gaussian, as defined in Eq. (3.39), can be used. The Wigner functional for the IPO is expressed as a generating functional $\mathcal{W}_\mathcal{G}[\alpha,\beta]$. An operator $\hat{\mathcal{C}}$, which is called the construction operator [17], is applied to the generating functional in order to get the Wigner functional for the IPO

$$W_{\hat{P}_\Delta}[\alpha,\beta] = \hat{\mathcal{C}}\mathcal{W}_\mathcal{G}[\alpha,\beta] \mid_{\mu_1=\mu_2^*=\eta_1=\eta_2^*=0}, \tag{4.10}$$

where μ and η are generating parameter fields, and the double coherent-state assisted Wigner functional is used for $\mathcal{W}_\mathcal{G}[\alpha,\beta]$, which was provided in Eq. (3.14). The generating functional idea here is similar to the one presented for calculating the Wigner functional for the number operator. The construction operator contains a kernel and derivatives of the parameter fields, which brings Eq. (4.11) to [17]

$$\begin{aligned} &i\hbar\frac{\mathrm{d}}{\mathrm{d}z}W_{\hat{\rho}}[\alpha,\beta](z) \\ &= \hat{\mathcal{C}}\left(\mathcal{W}_\mathcal{G}[\alpha,\beta] \star\star W_{\hat{\rho}}[\alpha,\beta](z) - W_{\hat{\rho}}[\alpha,\beta](z) \star\star \mathcal{W}_\mathcal{G}[\alpha,\beta]\right) \mid_{\mu_1=\mu_2^*=\eta_1=\eta_2^*=0}. \end{aligned} \tag{4.11}$$

4.1 Generating Wigner functional for the IPO

The generating Wigner functional for the infinitesimal propagation operator is calculated first, for this purpose, the coherent-state assisted approach is used and was provided in Eq. (3.51). Firstly the inner product of the IPO is taken with respect to coherent states, $\langle \alpha_1, \beta_1|$ and $|\alpha_2, \beta_2\rangle$, that uses the complex field variables α_1, β_1, α_2 and β_2 which will be integrated over. The coherent states serve as an over-complete basis that allows to express the creation and annihilation operators, $\hat{G}^\dagger(\mathbf{k}, \omega, z)$ and $\hat{G}(\mathbf{k}, \omega, z)$, in the IPO in a simple way. The Wigner functional for coherent states needs to be used twice to obtain the IPO in terms of Wigner functionals. The inner product produces

$$\langle \alpha_1, \beta_1| \hat{P}_\Delta |\alpha_2, \beta_2\rangle = \langle \alpha_1|\alpha_2\rangle \langle \beta_1|\beta_2\rangle \left(\beta_1^* \diamond T \diamond \diamond \alpha_2\alpha_2 + \alpha_1^*\alpha_1^* \diamond \diamond T^* \diamond \beta_2\right), \tag{4.12}$$

where $T = T(\mathbf{k}, \mathbf{k}_1, \mathbf{k}_2) = N'(\omega)N'(\omega_1)N'(\omega_2)V(\mathbf{k}, \mathbf{k}_1, \mathbf{k}_2, \omega, \omega_1, \omega_2)$, and the triple diamond product, which is associative, is

$$\begin{aligned} &\beta_1^* \diamond T \diamond \diamond \alpha_2\alpha_2 + \alpha_1^*\alpha_1^* \diamond \diamond T^* \diamond \beta_2 \\ &= \int (\beta_1^*(\mathbf{k})T(\mathbf{k}, \mathbf{k}_1, \mathbf{k}_2)\alpha_2(\mathbf{k}_1)\alpha_2(\mathbf{k}_2) \\ &+\alpha_1^*(\mathbf{k}_2)\alpha_1^*(\mathbf{k}_1)T^*(\mathbf{k}, \mathbf{k}_1, \mathbf{k}_2)\beta_2(\mathbf{k})) \, đ\mathbf{k}đ\mathbf{k}_1đ\mathbf{k}_2. \end{aligned} \tag{4.13}$$

The expression $\langle \alpha_1|\alpha_2\rangle \langle \beta_1|\beta_2\rangle$ is simplified, and produces

$$\begin{aligned} &\langle \alpha_1, \beta_1| \hat{P}_\Delta |\alpha_2, \beta_2\rangle = (\beta_1^* \diamond T \diamond \diamond \alpha_2\alpha_2 + \alpha_1^*\alpha_1^* \diamond \diamond T^* \diamond \beta_2) \\ &\times \exp\left(-\frac{1}{2}\|\alpha_1\|^2 - \frac{1}{2}\|\alpha_2\|^2 - \frac{1}{2}\|\beta_1\|^2 - \frac{1}{2}\|\beta_2\|^2 + \alpha_1^* \diamond \alpha_2 + \beta_1^* \diamond \beta_2\right). \end{aligned} \tag{4.14}$$

The reader is reminded that $T(\mathbf{k}, \mathbf{k}_1, \mathbf{k}_2)$ and $V(\mathbf{k}, \mathbf{k}_1, \mathbf{k}_2)$ are special types of kernels which are called vertex kernels. The kernels depend on three transverse wave vectors and can thus be diamond contracted three times. Eq. (4.14) needs to be brought into a form where the integral of the isotropic Gaussian, Eq. (3.39), can be used. Therefore, a generating functional approach is used. The generating functional for Eq. (4.14) is given by [17]

$$\begin{aligned} \mathcal{G}[\alpha_1, \alpha_2, \beta_1, \beta_2] = \exp\Bigg(&-\frac{1}{2}\|\alpha_1\|^2 - \frac{1}{2}\|\alpha_2\|^2 - \frac{1}{2}\|\beta_1\|^2 - \frac{1}{2}\|\beta_2\|^2 \\ &+ \alpha_1^* \diamond \alpha_2 + \beta_1^* \diamond \beta_2 + \alpha_1^* \diamond \mu_1 + \mu_2^* \diamond \alpha_2 + \beta_1^* \diamond \eta_1 + \eta_2^* \diamond \beta_2\Bigg). \end{aligned} \tag{4.15}$$

The generating functional for the inner-product of the IPO also depends on the generating parameter fields, μ, and η. However, the parameter dependence is ignored for simplicity. The construction operator is [17]

$$\hat{\mathcal{C}} = \frac{\delta}{\delta\eta_1} \diamond T \diamond \diamond \frac{\delta}{\delta\mu_2^*}\frac{\delta}{\delta\mu_2^*} + \frac{\delta}{\delta\mu_1}\frac{\delta}{\delta\mu_1} \diamond \diamond T^* \diamond \frac{\delta}{\delta\eta_2^*}. \tag{4.16}$$

In terms of integrals, the construction operator will have the form

$$\begin{aligned}\hat{\mathcal{C}} = \int \Bigg(&\frac{\delta}{\delta\eta_1(\mathbf{k}')} T(\mathbf{k}', \mathbf{k}_1', \mathbf{k}_2') \frac{\delta}{\delta\mu_2^*(\mathbf{k}_1')}\frac{\delta}{\delta\mu_2^*(\mathbf{k}_2')} \\ &+ \frac{\delta}{\delta\mu_1(\mathbf{k}_2')}\frac{\delta}{\delta\mu_1(\mathbf{k}_1')} T^*(\mathbf{k}', \mathbf{k}_1', \mathbf{k}_2') \frac{\delta}{\delta\eta_2^*(\mathbf{k}')} \Bigg) đ\mathbf{k}' đ\mathbf{k}_1' đ\mathbf{k}_2'.\end{aligned} \tag{4.17}$$

It is possible to check that $\langle \alpha_1, \beta_1 | \, \hat{P}_\Delta \, | \alpha_2, \beta_2 \rangle = \hat{\mathcal{C}}\mathcal{G} \mid_{\mu_1 = \mu_2^* = \eta_1 = \eta_2^* = 0}$, since the generating functional for the inner-product of the IPO and the construction operator is available. $\mathcal{G}$ is convenient for functional integration using complex fields. As mentioned before, the coherent-state assisted Wigner functional is used twice. The first two functional integrations will be carried out in detail over α_1 and α_2, which follows from the Wigner functional for the coherent-state assisted approach in Eq. (3.10), and is considered below

$$\begin{aligned}\tilde{\mathcal{W}}_{\mathcal{G}}[\alpha, \beta_1, \beta_2] &= N_0 \int \exp\Bigg(-2\|\alpha\|^2 + 2\alpha^* \diamond \alpha_1 + 2\alpha_2^* \diamond \alpha - \frac{1}{2}\|\alpha_1\|^2 \\ &- \frac{1}{2}\|\alpha_2\|^2 - \alpha_2^* \diamond \alpha_1 \Bigg) \mathcal{G}[\alpha_1, \alpha_2, \beta_1, \beta_2] \mathcal{D}^\circ[\alpha_1, \alpha_2] \\ &= N_0 \int \exp\big(-2\|\alpha\|^2 + 2\alpha^* \diamond \alpha_1 + 2\alpha_2^* \diamond \alpha - \|\alpha_1\|^2 \\ &- \|\alpha_2\|^2 - \alpha_2^* \diamond \alpha_1 - \frac{1}{2}\|\beta_1\|^2 - \frac{1}{2}\|\beta_2\|^2 + \alpha_1^* \diamond \alpha_2 \\ &+ \beta_1^* \diamond \beta_2 + \alpha_1^* \diamond \mu_1 + \mu_2^* \diamond \alpha_2 + \beta_1^* \diamond \eta_1 + \eta_2^* \diamond \beta_2 \Bigg) \mathcal{D}^\circ[\alpha_1, \alpha_2] \\ &= N_0 \exp\Bigg(-2\|\alpha\|^2 - \frac{1}{2}\|\beta_1\|^2 - \frac{1}{2}\|\beta_2\|^2 + \beta_1^* \diamond \beta_2 + \beta_1^* \diamond \eta_1 + \eta_2^* \diamond \beta_2 \Bigg) \\ &\times \int \exp\big(-\alpha_1^* \diamond \alpha_1 - \alpha_1^* \diamond (-\alpha_2 - \mu_1) - (\alpha_2^* - 2\alpha^*) \diamond \alpha_1 - \|\alpha_2\|^2 \\ &+ 2\alpha_2^* \diamond \alpha + \mu_2^* \diamond \alpha_2 \big) \mathcal{D}^\circ[\alpha_1, \alpha_2],\end{aligned} \tag{4.18}$$

where $\tilde{\mathcal{W}}_{\mathcal{G}}[\alpha,\beta_1,\beta_2]$ only contains the first Wigner functional for the coherent-state assisted approach, applying it a second time for β_1 and β_2 will produce $\mathcal{W}_{\mathcal{G}}[\alpha,\beta]$. It is now possible to use Eq. (3.39) to perform the integral over α_1, where the kernel equals to the identity kernel

$$
\begin{aligned}
&\tilde{\mathcal{W}}_{\mathcal{G}}[\alpha,\beta_1,\beta_2] \\
&= N_0 \exp\left(-2\|\alpha\|^2 - \frac{1}{2}\|\beta_1\|^2 - \frac{1}{2}\|\beta_2\|^2 + \beta_1^* \diamond \beta_2 + \beta_1^* \diamond \eta_1 + \eta_2^* \diamond \beta_2\right) \\
&\times \int \exp\left((2\alpha^* - \alpha_2^*) \diamond (\alpha_2 + \mu_1) - \|\alpha_2\|^2 + 2\alpha_2^* \diamond \alpha + \mu_2^* \diamond \alpha_2\right) \mathcal{D}^\circ[\alpha_2] \\
&= N_0 \exp\left(-2\|\alpha\|^2 - \frac{1}{2}\|\beta_1\|^2 - \frac{1}{2}\|\beta_2\|^2 + \beta_1^* \diamond \beta_2 + \beta_1^* \diamond \eta_1 + \eta_2^* \diamond \beta_2\right) \\
&\times \int \exp\left(2\alpha^* \diamond \alpha_2 - 2\alpha_2^* \diamond \alpha_2 - \alpha_2^* \diamond \mu_1 + 2\alpha_2^* \diamond \alpha + \mu_2^* \diamond \alpha_2\right. \\
&\left. + 2\alpha^* \diamond \mu_1\right) \mathcal{D}^\circ[\alpha_2] \\
&= N_0 \exp\left(-2\|\alpha\|^2 - \frac{1}{2}\|\beta_1\|^2 - \frac{1}{2}\|\beta_2\|^2 + \beta_1^* \diamond \beta_2 + \beta_1^* \diamond \eta_1 + \eta_2^* \diamond \beta_2\right) \\
&\times \int \exp\left(-2\alpha_2^* \diamond \alpha_2 - \alpha_2^* \diamond (\mu_1 - 2\alpha) - (-\mu_2^* - 2\alpha^*) \diamond \alpha_2\right. \\
&\left. + 2\alpha^* \diamond \mu_1\right) \mathcal{D}^\circ[\alpha_2] \\
&= \exp\left(-2\|\alpha\|^2 - \frac{1}{2}\|\beta_1\|^2 - \frac{1}{2}\|\beta_2\|^2 + \beta_1^* \diamond \beta_2 + \beta_1^* \diamond \eta_1 + \eta_2^* \diamond \beta_2\right. \\
&\left. + 2\alpha^* \diamond \mu_1\right) \exp\left(\frac{1}{2}(\mu_2^* + 2\alpha^*) \diamond (2\alpha - \mu_1)\right) \\
&= \exp\left(-\frac{1}{2}\|\beta_1\|^2 - \frac{1}{2}\|\beta_2\|^2 + \beta_1^* \diamond \beta_2 + \beta_1^* \diamond \eta_1 + \eta_2^* \diamond \beta_2 + \alpha^* \diamond \mu_1\right. \\
&\left. + \mu_2^* \diamond \alpha - \frac{1}{2}\mu_2^* \diamond \mu_1\right).
\end{aligned}
\tag{4.19}
$$

The IPO is partially transformed into a generating Wigner functional. All that is left is to repeat the process for the complex field variables, β_1 and β_2. The calculation is performed step by step below, noting that the coherent-

state assisted Wigner functional in Eq. (3.10) is used once again

$$
\begin{aligned}
&\mathcal{W}_{\mathcal{G}}[\alpha,\beta] = N_0 \int \exp\left(-2\|\beta\|^2 + 2\beta^* \diamond \beta_1 + 2\beta_2^* \diamond \beta - \frac{1}{2}\|\beta_1\|^2\right. \\
&\left. -\frac{1}{2}\|\beta_2\|^2 - \beta_2^* \diamond \beta_1\right) \tilde{\mathcal{W}}_{\mathcal{G}}[\alpha,\beta_1,\beta_2]\mathcal{D}^{\circ}[\beta_1,\beta_2] \\
&= N_0 \exp\left(\alpha^* \diamond \mu_1 + \mu_2^* \diamond \alpha - \frac{1}{2}\mu_2^* \diamond \mu_1 - 2\|\beta\|^2\right) \\
&\times \int \exp\left(-\|\beta_1\|^2 + 2\beta^* \diamond \beta_1 - \beta_2^* \diamond \beta_1 + \beta_1^* \diamond \beta_2 + \beta_1^* \diamond \eta_1\right. \\
&\left. +2\beta_2^* \diamond \beta - \|\beta_2\|^2 + \eta_2^* \diamond \beta_2\right) \mathcal{D}^{\circ}[\beta_1,\beta_2] \\
&= N_0 \exp\left(\alpha^* \diamond \mu_1 + \mu_2^* \diamond \alpha - \frac{1}{2}\mu_2^* \diamond \mu_1 - 2\|\beta\|^2\right) \\
&\times \int \exp\left(-\beta_1^* \diamond \beta_1 - \beta_1^* \diamond \left(-\beta_2 - \eta_1\right) - \left(\beta_2^* - 2\beta^*\right) \diamond \beta_1\right. \\
&\left. +2\beta_2^* \diamond \beta - \|\beta_2\|^2 + \eta_2^* \diamond \beta_2\right) \mathcal{D}^{\circ}[\beta_1,\beta_2] \\
&= N_0 \exp\left(\alpha^* \diamond \mu_1 + \mu_2^* \diamond \alpha - \frac{1}{2}\mu_2^* \diamond \mu_1 - 2\|\beta\|^2\right) \\
&\times \int \exp\left(\left(\beta_2^* - 2\beta^*\right) \diamond \left(-\beta_2 - \eta_1\right) + 2\beta_2^* \diamond \beta - \|\beta_2\|^2 + \eta_2^* \diamond \beta_2\right) \mathcal{D}^{\circ}[\beta_2] \\
&= N_0 \exp\left(\alpha^* \diamond \mu_1 + \mu_2^* \diamond \alpha - \frac{1}{2}\mu_2^* \diamond \mu_1 - 2\|\beta\|^2 + 2\beta^* \diamond \eta_1\right) \\
&\times \int \exp\left(-2\beta_2^* \diamond \beta_2 - \beta_2^* \diamond \eta_1 + 2\beta_2^* \diamond \beta + \eta_2^* \diamond \beta_2 + 2\beta^* \diamond \beta_2\right) \mathcal{D}^{\circ}[\beta_2] \\
&= N_0 \exp\left(\alpha^* \diamond \mu_1 + \mu_2^* \diamond \alpha - \frac{1}{2}\mu_2^* \diamond \mu_1 - 2\|\beta\|^2 + 2\beta^* \diamond \eta_1\right) \\
&\times \int \exp\left(-2\beta_2^* \diamond \beta_2 - \beta_2^* \diamond \left(\eta_1 - 2\beta\right) - \left(-\eta_2^* - 2\beta^*\right) \diamond \beta_2\right) \mathcal{D}^{\circ}[\beta_2] \\
&= \exp\left(\alpha^* \diamond \mu_1 + \mu_2^* \diamond \alpha - \frac{1}{2}\mu_2^* \diamond \mu_1 - 2\|\beta\|^2 + 2\beta^* \diamond \eta_1\right. \\
&\left. +\frac{1}{2}\left(\eta_2^* + 2\beta^*\right) \diamond \left(2\beta - \eta_1\right)\right) \\
&= \exp\left(\alpha^* \diamond \mu_1 + \mu_2^* \diamond \alpha - \frac{1}{2}\mu_2^* \diamond \mu_1 + \beta^* \diamond \eta_1 + \eta_2^* \diamond \beta - \frac{1}{2}\eta_2^* \diamond \eta_1\right).
\end{aligned}
\tag{4.20}
$$

where $\mathcal{W}_{\mathcal{G}}[\alpha,\beta]$ is the generating Wigner functional for the IPO, which can be seen in Eq. (4.10). The calculation for the generating Wigner functional of the IPO is concluded. It has been proven that [17]

$$\mathcal{W}_{\mathcal{G}}[\alpha,\beta]=\exp\left(\alpha^{*}\diamond\mu_{1}+\mu_{2}^{*}\diamond\alpha-\frac{1}{2}\mu_{2}^{*}\diamond\mu_{1}+\beta^{*}\diamond\eta_{1}+\eta_{2}^{*}\diamond\beta-\frac{1}{2}\eta_{2}^{*}\diamond\eta_{1}\right). \tag{4.21}$$

By means of the generation functional and the construction operator, the Wigner functional for the infinitesimal propagation operator can be obtained

$$W_{\hat{P}_{\Delta}}[\alpha,\beta]=\hat{\mathcal{C}}\mathcal{W}_{\mathcal{G}}[\alpha,\beta]\mid_{\mu_{1}=\mu_{2}^{*}=\eta_{1}=\eta_{2}^{*}=0}, \tag{4.22}$$

where $W_{\hat{P}_{\Delta}}[\alpha,\beta]$ is the Wigner functional for the IPO. To summarize what was done, a generating functional for the inner-product of the IPO with the pump and down-converted fields was calculated. The generating functional had a Gaussian form which was convenient for functional integration. The coherent-state assisted Wigner functional was used twice to obtain the generating Wigner functional for the IPO. The coherent-state assisted Wigner functional was used twice due to the IPO's dependence on the pump and down-converted fields. After that, the generating Wigner functional for the IPO simplifies to Eq. (4.21).

4.2 Wigner functional for the IPO

Since the calculation of the Wigner functional for the IPO is done, all that is left to do is to calculate the double star product of $\mathcal{W}_{\mathcal{G}}[\alpha,\beta]$ with $W_{\hat{\rho}}[\alpha,\beta](z)$ and $W_{\hat{\rho}}[\alpha,\beta](z)$ with $\mathcal{W}_{\mathcal{G}}[\alpha,\beta]$. Note that both $W_{\hat{\rho}}[\alpha,\beta](z)$, and $\mathcal{W}_{\mathcal{G}}[\alpha,\beta]$ are functionals of two complex field variables each. Thus, the star product is implemented twice. One star product belongs to α, and the other belongs to β. The star product was explained in chapter 3. The star product for two Wigner functionals is written in terms of complex field variables

$$\begin{aligned}W_{\hat{A}\hat{B}}&=W_{\hat{A}}\star W_{\hat{B}}\\&=N_{0}^{2}\int W_{\hat{A}}\left[\alpha-\alpha_{1}\right]W_{\hat{B}}\left[\alpha-\alpha_{2}\right]\exp\left(2\alpha_{1}^{*}\diamond\alpha_{2}-2\alpha_{2}^{*}\diamond\alpha_{1}\right)\mathcal{D}^{\circ}[\alpha_{1}]\mathcal{D}^{\circ}[\alpha_{2}].\end{aligned} \tag{4.23}$$

It is shown in appendix A, where the starting point was the star product of two Wigner functionals written in terms of the position and momentum

fields, q and p. Setting $W_{\hat{A}} = \mathcal{W}_{\mathcal{G}}[\alpha, \beta]$, and $W_{\hat{B}} = W_{\hat{\rho}}$, the star product is applied on the complex field α

$$
\begin{aligned}
&\mathcal{W}_{\mathcal{G}}[\alpha,\beta] \star W_{\hat{\rho}}[\alpha,\beta] \\
&= N_0^2 \int W_{\mathcal{G}}\left[\alpha-\alpha_1,\beta\right] W_{\hat{\rho}}\left[\alpha-\alpha_2,\beta\right] \exp\left(2\alpha_1^* \diamond \alpha_2 - 2\alpha_2^* \diamond \alpha_1\right) \mathcal{D}^{\circ}[\alpha_1]\mathcal{D}^{\circ}[\alpha_2] \\
&= N_0^2 \int W_{\hat{\rho}}\left[\alpha-\alpha_2,\beta\right] \exp\Bigg(2\alpha_1^* \diamond \alpha_2 - 2\alpha_2^* \diamond \alpha_1 + (\alpha^* - \alpha_1^*) \diamond \mu_1 \\
&+\mu_2^* \diamond (\alpha-\alpha_1) - \frac{1}{2}\mu_2^* \diamond \mu_1 + \beta^* \diamond \eta_1 + \eta_2^* \diamond \beta - \frac{1}{2}\eta_2^* \diamond \eta_1\Bigg) \mathcal{D}^{\circ}[\alpha_1]\mathcal{D}^{\circ}[\alpha_2] \\
&= N_0^2 \int W_{\hat{\rho}}\left[\alpha-\alpha_2,\beta\right] \exp\Bigg(- \alpha_1^* \diamond (\mu_1 - 2\alpha_2) + (-2\alpha_2^* - \mu_2^*) \diamond \alpha_1 \\
&+\alpha^* \diamond \mu_1 + \mu_2^* \diamond \alpha - \frac{1}{2}\mu_2^* \diamond \mu_1 + \beta^* \diamond \eta_1 + \eta_2^* \diamond \beta - \frac{1}{2}\eta_2^* \diamond \eta_1\Bigg) \mathcal{D}^{\circ}[\alpha_1]\mathcal{D}^{\circ}[\alpha_2].
\end{aligned}
\tag{4.24}
$$

A result derived in appendix C, Eq. (C.8), which contains delta functionals is now used and removes the functional integrals above

$$
\begin{aligned}
&= W_{\hat{\rho}}\left[\alpha^* + \frac{1}{2}\mu_2^*, \alpha - \frac{1}{2}\mu_1, \beta\right] \exp\Bigg(\alpha^* \diamond \mu_1 + \mu_2^* \diamond \alpha - \frac{1}{2}\mu_2^* \diamond \mu_1 \\
&+\beta^* \diamond \eta_1 + \eta_2^* \diamond \beta - \frac{1}{2}\eta_2^* \diamond \eta_1\Bigg) \\
&= \mathcal{W}_{\mathcal{G}}[\alpha,\beta] W_{\hat{\rho}}\left[\alpha^* + \frac{1}{2}\mu_2^*, \alpha - \frac{1}{2}\mu_1, \beta\right].
\end{aligned}
\tag{4.25}
$$

The first star product is completed. The second star product, which is over β, is of interest below

$$\begin{aligned}
&\mathcal{W}_{\mathcal{G}}[\alpha,\beta]\star\star W_{\hat{\rho}}[\alpha,\beta]\\
&=N_0^2\int\mathcal{W}_{\mathcal{G}}\left[\alpha,\beta-\beta_1\right]W_{\hat{\rho}}\left[\alpha^*+\frac{1}{2}\mu_2^*,\alpha-\frac{1}{2}\mu_1,\beta-\beta_2\right]\\
&\times\exp\left(2\beta_1^*\diamond\beta_2-2\beta_2^*\diamond\beta_1\right)\mathcal{D}^{\circ}[\beta_1]\mathcal{D}^{\circ}[\beta_2]\\
&=N_0^2\int W_{\hat{\rho}}\left[\alpha^*+\frac{1}{2}\mu_2^*,\alpha-\frac{1}{2}\mu_1,\beta-\beta_2\right]\exp\Bigg(\alpha^*\diamond\mu_1+\mu_2^*\diamond\alpha-\frac{1}{2}\mu_2^*\diamond\mu_1\\
&+(\beta^*-\beta_1^*)\diamond\eta_1+\eta_2^*\diamond(\beta-\beta_1)-\frac{1}{2}\eta_2^*\diamond\eta_1+2\beta_1^*\diamond\beta_2-2\beta_2^*\diamond\beta_1\Bigg)\\
&\times\mathcal{D}^{\circ}[\beta_1]\mathcal{D}^{\circ}[\beta_2].
\end{aligned}\tag{4.26}$$

The above equation is obtained by using Eqs. (4.23) and (4.24).

$$\begin{aligned}
&\mathcal{W}_{\mathcal{G}}[\alpha,\beta]\star\star W_{\hat{\rho}}[\alpha,\beta]\\
&=N_0^2\int W_{\hat{\rho}}\left[\alpha^*+\frac{1}{2}\mu_2^*,\alpha-\frac{1}{2}\mu_1,\beta-\beta_2\right]\exp\Bigg(\alpha^*\diamond\mu_1+\mu_2^*\diamond\alpha-\frac{1}{2}\mu_2^*\diamond\mu_1\\
&+(-\eta_2^*-2\beta_2^*)\diamond\beta_1-\beta_1^*\diamond(\eta_1-2\beta_2)-\frac{1}{2}\eta_2^*\diamond\eta_1+\beta^*\diamond\eta_1+\eta_2^*\diamond\beta\Bigg)\\
&\times\mathcal{D}^{\circ}[\beta_1]\mathcal{D}^{\circ}[\beta_2]\\
&=W_{\hat{\rho}}\left[\alpha^*+\frac{1}{2}\mu_2^*,\alpha-\frac{1}{2}\mu_1,\beta^*+\frac{1}{2}\eta_2^*,\beta-\frac{1}{2}\eta_1\right]\exp\Bigg(\alpha^*\diamond\mu_1+\mu_2^*\diamond\alpha\\
&-\frac{1}{2}\mu_2^*\diamond\mu_1-\frac{1}{2}\eta_2^*\diamond\eta_1+\beta^*\diamond\eta_1+\eta_2^*\diamond\beta\Bigg)\\
&=W_{\hat{\rho}}\left[\alpha^*+\frac{1}{2}\mu_2^*,\alpha-\frac{1}{2}\mu_1,\beta^*+\frac{1}{2}\eta_2^*,\beta-\frac{1}{2}\eta_1\right]\mathcal{W}_{\mathcal{G}}[\alpha,\beta].
\end{aligned}\tag{4.27}$$

Using the same technique, it can be shown that

$$\begin{aligned}
&W_{\hat{\rho}}[\alpha,\beta]\star\star\mathcal{W}_{\mathcal{G}}[\alpha,\beta]\\
&=W_{\hat{\rho}}\left[\alpha^*-\frac{1}{2}\mu_2^*,\alpha+\frac{1}{2}\mu_1,\beta^*-\frac{1}{2}\eta_2^*,\beta+\frac{1}{2}\eta_1\right]\mathcal{W}_{\mathcal{G}}[\alpha,\beta].
\end{aligned}\tag{4.28}$$

Armed with the star products, construction operator, and the IPE in terms of Wigner functionals, the main goal of the chapter is resumed [17]

$$
\begin{aligned}
&i\hbar\frac{\mathrm{d}}{\mathrm{d}z}W_{\hat{\rho}}[\alpha,\beta](z)\\
&=\hat{\mathcal{C}}\left(\mathcal{W}_{\mathcal{G}}[\alpha,\beta]\star\star W_{\hat{\rho}}[\alpha,\beta](z)-W_{\hat{\rho}}[\alpha,\beta](z)\star\star\mathcal{W}_{\mathcal{G}}[\alpha,\beta]\right)|_{\mu_1=\mu_2^*=\eta_1=\eta_2^*=0}\\
&=\hat{\mathcal{C}}\left(W_{\hat{\rho}}\left[\alpha^*+\frac{1}{2}\mu_2^*,\alpha-\frac{1}{2}\mu_1,\beta^*+\frac{1}{2}\eta_2^*,\beta-\frac{1}{2}\eta_1\right]\mathcal{W}_{\mathcal{G}}[\alpha,\beta]\right.\\
&\left.-W_{\hat{\rho}}\left[\alpha^*-\frac{1}{2}\mu_2^*,\alpha+\frac{1}{2}\mu_1,\beta^*-\frac{1}{2}\eta_2^*,\beta+\frac{1}{2}\eta_1\right]\mathcal{W}_{\mathcal{G}}[\alpha,\beta]\right)|_{\mu_1=\mu_2^*=\eta_1=\eta_2^*=0}.
\end{aligned}
\tag{4.29}
$$

From this point onwards, most of the expressions were taken from the notes of my co-supervisor, FS Roux, which was shared in private communication. The construction operator can be evaluated, and the expression simplifies to [17]

$$
\begin{aligned}
&i\hbar\frac{\mathrm{d}}{\mathrm{d}z}W_{\hat{\rho}}[\alpha,\beta](z)\\
&=2\beta^*\diamond T\diamond\diamond\alpha\frac{\delta W_{\hat{\rho}}}{\delta\alpha^*}-\frac{\delta W_{\hat{\rho}}}{\delta\beta}\diamond T\diamond\diamond\alpha\alpha-\frac{1}{4}\frac{\delta^3 W_{\hat{\rho}}}{\delta\beta\delta\alpha^*\delta\alpha^*}\diamond\diamond\diamond T\\
&-2\frac{\delta W_{\hat{\rho}}}{\delta\alpha}\alpha^*\diamond\diamond T^*\diamond\beta+\alpha^*\alpha^*\diamond\diamond T^*\diamond\frac{\delta W_{\hat{\rho}}}{\delta\beta^*}+\frac{1}{4}\frac{\delta^3 W_{\hat{\rho}}}{\delta\beta^*\delta\alpha\delta\alpha}\diamond\diamond\diamond T^*.
\end{aligned}
\tag{4.30}
$$

Once again, the equation is written in terms of integrals [17]

$$
\begin{aligned}
&i\hbar\frac{\mathrm{d}}{\mathrm{d}z}W_{\hat{\rho}}[\alpha,\beta](z)\\
&=\int\left[2\beta^*(\mathbf{k}_3)T(\mathbf{k}_1,\mathbf{k}_2,\mathbf{k}_3)\alpha(\mathbf{k}_1)\frac{\delta W_{\hat{\rho}}}{\delta\alpha^*(\mathbf{k}_2)}-\frac{\delta W_{\hat{\rho}}}{\delta\beta(\mathbf{k}_3)}T(\mathbf{k}_1,\mathbf{k}_2,\mathbf{k}_3)\alpha(\mathbf{k}_1)\alpha(\mathbf{k}_2)\right.\\
&-\frac{1}{4}\frac{\delta^3 W_{\hat{\rho}}}{\delta\beta(\mathbf{k}_3)\delta\alpha^*(\mathbf{k}_1)\delta\alpha^*(\mathbf{k}_2)}T(\mathbf{k}_1,\mathbf{k}_2,\mathbf{k}_3)-2\frac{\delta W_{\hat{\rho}}}{\delta\alpha(\mathbf{k}_1)}\alpha^*(\mathbf{k}_2)T^*(\mathbf{k}_1,\mathbf{k}_2,\mathbf{k}_3)\beta(\mathbf{k}_3)\\
&+\alpha^*(\mathbf{k}_1)\alpha^*(\mathbf{k}_2)T^*(\mathbf{k}_1,\mathbf{k}_2,\mathbf{k}_3)\frac{\delta W_{\hat{\rho}}}{\delta\beta^*(\mathbf{k}_3)}\\
&\left.+\frac{1}{4}\frac{\delta^3 W_{\hat{\rho}}}{\delta\beta^*(\mathbf{k}_3)\delta\alpha(\mathbf{k}_2)\delta\alpha(\mathbf{k}_1)}T^*(\mathbf{k}_1,\mathbf{k}_2,\mathbf{k}_3)\right]đ\mathbf{k}_1đ\mathbf{k}_2đ\mathbf{k}_3.
\end{aligned}
\tag{4.31}
$$

4.3 The semiclassical approximation and Magnus expansion

An assumption about the pump beam is now made. It is assumed that the pump beam remains a coherent state during SPDC [17]. The form for the Wigner functional of a coherent state was shown in section 3.2 and is given below [17, 21]

$$W[\alpha] = N_0 \exp\left(-2\|\alpha - \tilde{\alpha}\|^2\right), \tag{4.32}$$

where $\tilde{\alpha}$ is a point on functional phase space and will be referred to as the parameter function. Since the peak of $W[\alpha]$ on functional phase space is located at $\tilde{\alpha}$, and the pump field is undepleted, it is the "most classical" point. The state with a coherent pump beam is then represented by [17]

$$W_{\hat{\rho}}[\alpha, \beta](z) = N_0 \exp\left(-2\left\|\beta - \tilde{\zeta}(z)\right\|^2\right) W_{\hat{\sigma}}, \tag{4.33}$$

where $W_{\hat{\sigma}}$ is the Wigner functional for the down-converted beams and $\tilde{\zeta}(z)$ is called the pump parameter function. The Wigner functional for the state is just the Wigner functional for the pump beam multiplied by the Wigner functional for the down-converted beams. According to Eq. (3.16), it follows that the pump and down-converted beams are not entangled [17]. The updated Wigner functional for the state is substituted into Eq. (4.31), and the total derivative over z is taken. The total derivative was demonstrated in Eq. (3.27) where in this case $F = W_{\hat{\rho}}$, $f_1 = \tilde{\zeta}(z)$, and $f_2 = \tilde{\zeta}^*(z)$. The result is written in terms of integrals instead of diamond products and rearranged

in terms of $\frac{\partial W_{\hat{\sigma}}}{\partial z}$ [17]

$$
\begin{aligned}
i\hbar\frac{\partial W_{\hat{\sigma}}}{\partial z} &= -2i\hbar\int\left(\beta^*(\mathbf{k})-\tilde{\zeta}^*(\mathbf{k},z)\right)\frac{\mathrm{d}\tilde{\zeta}(\mathbf{k},z)}{\mathrm{d}z}đ\mathbf{k}W_{\hat{\sigma}}\\
&- 2i\hbar\int\frac{\mathrm{d}\tilde{\zeta}^*(\mathbf{k},z)}{\mathrm{d}z}\left(\beta(\mathbf{k})-\tilde{\zeta}(\mathbf{k},z)\right)đ\mathbf{k}W_{\hat{\sigma}}\\
&- 2\int\Big[\alpha^*(\mathbf{k}_1)\alpha^*(\mathbf{k}_2)T^*(\mathbf{k}_1,\mathbf{k}_2,\mathbf{k}_3,z)\left(\beta(\mathbf{k}_3)-\tilde{\zeta}(\mathbf{k}_3,z)\right)W_{\hat{\sigma}}\\
&+\frac{\delta W_{\hat{\rho}}}{\delta\alpha(\mathbf{k}_1)}\alpha^*(\mathbf{k}_2)T^*(\mathbf{k}_1,\mathbf{k}_2,\mathbf{k}_3,z)\beta(\mathbf{k}_3)\\
&+\frac{1}{4}\frac{\delta^2 W_{\hat{\sigma}}}{\delta\alpha(\mathbf{k}_1)\delta\alpha(\mathbf{k}_2)}T^*(\mathbf{k}_1,\mathbf{k}_2,\mathbf{k}_3,z)\left(\beta(\mathbf{k}_3)-\tilde{\zeta}(\mathbf{k}_3,z)\right)\\
&-\left(\beta^*(\mathbf{k}_3)-\tilde{\zeta}^*(\mathbf{k}_3,z)\right)T(\mathbf{k}_1,\mathbf{k}_2,\mathbf{k}_3,z)\alpha(\mathbf{k}_1)\alpha(\mathbf{k}_2)W_{\hat{\sigma}}\\
&-\beta^*(\mathbf{k}_3)T(\mathbf{k}_1,\mathbf{k}_2,\mathbf{k}_3,z)\alpha(\mathbf{k}_1)\frac{\delta W_{\hat{\sigma}}}{\delta\alpha^*(\mathbf{k}_2)}\\
&-\frac{1}{4}\left(\beta^*(\mathbf{k}_3)-\tilde{\zeta}^*(\mathbf{k}_3,z)\right)T(\mathbf{k}_1,\mathbf{k}_2,\mathbf{k}_3,z)\frac{\delta^2 W_{\hat{\sigma}}}{\delta\alpha^*(\mathbf{k}_1)\delta\alpha^*(\mathbf{k}_2)}\Big]đ\mathbf{k}_1đ\mathbf{k}_2đ\mathbf{k}_3.
\end{aligned}
\tag{4.34}
$$

The semiclassical approximation is used and is valid when the state of the pump beam does not change, i.e./, if the photon number is much greater than 1, which essentially sets $\beta=\tilde{\zeta}$ [17]. The above expression reduces to [17]

$$
\begin{aligned}
i\hbar\frac{\partial W_{\hat{\sigma}}}{\partial z} &= 2\int\Big[\tilde{\zeta}^*(\mathbf{k}_3,z)T(\mathbf{k}_1,\mathbf{k}_2,\mathbf{k}_3,z)\alpha(\mathbf{k}_1)\frac{\delta W_{\hat{\sigma}}}{\delta\alpha^*(\mathbf{k}_2)}\\
&-\frac{\delta W_{\hat{\sigma}}}{\delta\alpha(\mathbf{k}_1)}\alpha^*(\mathbf{k}_2)T^*(\mathbf{k}_1,\mathbf{k}_2,\mathbf{k}_3,z)\tilde{\zeta}(\mathbf{k}_3,z)\Big]đ\mathbf{k}_1đ\mathbf{k}_2đ\mathbf{k}_3.
\end{aligned}
\tag{4.35}
$$

In order to neaten the expression, a kernel H is defined [17, 20]

$$
H(\mathbf{k}_1,\mathbf{k}_2,z)=\frac{-4i}{\hbar}\int\tilde{\zeta}^*(\mathbf{k})T(\mathbf{k}_1,\mathbf{k}_2,\mathbf{k},z)đ\mathbf{k},
\tag{4.36}
$$

where the z dependence of $\tilde{\zeta}$ is now dropped since solving for $\tilde{\zeta}$ would be complicated [17]. The parameter function is now defined as [20]

$$
\tilde{\zeta}(\mathbf{k})=\sqrt{2\pi}\zeta_0 w_p h(\omega-\omega_p,\delta_p)\exp\left(-\frac{1}{4}w_p^2\|\mathbf{k}\|^2\right),
\tag{4.37}
$$

where w_p is the pump beam waist radius which is chosen to not change with the propagation distance, $|\zeta_0|^2$ is the pump power which is assumed not to deplete [17], and the narrow spectral function was explained in chapter 3, but is repeated for convenience

$$h(\omega - \omega_p, \delta_p) = \sqrt{\frac{\sqrt{2}}{\sqrt{\pi}\delta_p}} \exp\left(-\frac{(\omega - \omega_p)^2}{\delta_p^2}\right) \tag{4.38}$$

is a narrow function with a width of δ_p that represents the angular frequency which has the following property [20]

$$\frac{1}{2\pi} \int h^2(\omega - \omega_p, \delta_p) d\omega = 1. \tag{4.39}$$

Substituting the definition of $H(\mathbf{k}_1, \mathbf{k}_2, z)$ produces the evolution equation [17]

$$\frac{\partial W_{\hat{\sigma}}}{\partial z} = \frac{1}{2} \frac{\delta W_{\hat{\sigma}}}{\delta \alpha^*} \diamond H \diamond \alpha + \frac{1}{2} \alpha^* \diamond H^* \diamond \frac{\delta W_{\hat{\sigma}}}{\delta \alpha}. \tag{4.40}$$

The following ansatz will be used as the Wigner functional for type I SPDC, which is the solution to Eq. (D.1) [17, 20]

$$W_{\hat{\sigma}} = N_0 \exp(-2\alpha^* \diamond A(z) \diamond \alpha - \alpha \diamond B(z) \diamond \alpha - \alpha^* \diamond B^*(z) \diamond \alpha^*), \tag{4.41}$$

where A and B are the unknown SPDC kernels. The equation above assumes that the initial seed field is a vacuum and that the vacuum state evolves with a Bogoliubov transformation through the crystal [20]. The expression $W_{\hat{\sigma}}$ only contains the SPDC down-converted fields. Since type I SPDC is utilized, the outgoing photons are indistinguishable due to the photons having the same polarization. $W_{\hat{\sigma}}$ is substituted into the evolution equation, and a system of SPDC kernel differential equations is extracted. The SPDC kernel differential equation can be solved by back-substitution and is shown in appendix D to obtain [17]

$$\begin{aligned} A(z) = \mathbb{1} &+ \int_0^z \int_0^{z_1} \mathcal{Z}\{H^*(z_1) \diamond H(z_2)\} dz_2 dz_1 \\ &+ \int_0^z \int_0^{z_1} \int_0^{z_2} \int_0^{z_3} \mathcal{Z}\{H^*(z_1) \diamond H(z_2) \diamond H^*(z_3) \diamond H(z_4)\} dz_4 dz_3 dz_2 dz_1 + \ldots, \end{aligned} \tag{4.42}$$

and [17]

$$\begin{aligned} B(z) &= \int_0^z H(z_1)dz_1 \\ &+ \int_0^z \int_0^{z_1} \int_0^{z_2} \mathcal{Z}\{H(z_1) \diamond H^*(z_2) \diamond H(z_3)\} dz_3 dz_2 dz_1 + \ldots, \end{aligned} \tag{4.43}$$

where [17]

$$\begin{aligned} &\mathcal{Z}\left\{H_1(z_1) \diamond \cdots \diamond H_n(z_n)\right\} \\ &= \frac{1}{2}\left[H_1(z_1) \diamond \mathcal{Z}\left\{H_2(z_2) \diamond \cdots \diamond H_n(z_n)\right\}\right. \\ &\left. + \mathcal{Z}\left\{H_1(z_2) \diamond \cdots \diamond H_{n-1}(z_n)\right\} \diamond H_n(z_1)\right], \end{aligned} \tag{4.44}$$

and $\mathcal{Z}\left\{H_1(z_1)\right\} = H_1(z_1)$. The down-converted state as a twin-beam squeezed vacuum state is given by

$$\begin{aligned} W_{\hat{\sigma}}[\alpha, \beta] &= N_0^2 \exp\left(-2\alpha^* \diamond A(z) \diamond \alpha - 2\beta^* \diamond A(z) \diamond \beta - 2\alpha^* \diamond B(z) \diamond \beta^*\right. \\ &\left. -2\beta \diamond B(z)^* \diamond \alpha\right), \end{aligned} \tag{4.45}$$

where the kernels A and B are the type I SPDC kernels. Ghost imaging requires spatially separated signal and idler beams and is considered in Eq. (4.45). The idler beam is labeled as α, and β will now represent the signal beam. The normalization of the state is important

$$\begin{aligned} &\int W_{\hat{\sigma}}[\alpha, \beta] \mathcal{D}^\circ[\alpha, \beta] \\ &= N_0^2 \int \exp\left(-2\alpha^* \diamond A(z) \diamond \alpha - 2\beta^* \diamond A(z) \diamond \beta - 2\alpha^* \diamond B(z) \diamond \beta^*\right. \\ &\left. -2\beta \diamond B(z)^* \diamond \alpha\right) \mathcal{D}^\circ[\alpha, \beta] \\ &= \frac{1}{\det(A) \det\left(A - B \diamond (A^*)^{-1} \diamond B^*\right)}. \end{aligned} \tag{4.46}$$

The functional integral, Eq. (3.39), was used twice to obtain the final result. For the state to be normalized, it follows that $A^{-1} = A - B \diamond (A^*)^{-1} \diamond B^*$, which will be used in the next chapter.

Chapter 5

Quantum ghost imaging

The setup of ghost imaging requires an entangled signal and idler beam in the transverse momentum degree of freedom. The signal beam interacts with the object and travels to the bucket detector whereas the idler beam is incident on the CCD array or scanning detector. The idler photons, that are coincident with the signal photons incident on the bucket detector, produce a picture of the object without interacting with it, hence the name ghost imaging. The basic setup can be seen in figure 5.1. The bucket detector is a detector which detects the signal beam after it has interacted with the object and has a large transverse surface area that provides a binary output on whether a photon is detected or not, whilst the CCD array can be thought of comprising many single pixel detectors that records photons in the transverse plane. The bucket detector contains spatial resolution, whilst the idler photon channel contains information about the object. Both pieces of information is required to produce an image. The special role of entanglement for ghost imaging is pointed out on page 44 in Chapter 3.

The purpose of the v shaped mirror in figure 5.1 is to separate the signal and idler beams into specific paths or channels. This setup with the v shaped mirror works due to the signal and idler SPDC beams emitted in cones, i.e. they are already spatially separated. The ghost imaging setup also requires lenses in-between the object and the crystal plane and is ignored in the diagram for simplicity. The aim of this project is to calculate the resolution of ghost imaging by using Wigner functionals for one photon.

For the purposes of this project, the object is located at a distance z_0 from the v shaped mirror and will be an aperture. The aperture will be modeled as a transmission function, $t(x, y, z_0)$, that only lets light through at the

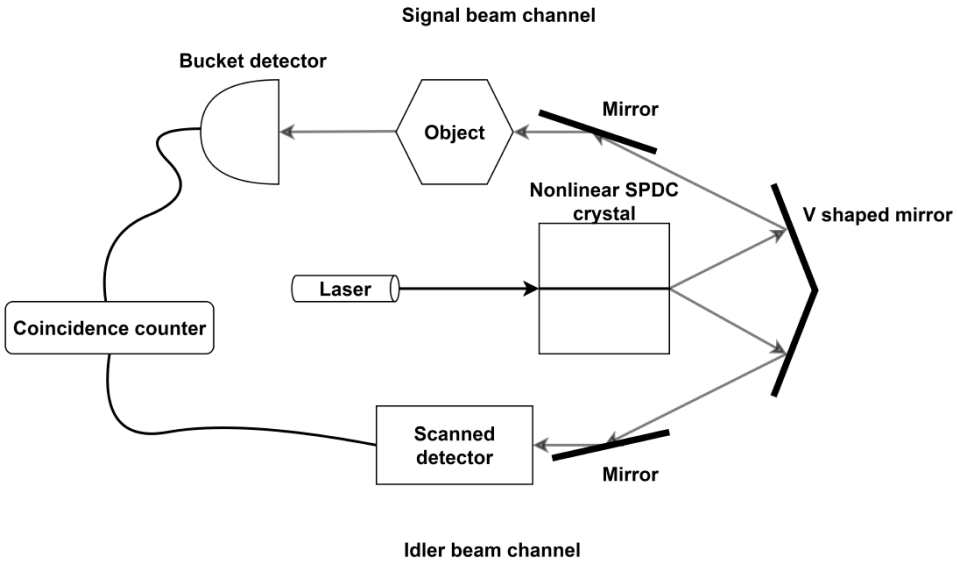

Figure 5.1: *The basic setup for ghost imaging using entangled photons produced by SPDC.*

location of the point-like aperture. The image of the point like aperture is the point spread function (PSF), which will be calculated for two cases, the thin and extreme crystal cases. $t^2(x)$ will be modeled as a delta function, and therefore $\|t(x)\| = 1$. It is approximated by a delta function in order to select a point on the transversal plane in which the aperture is located, and to focus the incident rays on the object through the aperture. Light of an infinite amplitude is then transmitted through the object, which leads to modeling $t^2(\mathbf{X}) = \delta(\mathbf{X} - \mathbf{X}')$, where $\mathbf{X}'$ is the transverse position of the aperture.

The system is modeled in such a way that the lost photons are not of interest in the analysis. In other words, only the photons passing through the aperture is considered. The state is then normalized, and as a consequence, the system is unitary, or reversible. For a real physical process, such a system would not be reversible since some photons would be absorbed by the object, and information will be lost, i.e. the system will be a lossy process. For the purpose of this dissertation, the transverse spatial properties which produce an image are of interest, therefore modeling the process to be unitary is sufficient.

The detectors in the ghost imaging setup are modeled in terms of Wigner functionals, and was introduced in section 3.3. The generating Wigner functional for an arbitrary detector kernel, D, was provided to me by my co-supervisor, FS Roux, and is given below

$$\mathcal{W}(J) = \left(\frac{2}{1+J}\right)^{\mathrm{tr}(D)} \exp\left(-2\left(\frac{1-J}{1+J}\right)\alpha^* \diamond D \diamond \alpha\right), \tag{5.1}$$

where J is the generating parameter. The detector Wigner functional for the detection of n photons can be obtained from Eq. 5.5 by

$$\frac{\partial^n \mathcal{W}(J)}{\partial J^n} \mid_{J=0}. \tag{5.2}$$

The detector kernel for the bucket detector is given as the identity kernel, $\mathbb{1}$ and produces the generating Wigner functional for the bucket detector given by

$$\mathcal{W}_B(J) = \frac{N_0}{(1+J)^{\Omega}} \exp\left(-2\left(\frac{1-J}{1+J}\right)\|\beta\|^2\right), \tag{5.3}$$

where β is a complex field variable that represents the signal beam, which interacts with the object. The detector kernel for a single pixel in the CCD array to be used in Eq. (5.5) is given by $D = M(\mathbf{k}_1, \omega_1, \mathbf{X}_0)M^*(\mathbf{k}_2, \omega_2, \mathbf{X}_0)$. The function $M(\mathbf{k}_1, \omega, \mathbf{X}_0)$ represents one pixel in the CCD array at position $\mathbf{X}_0$ and its width is given as the size of a pixel on the CCD array, w_0. $M(\mathbf{k}_1, \omega, \mathbf{X}_0)$ reads

$$M(\mathbf{k}_1, \omega, \mathbf{X}_0) = N_M h(\omega - \omega_d, \delta_d) \exp\left(-\frac{1}{4}w_0^2|\mathbf{k}_1|^2 + i\mathbf{X}_0 \cdot \mathbf{k}_1\right), \tag{5.4}$$

where N_M is a normalization constant such that $\mathrm{tr}(D) = 1$, $h(\omega - \omega_d, \delta_d)$ is a narrow spectral function[1] that has its maximum value at ω_d with spectral bandwidth δ_d, and w_0 is the size of a single pixel on the CCD array. Given the definition of D above, and $\mathrm{tr}(D) = 1$, the generating Wigner functional for the CCD array then becomes

$$\mathcal{W}_A(K) = \frac{2}{1+K} \exp\left(-2\left(\frac{1-K}{1+K}\right)\alpha^* \diamond MM^* \diamond \alpha\right). \tag{5.5}$$

[1]The narrow spectral function was explained in chapter 4.

The detector kernel depends on the position of the pixels on the CCD array, $\mathbf{X}_0$, located on the transverse plane. Figure 3.1 depicts a few pixels in a CCD array. The purpose of the CCD detector is to detect idler photons which are coincident with the signal photons arriving from SPDC and to provide spatial resolution i.e the position of the photon detected on the transverse plane. One of the main aims of this project is to obtain a photon probability distribution over the transverse plane on the CCD array. The procedure of obtaining the probability distribution is to take the expectation value of the detection operators and divide it by a normalization factor. This probability distribution arises as a result of the coincidence counts between the signal and idler photons. Let the idler beam be α, and the signal beam, which interacts with the object, be β. The expectation value is then given by

$$\langle W_B W_A \rangle = \int W_{\hat{S}\hat{\rho}\hat{S}^\dagger}[\alpha, \beta] W_B[\beta] W_A[\alpha] \mathcal{D}^\circ[\alpha, \beta], \tag{5.6}$$

where $W_{\hat{S}\hat{\rho}\hat{S}^\dagger}$ is the Wigner functional of the state after SPDC, evolved by an operator $\hat{S}$ due to interaction with the object. The Wigner functionals, W_B and W_A, represent the Wigner functionals for the bucket detector and CCD array. The generating Wigner functional method will be used in the actual calculations. Eq. (5.6) will be multiplied by a normalization factor, μ, to obtain a probability distribution.

5.1 The object

The main goal of this section is to obtain the Wigner functional for the SPDC state after it has interacted with the object. It is done by defining an operator representing the object and transforming the Wigner functional for the SPDC state, Eq. (4.45), with star products for the Wigner functionals of the object operator. This section is started with a basic description of the object and the reasoning behind ghost images due to the presence of the object. As mentioned earlier in this chapter, the process will be modeled to be unitary, and only the photons transmitted through the object are considered.
The ghost imaging object will be modeled as an aperture, however for illustration purposes, consider it to be an aperture with an arrow as shown in figure 5.2. One may ask, why does an image of the object form on the CCD array even though the idler photons, which are incident on the detector, have

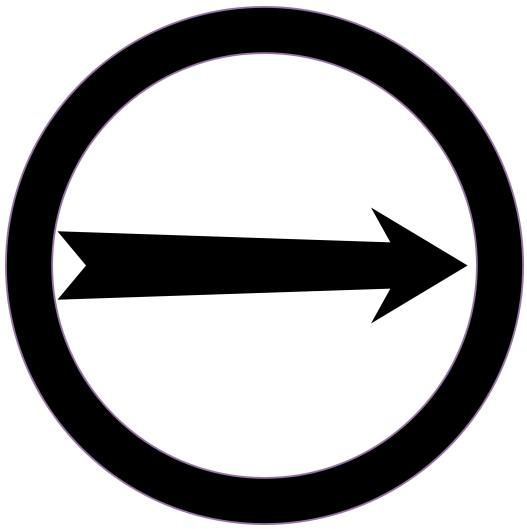

Figure 5.2: *An aperture with an arrow representing the object.*

never interacted with the object? In order to answer, consider incident signal photons on the object in figure 5.2. The first case is where the signal photons get absorbed by the arrow and do not get detected by the bucket detector. Therefore there are no coincidences between the idler and signal photons when the signal photons get absorbed. In this case, despite the idler photons reaching the CCD array, they do not get registered due to no coincidence since the signal photons get absorbed by the arrow. The second case is where the signal photons are transmitted through the aperture and are coincident with the idler photons. These photons will be registered, and after a sufficient number of coincident photons, a ghost image will form on the CCD array. The CCD array contains the spatial resolution, whereas the signal beam channel contains information about the object. The tactic of coincidence also reduces error caused by stray photons in the environment.
It is also possible to get an image of the object if the signal photons that interact with the object are backscattered onto a mirror on the SPDC crystals surface and then incident on a screen [22].
The objective is now to provide an operator for the object which evolves the signal photon field found in the Wigner functional for the SPDC state. The idea is to only affect the signal beam in the SPDC Wigner functional since only the signal beam interacts with the object. This operator will be labeled as $\hat{S}$ and was provided to me by my co-supervisor, FS Roux, in private

communication. The operator can be represented as

$$\begin{aligned}\hat{S} &= \sum_{j=0}^{\infty} \frac{1}{j!} \left[\int |\mathbf{k}\rangle E(\mathbf{k},\mathbf{k}') \langle \mathbf{k}'| đ\mathbf{k} đ\mathbf{k}' \right]^{\otimes j} \\ &= \exp_{\otimes} \left(\int |\mathbf{k}\rangle E(\mathbf{k},\mathbf{k}') \langle \mathbf{k}'| đ\mathbf{k} đ\mathbf{k}' \right),\end{aligned} \tag{5.7}$$

where $\mathbf{k}$ and $\mathbf{k}'$ are the transverse wave vectors, $\otimes$ represents the tensor product, and $E(\mathbf{k},\mathbf{k}')$ is a Toeplitz kernel which contains information about the position of the aperture on the transverse plane, as well as the aperture size. The operator is unitary if $E^{\dagger}(\mathbf{k},\mathbf{k}') = -E(\mathbf{k}',\mathbf{k})$. The Toeplitz kernel, which was also provided to me by FS Roux, was examined in section 3.1, the one used here is

$$E(\mathbf{k}_1,\mathbf{k}_2,\omega_1,\omega_2) = 2\pi\delta(\omega_1-\omega_2) \int t(\mathbf{X}) \exp\left(i\left(\mathbf{k}_1-\mathbf{k}_2\right)\cdot\mathbf{X}\right) d^2\mathbf{X}, \tag{5.8}$$

where $t(\mathbf{X})$ is the transmission function, and dictates how much light exits the aperture and has a magnitude smaller than or equal to 1. The width of the transmission function is equal to the width of the aperture. And $\mathbf{X}$ is a two-dimensional vector on the transverse plane. $E(\mathbf{k}_1,\mathbf{k}_2,\omega_1,\omega_2)$ is the only kernel with information about the object since it contains the transmission function.
A conversation with my co-supervisor, FS Roux, had resulted in the Wigner functional representation of Eq. (5.7)

$$W_{\hat{S}}[\beta] = N \exp\left(-2\beta^* \diamond H \diamond \beta\right), \tag{5.9}$$

where

$$N = \frac{N_0}{\det\left[\mathbb{1}+E\right]}, \tag{5.10}$$

and

$$H = (\mathbb{1}-E) \diamond (\mathbb{1}+E)^{-1}. \tag{5.11}$$

The SPDC and object Wigner functional is obtained, where E is given by Eq. (5.8). These Wigner functionals must be combined in a way that evolves the signal beam, β, of the SPDC Wigner functional with respect to the object operator since this is the beam in contact with the object. The star product

will be used to combine Wigner functionals

$$\begin{aligned} W_{\hat{S}\hat{\rho}\hat{S}^\dagger}[\alpha,\beta] &= W_{\hat{S}}[\beta] \star W_{\hat{\rho}}[\alpha,\beta] \star W_{\hat{S}^\dagger}[\beta] \\ &= \frac{N^2 N_0}{\det\left(H+H^\dagger\right)} \int \exp\left[-2\alpha_a^* \diamond H_p \diamond \alpha_a - 2\beta^* \diamond H_p \diamond \beta\right. \\ &\left. +2\alpha_a^* \diamond H_n \diamond \beta + 2\beta^* \diamond H_n^\dagger \diamond \alpha_a\right] W_{\hat{\rho}}[\alpha,\alpha_a]\mathcal{D}^\circ[\alpha_a], \end{aligned} \tag{5.12}$$

where $H_p = \left(\mathbb{1} + H \diamond H^\dagger\right) \diamond \left(H + H^\dagger\right)^{-1}$ and $H_n = (\mathbb{1} + H) \diamond \left(\mathbb{1} - H^\dagger\right) \diamond \left(H + H^\dagger\right)^{-1}$. The expression above was given to me by my co-supervisor, FS Roux, however, my derivation of Eq. (5.12) is provided in appendix E. A quick observation of Eq. (5.12) reveals that the idler beam, α, is untouched by the star product. This concludes section 5.1. In the next section, we will use Eq. (5.12) in order to calculate the point spread function.

5.2 Probability distribution

The main objective of this section is to calculate and interpret the point spread function (PSF). The starting point is the simplification of the trace in Eq. (5.6). However, to mathematically simplify the calculation, the generating Wigner functionals for the detection kernels is used instead of directly using the Wigner functionals. A single derivative of the expression with respect to the generating parameters is then taken for a single photon which is labeled as $\mathcal{R} = \mathcal{R}(\mathbf{X}_0, \mathbf{X}')$ where $\mathbf{X}_0$ is the pixel position on the CCD array and $\mathbf{X}'$ is the aperture position

$$\mathcal{R} = \frac{\partial^2}{\partial J \partial K} \left[\mathrm{tr}\left(W_{\hat{S}\hat{\rho}\hat{S}^\dagger}[\alpha,\beta]\mathcal{W}_B[\beta]\mathcal{W}_A[\alpha]\right)\right]\Big|_{J,K=0}, \tag{5.13}$$

where J and K are the generating parameters for the bucket detector and CCD array respectively. $\mathcal{R}$ is a probability distribution for the detection of a photon. The functional integral of the trace can be separated since the bucket detector only depends on the signal field, and the CCD array only depends on the idler field. This results in

$$\begin{aligned} &\mathrm{tr}\left(W_{\hat{S}\hat{\rho}\hat{S}^\dagger}[\alpha,\beta]\mathcal{W}_B[\beta]\mathcal{W}_A[\alpha]\right) \\ &= \int W_{\hat{S}\hat{\rho}\hat{S}^\dagger}[\alpha,\beta]\mathcal{W}_B[\beta]\mathcal{D}^\circ[\beta]\mathcal{W}_A[\alpha]\mathcal{D}^\circ[\alpha]. \end{aligned} \tag{5.14}$$

The functional integration of the expression above is given in appendix F and results in

$$\begin{aligned}
&\mathrm{tr}\left(W_{\hat{S}\hat{\rho}\hat{S}^\dagger}[\alpha,\beta]\mathcal{W}_B[\beta]\mathcal{W}_A[\alpha]\right) \\
&= \frac{2N_0}{(1+K)\det\left[\mathbb{1}+JE\diamond E\right]\det\left[A+(\frac{1-K}{1+K})MM^*\right]} \\
&\times \frac{1}{\det\left[D_E+A-B\diamond(A^T+(\frac{1-K}{1+K})M^*M)^{-1}\diamond B^*\right]},
\end{aligned} \tag{5.15}$$

where the definition of kernel D_E is

$$D_E = (\mathbb{1}-JE\diamond E)\diamond(\mathbb{1}+JE\diamond E)^{-1}. \tag{5.16}$$

Upon inspecting Eq. (5.15), it is evident that it depends on the SPDC kernels, A and B, as expected. It is also a function of the object toeplitz kernel, E, which is modeled as an aperture and hidden in the definition of D_E. The number of photons are not specified as yet, thus the dependence on the generating parameters J and K.
The derivative of the trace with respect to the generating parameters is now of concern in order to select one photon. After performing the derivatives, the probability distribution, $\mathcal{R}$, is simplified to be

$$\mathcal{R} \approx \frac{M\diamond B^*\diamond E\diamond E\diamond B\diamond M^*}{4}. \tag{5.17}$$

A detailed derivation of Eq. (5.17) is done by me and can be found in appendix G.
Two forms of $\mathcal{R}$ can be obtained. One for the extreme thin crystal limit, and one for the rational thin crystal limit. In both cases, only the first nonzero term in both the SPDC kernels, A and B, are considered. For the extreme thin crystal limit, it is considered that $z \approx 0$ in the integrand of the SPDC kernel, B. For the rational thin crystal limit, the z dependence remains and is included in the calculations. The PSF for the extreme crystal case is considered first.

5.3 The point spread function

The purpose of this section is to calculate the final simplified result for the PSF as well as its conditional photon probability distribution and is done

independently. It is possible to extract them from $\mathcal{R}$. The probability distribution simplifies to a Gaussian

$$\mathcal{R} = \frac{Q}{4} \int t^2(\mathbf{X}) \exp\left(-\frac{2|\mathbf{X}_0 - \mathbf{X}|^2}{w_0^2} - \frac{2|\mathbf{X}|^2}{w_p^2} \right) d^2\mathbf{X}. \tag{5.18}$$

A full derivation of Eq. (5.18) which was done independently and is provided in appendix H. Isolating the (ghost) image from the final result, one obtains

$$\begin{aligned} T(\mathbf{X}_0) &= \int t(\mathbf{X})^2 \exp\left(-\frac{2|\mathbf{X}_0 - \mathbf{X}|^2}{w_0^2} - \frac{2|\mathbf{X}|^2}{w_p^2} \right) d^2\mathbf{X} \\ &= \int t(\mathbf{X})^2 h\left(\mathbf{X}_0, \mathbf{X}\right) d^2\mathbf{X}, \end{aligned} \tag{5.19}$$

where $h\left(\mathbf{X}_0, \mathbf{X}\right)$ is the point spread function. If the transmission function is modeled as a point aperture located at $\mathbf{X}'$, $t^2(\mathbf{X}) = \delta\left(\mathbf{X} - \mathbf{X}'\right)$, then the point spread function is the image. The point spread function is

$$h\left(\mathbf{X}_0, \mathbf{X}'\right) = \exp\left(-\frac{2|\mathbf{X}_0 - \mathbf{X}'|^2}{w_0^2} - \frac{2|\mathbf{X}'|^2}{w_p^2} \right), \tag{5.20}$$

where $\mathbf{X}_0$ is the pixel position. $h\left(\mathbf{X}_0, \mathbf{X}'\right)$ is the point spread function as recorded by the pixel located there. From the equation above, it looks as if the signal beam incident on the object were a Gaussian beam with the same beam waist as the pump beam. It is now important to discuss resolution. Resolution is the minimal distance at which two points in the image can be distinguished [13]. The definition implies that a decrease in the FWHM (full width at half maximum) results in an increase in the obtained image quality due to the optical systems ability to differentiate between finer details. In other words, the smaller the FWHM resolution, the sharper the PSF and the clearer the image. The FWHM resolution is equal to the pixel size, w_0, times a constant, which will be ignored.

Coming back to equation (5.20), it is desirable to have an effect of w_p in the PSF. According to the PSF obtained, the aperture position needs to be shifted to retain the beam waist. Consider the aperture to be shifted horizontally by 1 unit. For convenience of analysis, the movement of the aperture will only be in the horizontal direction since the results are symmetric in the vertical direction, i.e. $X_{0y} = X'_y = 0$. It is important to note that all the

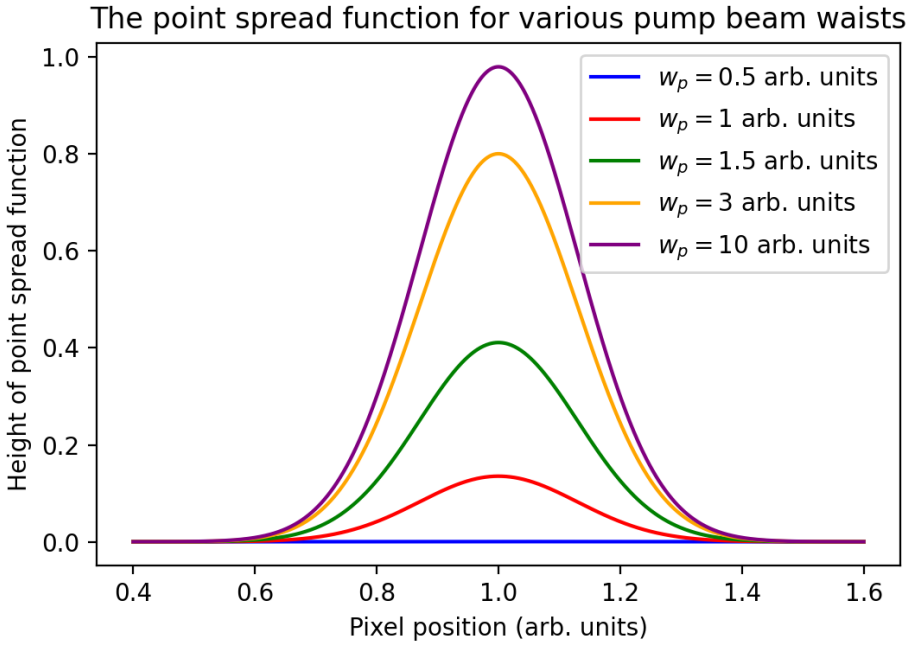

Figure 5.3: *A depiction of the point spread function for various pump beam waists which are given in the legend. The units "arb. units"" represents arbitrary units. The aperture is moved by 1 unit in the* $\hat{\boldsymbol{x}}$ *direction on the transverse plane.*

units are ignored since it cancels out in the argument of the exponential in Eq. (5.20).

For a fixed w_0, an increase in the pump beam waist results in a sharper point spread function. Similarly, a decrease in the beam waist leads to a flatter point spread function with a smaller FWHM and can be seen in figure 5.3. The brightness of the image is dependent on w_p since the amplitude of the image increases. The beam waist can be calculated by using the following formula

$$z_R = \frac{kw_p^2}{2}, \tag{5.21}$$

where z_R is the Rayleigh range, and k is the wave number.

For a fixed pump beam waist, a smaller w_0 will produce a smaller FWHM, and a larger w_0 will produce a larger FWHM which can be seen in figure 5.4. The brightness of the image is independent of the pixel size, i.e. the

amplitude does not change with a change in w_0.

A question arises as to what happens when the aperture is moved further

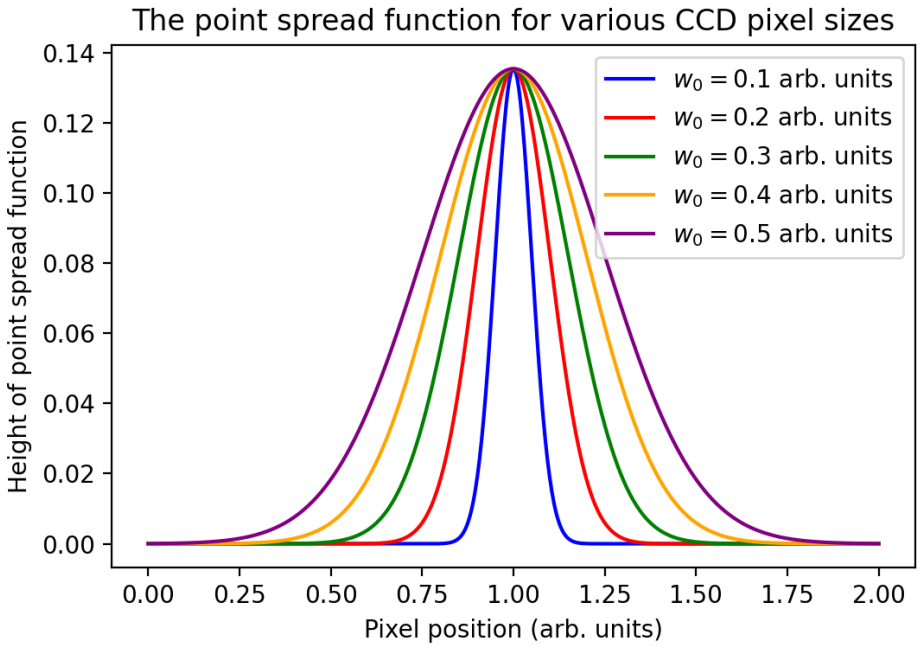

Figure 5.4: *A depiction of the point spread function for pixel sizes which are given in the legend. The aperture is moved by 1 unit in the $\hat{\boldsymbol{x}}$ direction on the transverse plane.*

away from the signal beam. For a fixed pixel size and beam waist, the increase of the aperture distance accelerates the decrease of the PSF and is shown in figure 5.5.

The point spread function is illustrated in figure 5.6. Note that the figure has a displaced aperture and aims to show that the image and point spread function is dependent on the position of the aperture. The point spread function is not shift invariant. It contains an amplitude function containing the pump beam waist which increases the amplitude of the point spread function for a decreasing pump beam waist.

The case where two apertures are involved is now considered. The first aperture is a labeled as $\mathbf{X}'$, and the second aperture is labeled as $\mathbf{X}'_1$. An image of these two apertures is obtained by modifying the transmission function as

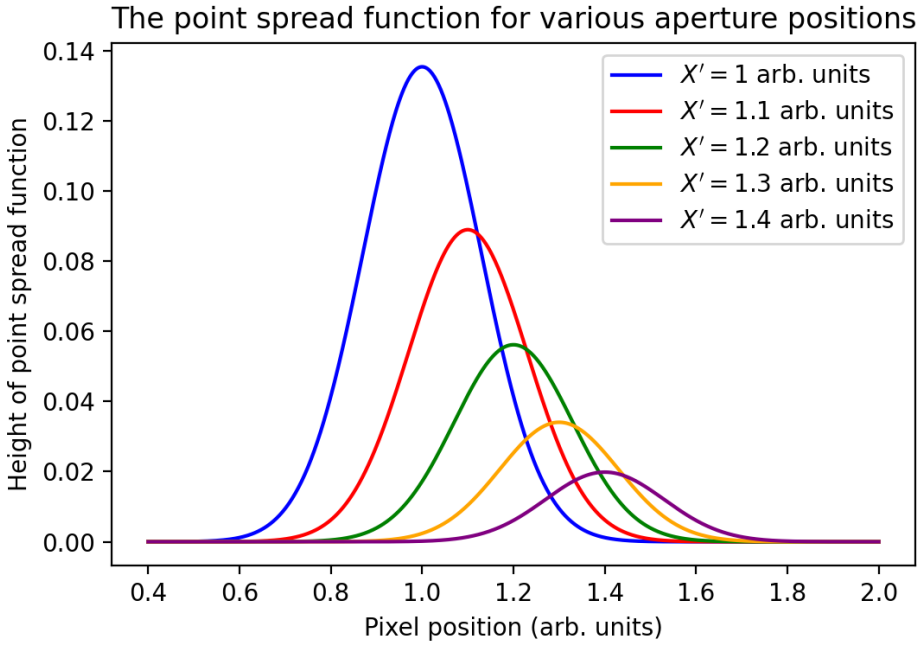

Figure 5.5: *A depiction of the point spread function for different aperture positions which are given in the legend.*

follows

$$t^2(\mathbf{X}) = \frac{\delta(\mathbf{X} - \mathbf{X}') + \delta(\mathbf{X} - \mathbf{X}'_1)}{2}. \tag{5.22}$$

The result is a sum of PSF's which is shown in figure 5.7.

And finally the case where there is a fixed distance between two apertures with varying pixel sizes, is depicted in figure 5.8. The image for a small aperture size clearly shows two Gaussian distributions, each representing an aperture. As the pixel size increases, it becomes increasingly difficult to distinguish between these apertures in the image. The resolution is the minimum distance to resolve two points. In this case the points are the apertures and is equal to 1 unit. When the pixel size increases, a single Gaussian distribution is obtained and is depicted in purple. The distance between the two apertures on the image is approximated via calculation of the FWHM of the single Gaussian shown in purple. A FWHM>1 unit is obtained which can be observed by the shape of the Gaussian in figure 5.8. The case of FWHM> d, where d is the distance between apertures, means

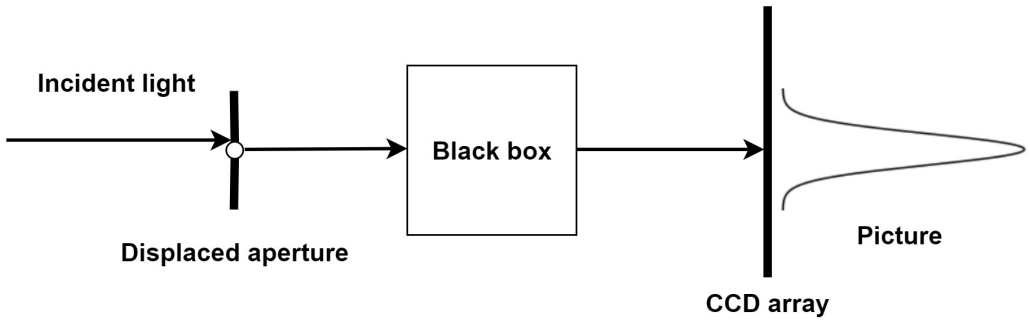

Figure 5.6: *An illustration of the point spread function. The aperture is the object and is modeled as a point, however it is magnified in this diagram. An input signal beam which is incident on the displaced aperture. An image is then obtained as a result of the ghost imaging setup. The image is dependent on the apertures position and is quantified by the point spread function.*

that the apertures on the image is not resolved. In other words, it will be impossible to see the different apertures in the image due to a large pixel size.
The resolution limit for the setup is also discussed. The resolution limit is w_0, since it is the pixel size on the CCD array. Therefore if two apertures of a distance less than w_0 is considered, then the setup will not be able to resolve the two apertures in the image. In order for an object to be resolvable, the following criteria needs to be satisfied

$$d > w_0. \tag{5.23}$$

As a side-note, altering the beam waist will only contribute to a change in the amplitude of the image.
The conditional probability of photons are now of interest. The probability distribution, $\mathcal{R}$, is not normalized due to an approximation made as a result of an inefficient SPDC process, as mentioned in appendix G. Therefore, $\mathcal{R}$ is written in terms of a condition probability and normalized as follows

$$\begin{aligned} \frac{\mathcal{R}}{\tilde{N}} &= \frac{\tilde{P}(D_1 \cap D_2)}{\tilde{N}} = \frac{\tilde{P}(D_1|D_2)\tilde{P}(D_2)}{\tilde{N}_1\tilde{N}_2} \\ \implies \frac{\mathcal{R}}{\tilde{N}} &= P(D_1 \cap D_2) = P(D_1|D_2)P(D_2), \end{aligned} \tag{5.24}$$

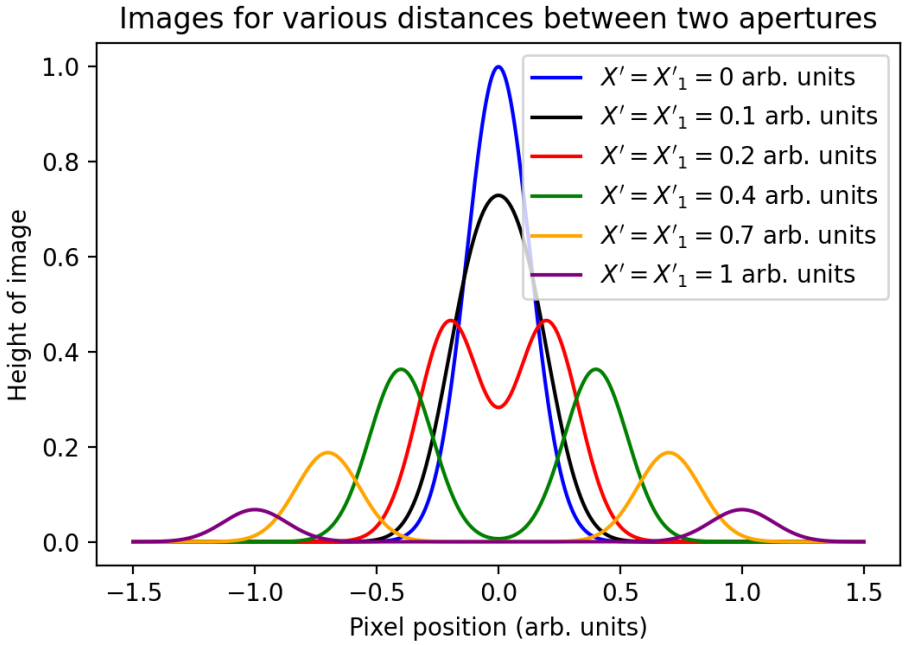

Figure 5.7: *The images of two apertures with varying distances apart. If the pump beam waist is increased, then the amplitude function is increased, which in turn increases the amplitudes of the images.*

where $P(D_1|D_2)$ is the normalized conditional probability of detecting a photon at detector D_1, given that a photon is detected at D_2, and $P(D_2)$ is the normalized probability of detecting a photon at detector D_2. The factor $P(D_1 \cap D_2)$ represents detecting photons at both detectors D_1 and D_2, therefore it is the normalized probability of detecting coincident photons. The probabilities containing tildes are unnormalized probabilities. The normalization factors associated with these probabilities are also given with a tilde which form the normalized probabilities. It is possible to find the conditional probability of detecting a photon at $\mathbf{X}_0$, by normalizing $\mathcal{R}$

$$\begin{aligned} \frac{\mathcal{R}}{\mu} &= P(D_1|D_2) = \frac{\mathcal{R}}{\tilde{N}P(D_2)} \\ &= \frac{1}{\mu}\int t(\mathbf{X})^2 \exp\left(-\frac{2|\mathbf{X}_0 - \mathbf{X}|^2}{w_0^2} - \frac{2|\mathbf{X}|^2}{w_p^2}\right) d^2\mathbf{X}, \end{aligned} \tag{5.25}$$

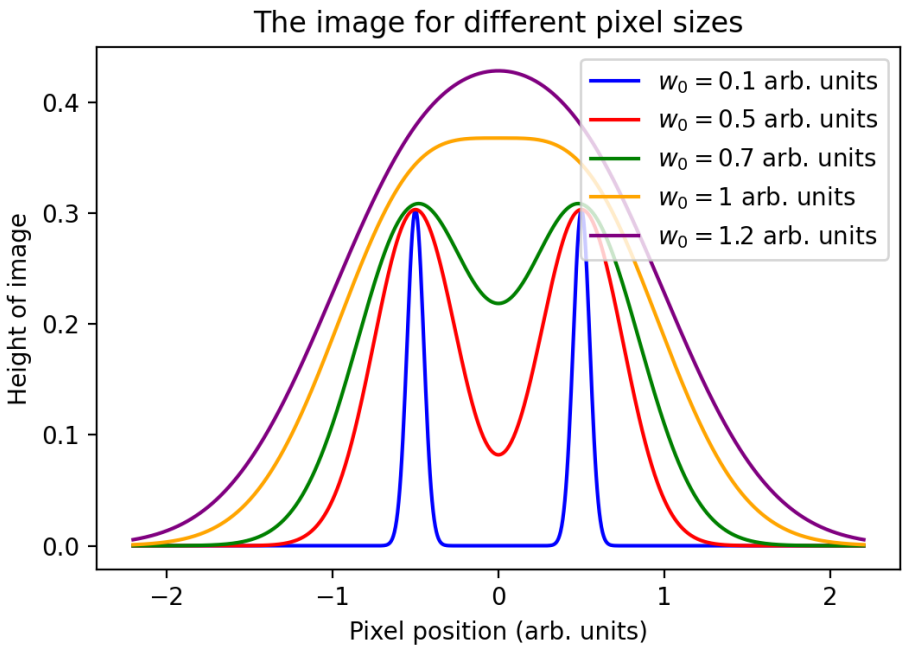

Figure 5.8: *The images for different CCD pixel sizes with two apertures at a distance of 1 unit apart.*

where

$$\mu = \int \mathcal{R} d^2\mathbf{X}_0 = \frac{\pi w_0^2}{2} \int t(\mathbf{X})^2 \exp\left(-\frac{2|\mathbf{X}|^2}{w_p^2}\right) d^2\mathbf{X}. \tag{5.26}$$

A point aperture is considered, which implies $t(\mathbf{X})^2 = \delta(\mathbf{X} - \mathbf{X}')$

$$P(D_1|D_2) = \frac{1}{\mu} \exp\left(-\frac{2|\mathbf{X}_0 - \mathbf{X}'|^2}{w_0^2} - \frac{2|\mathbf{X}'|^2}{w_p^2}\right), \tag{5.27}$$

with

$$\mu = \frac{\pi w_0^2}{2} \exp\left(-\frac{2|\mathbf{X}'|^2}{w_p^2}\right). \tag{5.28}$$

Therefore

$$P(D_1|D_2) = \frac{2}{\pi w_0^2} \exp\left(-\frac{2|\mathbf{X}_0 - \mathbf{X}'|^2}{w_0^2}\right). \tag{5.29}$$

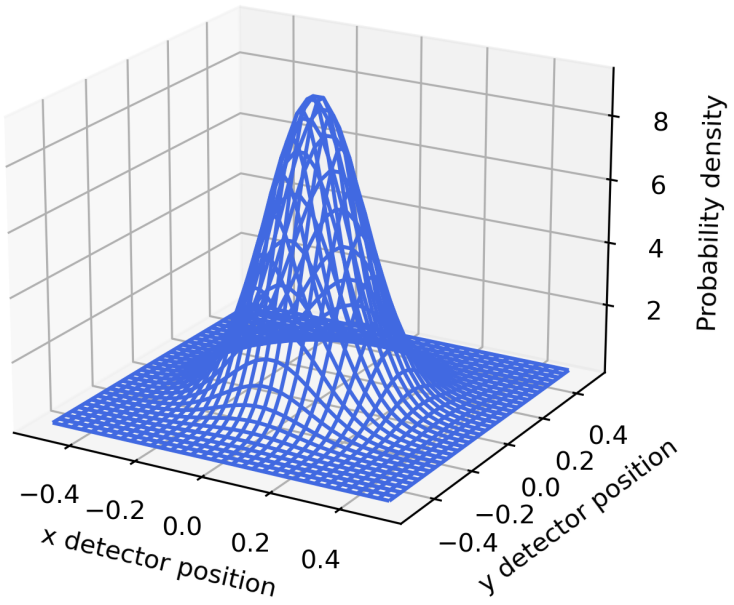

Figure 5.9: *The conditional photon probability distribution for the object located at the origin of the transverse plane for a CCD pixel size of 0.26. The detector positions have arbitrary units.*

The shape of $P(D_1|D_2)$ does not vary when the aperture position varies, and the material dependencies are removed due to its normalization. The height of the ghost image peak only depends on the pixel size, w_0. The lower the pixel size, the higher the peak.
To get an aesthetic idea of the conditional photon probability distribution, an example whereby the object is located at the origin is used, i.e. $\mathbf{X}' = 0$, and a pixel size of 0.26. Using these numerical values, it is then possible to graph out a picture of the ghost image. It is done in figure 5.9. The point spread function for the rational thin crystal limit was calculated independently, which used an approximation for the z dependence in the bilinear kernel, $H(z)$. The bilinear kernel can be found in the SPDC kernel, B. After calculating the PSF, the same image as for the extreme thin crystal limit is obtained. The proof can be found in appendix I.

Chapter 6

Conclusion

The Maxwell's equations for light in a medium were used to calculate an equation for the scalar field in the co-propagating frame, and the IPO was then extracted. Thereafter, the use of Wigner functionals in SPDC were discussed and the evolution equation was then calculated.
The main aim of this study was to compute the resolution of ghost imaging using the thorough description in terms of Wigner functional theory. Chapter 5 contains a detailed discussion of the results. These results for ghost imaging were obtained for two instances, which were the extreme thin crystal limit and the rational thin crystal limit resulting in the same images. In both cases, only the first nonzero term in the Magnus expansion for SPDC kernels A and B were retained, and used in the Wigner functional for the SPDC state. The first term of A is the identity kernel, and the first term for B is the integral of the bilinear kernel $H(z)$ with respect to the propagation through the crystal. In the extreme thin crystal limit, the z dependence of $H(z)$ was removed from the SPDC kernel, B. In the rational thin crystal limit, the z dependence was retained and approximated using a Taylor expansion. The resulting image and conditional photon probability distribution from both cases are the same.
The main results from this dissertation reads that the image of a point object obtained depends on the CCD pixel size, aperture position, and the beam waist. Moreover, the ghost imaging model calculations show that the resolution is equal to the CCD pixel size. The resolution is thus only limited by the CCD pixel size, i.e. an object smaller than the CCD pixel size cannot be resolved. Another result obtained was that the image position depends on the position of the object. Movement of the object away from the incidence

of the signal beam resulted in a decreasing height of the image, in other words, the amplitude of the image decreases as the aperture is pulled away. An additional effect of moving the point aperture position by a distance, $\mathbf{X}'$, results in the movement of the image position by $\mathbf{X}'$.
The dependence on the beam waist on the image was discussed. An increase in the beam waist leads to an increase in the amplitude of the image, which increases the brightness.
Most of these results are to be expected for a crystal with sufficiently large surface area. The unusual result is the dependence of the resolution solely on the CCD pixel size due to the near field model.

Bibliography

[1] Robert W. Boyd. *Nonlinear Optics, Third Edition*. Academic Press, Inc., USA, 3rd edition, 2008.

[2] Christophe Couteau. Spontaneous parametric down-conversion. *Contemporary Physics*, 59(3):291–304, Jul 2018. URL: http://dx.doi.org/10.1080/00107514.2018.1488463, doi:10.1080/00107514.2018.1488463.

[3] Thomas L. Curtright and Cosmas K. Zachos. Quantum mechanics in phase space. *Asia Pacific Physics Newsletter*, 01(01):37–46, May 2012. URL: http://dx.doi.org/10.1142/S2251158X12000069, doi:10.1142/s2251158x12000069.

[4] Jonathan P. Dowling and Kaushik P. Seshadreesan. Quantum optical technologies for metrology, sensing, and imaging. *Journal of Lightwave Technology*, 33(12):2359–2370, Jun 2015. URL: https://doi.org/10.1109%2Fjlt.2014.2386795, doi:10.1109/jlt.2014.2386795.

[5] Peter D. Drummond and Mark Hillery. *The Quantum Theory of Nonlinear Optics*. Cambridge University Press, 2014. doi:10.1017/CBO9780511783616.

[6] Christopher Gerry and Peter Knight. *Introductory Quantum Optics*. Cambridge University Press, 2004. doi:10.1017/CBO9780511791239.

[7] J N Kriel, F G Scholtz, and J D Thom. Moyal implementation of flow equations—a non-perturbative approach to quantum many-body systems. *Journal of Physics A: Mathematical and Theoretical*, 40(31):9483, jul 2007. URL: https://dx.doi.org/10.1088/1751-8113/40/31/023, doi:10.1088/1751-8113/40/31/023.

[8] Paul G. Kwiat, Klaus Mattle, Harald Weinfurter, Anton Zeilinger, Alexander V. Sergienko, and Yanhua Shih. New high-intensity source of polarization-entangled photon pairs. *Phys. Rev. Lett.*, 75:4337–4341, Dec 1995. URL: https://link.aps.org/doi/10.1103/PhysRevLett.75.4337, doi:10.1103/PhysRevLett.75.4337.

[9] C. K. Law and J. H. Eberly. Analysis and interpretation of high transverse entanglement in optical parametric down conversion. *Phys. Rev. Lett.*, 92:127903, Mar 2004. URL: https://link.aps.org/doi/10.1103/PhysRevLett.92.127903, doi:10.1103/PhysRevLett.92.127903.

[10] Wilhelm Magnus. On the exponential solution of differential equations for a linear operator. *Communications on Pure and Applied Mathematics*, 7(4):649–673, 1954. URL: https://onlinelibrary.wiley.com/doi/abs/10.1002/cpa.3160070404, arXiv:https://onlinelibrary.wiley.com/doi/pdf/10.1002/cpa.3160070404, doi:https://doi.org/10.1002/cpa.3160070404.

[11] T. J. Moir. Toeplitz matrices for linear time-invariant systems, an illustration of their application to Wiener filters and estimators. *International Journal of Systems Science*, 49(4):800–817, 2018. arXiv:https://doi.org/10.1080/00207721.2017.1419306, doi:10.1080/00207721.2017.1419306.

[12] J. E. Moyal. Quantum mechanics as a statistical theory. *Mathematical Proceedings of the Cambridge Philosophical Society*, 45(1):99–124, 1949. doi:10.1017/S0305004100000487.

[13] Alexander Ng and Justiaan Swanevelder. Resolution in ultrasound imaging. *Continuing Education in Anaesthesia Critical Care & Pain*, 11(5):186–192, 08 2011. arXiv:https://academic.oup.com/bjaed/article-pdf/11/5/186/794418/mkr030.pdf, doi:10.1093/bjaceaccp/mkr030.

[14] Pedro Otero Casal. *Spontaneous Parametric Down-Conversion*. Number FYSPROJ1250 in FYSAST. 2022.

[15] Filippus S. Roux. Combining spatiotemporal and particle-number degrees of freedom. *Phys. Rev. A*, 98:043841, Oct 2018. URL:

https://link.aps.org/doi/10.1103/PhysRevA.98.043841, doi:10.1103/PhysRevA.98.043841.

[16] Filippus S. Roux. Erratum: Combining spatiotemporal and particle-number degrees of freedom [phys. rev. a 98, 043841 (2018)]. *Phys. Rev. A*, 101:019903, Jan 2020. URL: https://link.aps.org/doi/10.1103/PhysRevA.101.019903, doi:10.1103/PhysRevA.101.019903.

[17] Filippus S. Roux. Parametric down-conversion beyond the semiclassical approximation. *Phys. Rev. Research*, 2:033398, Sep 2020. URL: https://link.aps.org/doi/10.1103/PhysRevResearch.2.033398, doi:10.1103/PhysRevResearch.2.033398.

[18] Filippus S. Roux. Quantifying entanglement of parametric down-converted states in all degrees of freedom. *Phys. Rev. Research*, 2:023137, May 2020. URL: https://link.aps.org/doi/10.1103/PhysRevResearch.2.023137, doi:10.1103/PhysRevResearch.2.023137.

[19] Filippus S. Roux. Spatiotemporal effects on squeezing measurements. *Phys. Rev. A*, 103:013701, Jan 2021. URL: https://link.aps.org/doi/10.1103/PhysRevA.103.013701, doi:10.1103/PhysRevA.103.013701.

[20] Filippus S. Roux. Stimulated parametric down-conversion for spatiotemporal metrology. *Phys. Rev. A*, 104:043514, Oct 2021. URL: https://link.aps.org/doi/10.1103/PhysRevA.104.043514, doi:10.1103/PhysRevA.104.043514.

[21] Filippus S. Roux and Nicolas Fabre. Wigner functional theory for quantum optics, 2020. arXiv:1901.07782.

[22] Yanhua Shih. The physics of ghost imaging. In *International Conference on Quantum Information*, page QTuB1. Optica Publishing Group, 2008. URL: https://opg.optica.org/abstract.cfm?URI=ICQI-2008-QTuB1, doi:10.1364/ICQI.2008.QTuB1.

[23] Gintaras Tamošauskas, Gvidas Beresnevičius, Darius Gadonas, and Audrius Dubietis. Transmittance and phase matching of BBO crystal in

the 3-5 μm range and its application for the characterization of mid-infrared laser pulses. *Optical Materials Express*, 8(6):1410, June 2018. doi:10.1364/OME.8.001410.

[24] S.P. Walborn, C.H. Monken, S. Pádua, and P.H. Souto Ribeiro. Spatial correlations in parametric down-conversion. *Physics Reports*, 495(4):87–139, 2010. URL: https://www.sciencedirect.com/science/article/pii/S0370157310001602, doi:https://doi.org/10.1016/j.physrep.2010.06.003.

Appendices

Appendix A

Coherent state star product

The following star product of two Wigner functionals in terms of coherent states is proved

$$\begin{aligned} &W_{\hat{A}\hat{B}} = W_{\hat{A}} \star W_{\hat{B}} \\ &= N_0^2 \int W_{\hat{A}}\left[\alpha - \alpha_1\right] W_{\hat{B}}\left[\alpha - \alpha_2\right] \exp\left(2\alpha_1^* \diamond \alpha_2 - 2\alpha_2^* \diamond \alpha_1\right) \mathcal{D}^\circ[\alpha_1]\mathcal{D}^\circ[\alpha_2]. \end{aligned} \tag{A.1}$$

Acknowledging the star product for two Wigner functionals in terms of position and momentum variables [21]

$$\begin{aligned} &W_{\hat{A}\hat{B}} = W_{\hat{A}} \star W_{\hat{B}} \\ &= N_0^2 \int W_{\hat{A}}\left[q - q_1, p - p_1\right] W_{\hat{B}}\left[q - q_2, p - p_2\right] \exp\left(2i\left(q_1 \diamond p_2 - q_2 \diamond p_1\right)\right) \\ &\times \mathcal{D}[q_1, q_2]\mathcal{D}^\circ[p_1, p_2]. \end{aligned} \tag{A.2}$$

Examining the exponent

$$\begin{aligned} &2i\left(q_1 \diamond p_2 - q_2 \diamond p_1\right) \\ &= 2i\left(q_1 \diamond p_2 - iq_1 \diamond q_2 + iq_1 \diamond q_2 - q_2 \diamond p_1\right) \\ &= 2\left(q_1 \diamond \left(ip_2 + q_2\right) + q_2 \diamond \left(-q_1 - ip_1\right)\right) \\ &= 2\sqrt{2}\left(q_1 \diamond \alpha_2 - q_2 \diamond \alpha_1\right) \\ &= 2\sqrt{2}\left(\left(\frac{\alpha_1 + \alpha_1^*}{\sqrt{2}}\right) \diamond \alpha_2 - \left(\frac{\alpha_2 + \alpha_2^*}{\sqrt{2}}\right) \diamond \alpha_1\right) \\ &= 2\left(\alpha_1 \diamond \alpha_2 + \alpha_1^* \diamond \alpha_2 - \alpha_2 \diamond \alpha_1 - \alpha_2^* \diamond \alpha_1\right) \\ &= 2\left(\alpha_1^* \diamond \alpha_2 - \alpha_2^* \diamond \alpha_1\right). \end{aligned} \tag{A.3}$$

The exponent transformation in terms of α is concluded, the dependence of $W_{\hat{A}}$ is now of interest. The position and momentum, q and p, are shifted by q_1 and p_1 respectively, and is equivalent to having $W_{\hat{A}}$ depend on $\tilde{\alpha} = \frac{1}{\sqrt{2}}(q - q_1 + ip - ip_1) = \alpha - \alpha_1$. A similar argument can be made for $W_{\hat{B}}$. Therefore, the star product simplifies to

$$\begin{aligned} W_{\hat{A}\hat{B}} &= W_{\hat{A}} \star W_{\hat{B}} \\ &= N_0^2 \int W_{\hat{A}}[\alpha - \alpha_1] W_{\hat{B}}[\alpha - \alpha_2] \exp\left(2\alpha_1^* \diamond \alpha_2 - 2\alpha_2^* \diamond \alpha_1\right) \mathcal{D}^\circ[\alpha_1]\mathcal{D}^\circ[\alpha_2]. \end{aligned} \tag{A.4}$$

The star product written in terms of complex field variables for two operators was shown, starting from the star product for two operators written in terms of p and q.

Appendix B

Proof for the discrete and finite isotropic Gaussian integral

This proof was done independently. Consider the isotropic Gaussian below

$$\begin{aligned}&\int \exp\left(-\mathrm{c}\alpha^* \diamond P \diamond \alpha - \alpha^* \diamond \beta - \beta' \diamond \alpha\right) \mathcal{D}^\circ[\alpha] \\ &= \frac{1}{c^\Omega \det[P]} \exp\left(\frac{1}{\mathrm{c}} \beta' \diamond P^{-1} \diamond \beta\right).\end{aligned} \tag{B.1}$$

where $\mathcal{D}^\circ[\alpha] = \frac{1}{(2\pi)^\Omega} \mathcal{D}[p]\mathcal{D}[q]$. The aim is to solve the Gaussian integral for the discrete case with finite dimension, then make the final result continuous and infinite-dimensional. Consider the exponent

$$\begin{aligned}&-\mathrm{c}\alpha^* \diamond P \diamond \alpha - \alpha^* \diamond \beta - \beta' \diamond \alpha \\ &= -\frac{\mathrm{c}}{2} \left(q(\mathbf{k}) - ip(\mathbf{k})\right) \diamond P(\mathbf{k}, \mathbf{k}') \diamond \left(q(\mathbf{k}') + ip(\mathbf{k}')\right) \\ &- \frac{1}{\sqrt{2}} \left(q(\mathbf{k}) - ip(\mathbf{k})\right) \diamond \beta(\mathbf{k}) - \frac{1}{\sqrt{2}} \beta'(\mathbf{k}) \diamond \left(q(\mathbf{k}) + ip(\mathbf{k})\right) \\ &= -\frac{\mathrm{c}}{2} \left[q(\mathbf{k}) \diamond P(\mathbf{k}, \mathbf{k}') \diamond q(\mathbf{k}') + iq(\mathbf{k}) \diamond P(\mathbf{k}, \mathbf{k}') \diamond p(\mathbf{k}')\right. \\ &\left. -ip(\mathbf{k}) \diamond P(\mathbf{k}, \mathbf{k}') \diamond q(\mathbf{k}') + p(\mathbf{k}) \diamond P(\mathbf{k}, \mathbf{k}') \diamond p(\mathbf{k}')\right] \\ &- \frac{1}{\sqrt{2}} \left(q(\mathbf{k}) - ip(\mathbf{k})\right) \diamond \beta(\mathbf{k}) - \frac{1}{\sqrt{2}} \beta'(\mathbf{k}) \diamond \left(q(\mathbf{k}) + ip(\mathbf{k})\right),\end{aligned} \tag{B.2}$$

which is discretized and made finite-dimensional

$$\begin{aligned} &-\sum_{n,j}^{N}\frac{\mathrm{c}}{2}\left[q_nP_{nj}q_j+iq_nP_{nj}p_j-ip_nP_{nj}q_j+p_nP_{nj}p_j\right] \\ &-\frac{1}{\sqrt{2}}\sum_{l}^{N}\left(\left(q_l-ip_l\right)\beta_l+\beta_l'\left(q_l+ip_l\right)\right), \end{aligned} \tag{B.3}$$

where the summation runs from 1 to the dimension, N, and P_{ij} are entries of a matrix $\mathbf{P}$ with dimensions $N\times N$, similarly, q_i is the ith entry of the column vector $\mathbf{q}$. The matrix $\mathbf{P}$ is assumed to be invertible. Written in terms of matrices

$$\begin{aligned} &-\frac{\mathrm{c}}{2}\left[\mathbf{q}^T\mathbf{P}\mathbf{q}+i\mathbf{q}^T\mathbf{P}\mathbf{p}-i\mathbf{p}^T\mathbf{P}\mathbf{q}+\mathbf{p}^T\mathbf{P}\mathbf{p}\right] \\ &-\frac{1}{\sqrt{2}}\left(\left(\mathbf{q}^T-i\mathbf{p}^T\right)\mathbf{p}\boldsymbol{\beta}+\boldsymbol{\beta}'^T\left(\mathbf{q}+i\mathbf{p}\right)\right). \end{aligned} \tag{B.4}$$

Since $\mathbf{P}$ is invertible, it has nonzero eigenvalues. To slightly simplify the calculations, it is also assumed that $\mathbf{P}$ is symmetric. Spectral decomposition is used on $\mathbf{P}$. Let the normalized eigenvectors be $\mathbf{U}^{(l)}$ for the lth eigenvalue. It is worth noting that the eigenvectors form projection matrices, in other words $\mathbf{U}^{(l)}\mathbf{U}^{(l)T}$ is the lth projection matrix. Therefore

$$\mathbf{P}=\sum_{l}\lambda_l\mathbf{U}^{(l)}\mathbf{U}^{(l)T}. \tag{B.5}$$

The subscript indices are reserved for matrix entries. Alternatively, a more general case of $\mathbf{P}$ can be considered, the case that $\mathbf{P}$ is normal. It can be done by assuming that the eigenvalues and eigenvectors are complex, however, the simpler case of a symmetric matrix $\mathbf{P}$ is considered here. Eq. (B.4) becomes

$$\begin{aligned} &-\frac{\mathrm{c}}{2}\sum_{l}\Big[\mathbf{q}^T\lambda_l\mathbf{U}^{(l)}\mathbf{U}^{(l)T}\mathbf{q}+i\mathbf{q}^T\lambda_l\mathbf{U}^{(l)}\mathbf{U}^{(l)T}\mathbf{p}-i\mathbf{p}^T\lambda_l\mathbf{U}^{(l)}\mathbf{U}^{(l)T}\mathbf{q} \\ &+\mathbf{p}^T\lambda_l\mathbf{U}^{(l)}\mathbf{U}^{(l)T}\mathbf{p}\Big]-\frac{1}{\sqrt{2}}\left(\left(\mathbf{q}^T-i\mathbf{p}^T\right)\boldsymbol{\beta}+\boldsymbol{\beta}'^T\left(\mathbf{q}+i\mathbf{p}\right)\right). \end{aligned} \tag{B.6}$$

A change of variables is now performed, let $q'_l = \mathbf{U}^{(l)T}\mathbf{q}$ and $p'_l = \mathbf{U}^{(l)T}\mathbf{p}$. Since these are elements of a matrix, the transpose has no effect on it.

$$\begin{aligned}
&-\frac{\mathrm{c}}{2}\sum_l \left[q'_l\lambda_l q'_l + iq'_l\lambda_l p'_l - ip'_l\lambda_l q'_l + p'_l\lambda_l p'_l\right] \\
&-\frac{1}{\sqrt{2}}\sum_l \left(\left(\mathbf{q}^T - i\mathbf{p}^T\right)\mathbf{U}^{(l)}\mathbf{U}^{(l)T}\boldsymbol{\beta} + \boldsymbol{\beta}'^T\mathbf{U}^{(l)}\mathbf{U}^{(l)T}\left(\mathbf{q}+i\mathbf{p}\right)\right) \\
=&-\frac{\mathrm{c}}{2}\sum_l \lambda_l\left[q_l'^2 + p_l'^2\right] \\
&-\frac{1}{\sqrt{2}}\sum_l \left(\left(q'_l - ip'_l\right)\tilde{\beta}_l + \tilde{\beta}'_l\left(q'_l + ip'_l\right)\right),
\end{aligned} \tag{B.7}$$

where $\tilde{\beta}_l = \mathbf{U}^{(l)T}\boldsymbol{\beta}$ and $\tilde{\beta}'_l = \mathbf{U}^{(l)T}\boldsymbol{\beta}'$. Grouping terms and completing the square

$$\begin{aligned}
=&\sum_l \left[-\frac{\mathrm{c}\lambda_l}{2}q_l'^2 - \frac{\mathrm{c}\lambda_l}{2}p_l'^2 - \frac{1}{\sqrt{2}}\left(\left(q'_l - ip'_l\right)\tilde{\beta}_l + \tilde{\beta}'_l\left(q'_l + ip'_l\right)\right)\right] \\
=&\sum_l \left[-\frac{\mathrm{c}\lambda_l}{2}q_l'^2 - \frac{\mathrm{c}\lambda_l}{2}p_l'^2 - \frac{1}{\sqrt{2}}\left(\tilde{\beta}_l + \tilde{\beta}'_l\right)q'_l - \frac{i}{\sqrt{2}}\left(\tilde{\beta}'_l - \tilde{\beta}_l\right)p'_l\right] \\
=&-\sum_l \frac{\mathrm{c}\lambda_l}{2}\left[q_l'^2 + \frac{\sqrt{2}}{\mathrm{c}\lambda_l}\left(\tilde{\beta}_l + \tilde{\beta}'_l\right)q'_l + \frac{1}{2\mathrm{c}^2\lambda_l^2}\left(\tilde{\beta}_l + \tilde{\beta}'_l\right)^2\right. \\
&+ p_l'^2 + \frac{i\sqrt{2}}{\mathrm{c}\lambda_l}\left(\tilde{\beta}'_l - \tilde{\beta}_l\right)p'_l - \frac{1}{2\mathrm{c}^2\lambda_l^2}\left(\tilde{\beta}'_l - \tilde{\beta}_l\right)^2 \\
&\left.+\frac{1}{2\mathrm{c}^2\lambda_l^2}\left(\tilde{\beta}'_l - \tilde{\beta}_l\right)^2 - \frac{1}{2\mathrm{c}^2\lambda_l^2}\left(\tilde{\beta}_l + \tilde{\beta}'_l\right)^2\right] \\
=&-\sum_l \frac{\mathrm{c}\lambda_l}{2}\left[\left(q'_l + \frac{1}{\sqrt{2}\mathrm{c}\lambda_l}\left(\tilde{\beta}_l + \tilde{\beta}'_l\right)\right)^2\right. \\
&\left.+\left(p'_l + \frac{i}{\sqrt{2}\mathrm{c}\lambda_l}\left(\tilde{\beta}'_l - \tilde{\beta}_l\right)\right)^2 - \frac{2\tilde{\beta}'_l\tilde{\beta}_l}{\mathrm{c}^2\lambda_l^2}\right] \\
=&-\sum_l \left[\frac{\mathrm{c}\lambda_l}{2}\left(q'_l + \frac{1}{\sqrt{2}\mathrm{c}\lambda_l}\left(\tilde{\beta}_l + \tilde{\beta}'_l\right)\right)^2\right. \\
&\left.+\frac{\mathrm{c}\lambda_l}{2}\left(p'_l + \frac{i}{\sqrt{2}\mathrm{c}\lambda_l}\left(\tilde{\beta}'_l - \tilde{\beta}_l\right)\right)^2 - \frac{\tilde{\beta}'_l\tilde{\beta}_l}{\mathrm{c}\lambda_l}\right].
\end{aligned} \tag{B.8}$$

Recall that the expression is broken into dimension N, therefore performing an N-dimensional integral for each variable, $\mathbf{p}$ and $\mathbf{q}$, produces $2N$ integrals

$$\begin{aligned}\int \exp\Bigg(-\sum_l \Bigg[&\frac{\mathrm{c}\lambda_l}{2}\left(q_l' + \frac{1}{\sqrt{2}\mathrm{c}\lambda_l}\left(\tilde{\beta}_l + \tilde{\beta}_l'\right)\right)^2 \\ &+\frac{\mathrm{c}\lambda_l}{2}\left(p_l' + \frac{i}{\sqrt{2}\mathrm{c}\lambda_l}\left(\tilde{\beta}_l' - \tilde{\beta}_l\right)\right)^2 - \frac{\tilde{\beta}_l'\tilde{\beta}_l}{\mathrm{c}\lambda_l}\Bigg]\Bigg) d^N\mathbf{p}d^N\mathbf{q}.\end{aligned} \tag{B.9}$$

A change of variables needs to be performed such that the integral is performed over $\mathbf{p}'$ and $\mathbf{q}'$. Consider the integral measure $d^N\mathbf{p}$. To change the integral measure to $d^N\mathbf{p}'$ a Jacobian is used, i.e. $d^N\mathbf{p} = \det(J)\, d^N\mathbf{p}' = \det\left(\frac{\partial(p_1,\ldots,p_N)}{\partial(p_1',\ldots,p_N')}\right) d^N\mathbf{p}'$. Recall that $p_l' = \mathbf{U}^{(l)T}\mathbf{p}$, therefore using the property of projection matrices $\mathbf{I} = \sum_j \mathbf{U}^{(j)}\mathbf{U}^{(j)T}$ where $\mathbf{I}$ is the N-dimensional identity matrix in this context, $\mathbf{p} = \sum_j \mathbf{U}^{(j)}p_j'$ is obtained. The Jacobian, $\mathbf{J}$, is constructed by the use of $J_{ij} = \frac{\partial p_i}{\partial p_j'}$

$$\begin{aligned}J_{ij} &= \frac{\partial p_i}{\partial p_j'} \\ &= \frac{\partial}{\partial p_j'}\sum_m U_i^{(m)}p_m' \\ &= U_i^{(j)}.\end{aligned} \tag{B.10}$$

$U_i^{(j)}$ is the element in the ith row of the jth eigenvector. Eq. (B.10) essentially means that the jth column of the Jacobian will contain the jth eigenvector, therefore the Jacobian is composed of the eigenvectors of matrix $\mathbf{P}$, it follows that the Jacobian is an orthogonal matrix. These types of matrices are typically used in similarity transformations to map a matrix into a diagonal matrix. One useful property of orthogonal matrices is $\mathbf{W}\mathbf{W}^T = \mathbf{I} \implies \det\left(\mathbf{W}\mathbf{W}^T\right) = 1 \implies \det(\mathbf{W}) = \pm 1$ for an orthogonal matrix, $\mathbf{W}$. However, the case where $\det(\mathbf{W}) = 1$ is considered. Since the orthogonal matrix equals to the Jacobian, it follows that $\det(\mathbf{J}) = \det\left(\frac{\partial(p_1,\ldots,p_N)}{\partial(p_1',\ldots,p_N')}\right) = 1$ which means that $d^N\mathbf{p} = d^N\mathbf{p}'$. A similar approach can be done for $\mathbf{q}$ which will produce $d^N\mathbf{q} = d^N\mathbf{q}'$. This brings the

isotropic Gaussian to

$$\begin{aligned}
&\int \exp\left(-\sum_l \left[\frac{\mathrm{c}\lambda_l}{2}\left(q_l' + \frac{1}{\sqrt{2}\mathrm{c}\lambda_l}\left(\tilde{\beta}_l + \tilde{\beta}_l'\right)\right)^2\right.\right. \\
&\left.\left. + \frac{\mathrm{c}\lambda_l}{2}\left(p_l' + \frac{i}{\sqrt{2}\mathrm{c}\lambda_l}\left(\tilde{\beta}_l' - \tilde{\beta}_l\right)\right)^2 - \frac{\tilde{\beta}_l'\tilde{\beta}_l}{\mathrm{c}\lambda_l}\right]\right) d^N\mathbf{p}' d^N\mathbf{q}' \\
&= \exp\left(\sum_l \frac{\tilde{\beta}_l'\tilde{\beta}_l}{\mathrm{c}\lambda_l}\right) \int \exp\left(-\sum_l \frac{\mathrm{c}\lambda_l}{2}\left(q_l' + \frac{1}{\sqrt{2}\mathrm{c}\lambda_l}\left(\tilde{\beta}_l + \tilde{\beta}_l'\right)\right)^2\right) d^N\mathbf{q}' \\
&\int \exp\left(-\sum_l \frac{\mathrm{c}\lambda_l}{2}\left(p_l' + \frac{i}{\sqrt{2}\mathrm{c}\lambda_l}\left(\tilde{\beta}_l' - \tilde{\beta}_l\right)\right)^2\right) d^N\mathbf{p}' \\
&= \exp\left(\sum_l \frac{\tilde{\beta}_l'\tilde{\beta}_l}{\mathrm{c}\lambda_l}\right) \left(\sqrt{\frac{2\pi}{\mathrm{c}}}\right)^N \frac{1}{\sqrt{\prod_n \lambda_n}} \left(\sqrt{\frac{2\pi}{\mathrm{c}}}\right)^N \frac{1}{\sqrt{\prod_n \lambda_n}} \\
&= \exp\left(\sum_l \frac{\tilde{\beta}_l'\tilde{\beta}_l}{\mathrm{c}\lambda_l}\right) \left(\frac{2\pi}{\mathrm{c}}\right)^N \frac{1}{\prod_n \lambda_n}.
\end{aligned} \tag{B.11}$$

The eigenvalues belong to matrix $\mathbf{P}$, therefore the product of all the eigenvalues of matrix $\mathbf{P}$ is equal to the determinant. The expressions $\tilde{\beta}_l = \mathbf{U}^{(l)T}\boldsymbol{\beta}$ and $\tilde{\beta}_l' = \mathbf{U}^{(l)T}\boldsymbol{\beta}'$, as defined earlier, will be used and brings the isotropic Gaussian to

$$\begin{aligned}
&\frac{(2\pi)^N}{\mathrm{c}^N \det(\mathbf{P})} \exp\left(\sum_l \frac{\boldsymbol{\beta}'^T \mathbf{U}^{(l)}\mathbf{U}^{(l)T}\boldsymbol{\beta}}{\mathrm{c}\lambda_l}\right) \\
&= \frac{(2\pi)^N}{\mathrm{c}^N \det(\mathbf{P})} \exp\left(\frac{1}{\mathrm{c}}\boldsymbol{\beta}'^T \sum_l \left(\frac{\mathbf{U}^{(l)}\mathbf{U}^{(l)T}}{\lambda_l}\right)\boldsymbol{\beta}\right) \\
&= \frac{(2\pi)^N}{\mathrm{c}^N \det(\mathbf{P})} \exp\left(\frac{1}{\mathrm{c}}\boldsymbol{\beta}'^T \mathbf{P}^{-1}\boldsymbol{\beta}\right).
\end{aligned} \tag{B.12}$$

It has just been shown that

$$\begin{aligned}&\int \exp\Big(-\frac{\mathrm{c}}{2}\left[\mathbf{qPq}+i\mathbf{qPp}-i\mathbf{pPq}+\mathbf{pPp}\right]\\&-\frac{1}{\sqrt{2}}\left(\left(\mathbf{q}-i\mathbf{p}\right)\boldsymbol{\beta}+\boldsymbol{\beta}'^{T}\left(\mathbf{q}+i\mathbf{p}\right)\right)\Big)\,d^{N}\mathbf{p}d^{N}\mathbf{q}\\&=\frac{(2\pi)^{N}}{\mathrm{c}^{N}\det(\mathbf{P})}\exp\left(\frac{1}{\mathrm{c}}\boldsymbol{\beta}'^{T}\mathbf{P}^{-1}\boldsymbol{\beta}\right).\end{aligned}\tag{B.13}$$

Both sides of the equation is divided by $(2\pi)^N$ and written in terms of $\boldsymbol{\beta}=\frac{\mathbf{q}+i\mathbf{p}}{\sqrt{2}}$

$$\begin{aligned}&\int \exp\left(-\mathrm{c}\left[\frac{(\mathbf{q}-i\mathbf{p})}{\sqrt{2}}\mathbf{P}\frac{(\mathbf{q}+i\mathbf{p})}{\sqrt{2}}\right]\right.\\&\left.-\frac{1}{\sqrt{2}}\left(\left(\mathbf{q}-i\mathbf{p}\right)\boldsymbol{\beta}+\boldsymbol{\beta}'^{T}\left(\mathbf{q}+i\mathbf{p}\right)\right)\right)\frac{1}{(2\pi)^{N}}d^{N}\mathbf{p}d^{N}\mathbf{q}\\&=\frac{1}{\mathrm{c}^{N}\det(\mathbf{P})}\exp\left(\frac{1}{\mathrm{c}}\boldsymbol{\beta}'^{T}\mathbf{P}^{-1}\boldsymbol{\beta}\right).\end{aligned}\tag{B.14}$$

Performing the substitution of $\boldsymbol{\alpha}$ on the left-hand side gives the final answer

$$\begin{aligned}&\int \exp\left(-\mathrm{c}\boldsymbol{\alpha}^{*}\mathbf{P}\boldsymbol{\alpha}-\boldsymbol{\alpha}^{*}\boldsymbol{\beta}-\boldsymbol{\beta}'^{T}\boldsymbol{\alpha}\right)D^{\circ}(\boldsymbol{\alpha})\\&=\frac{1}{\mathrm{c}^{N}\det(\mathbf{P})}\exp\left(\frac{1}{\mathrm{c}}\boldsymbol{\beta}'^{T}\mathbf{P}^{-1}\boldsymbol{\beta}\right),\end{aligned}\tag{B.15}$$

where $D^{\circ}(\boldsymbol{\alpha})=\frac{1}{(2\pi)^{N}}d^{N}\mathbf{p}d^{N}\mathbf{q}$. Analogously to Eq. (B.15), if the dimension is $N=\Omega=\mathrm{tr}(\mathbb{1})$ and instead of symmetric matrices, kernels are included, then Eq. (B.1) is obtained.

Another interesting expression which can be seen is the functional integral of a real field, in contrast to the functional integral over a complex field variable, α, shown above. The field q is considered since it is real. Essentially, the integral over q for the discrete case will be shown and will be performed much faster than for the complex case

$$\begin{aligned}&\int \exp\left(-\mathrm{c}q\diamond P\diamond q-q\diamond\beta\right)\mathcal{D}[q]\\&=\exp\left(\frac{\beta\diamond P^{-1}\diamond\beta}{4\mathrm{c}}\right)\frac{\pi^{\Omega/2}}{\mathrm{c}^{\Omega/2}\sqrt{\det\left(P\right)}}.\end{aligned}\tag{B.16}$$

Much like the case before, the exponent is discretized. Consider the assumptions and transformations of the previous case

$$\begin{aligned}
&- \mathrm{c}\mathbf{q}^T\mathbf{P}\mathbf{q} - \mathbf{q}^T\boldsymbol{\beta} \\
&= \sum_l \left[-\mathrm{c}\lambda_l q_l'^2 - q_l'\tilde{\beta}_l\right] \\
&= -\sum_l \mathrm{c}\lambda_l \left(q_l' + \frac{\tilde{\beta}_l}{2\mathrm{c}\lambda_l}\right)^2 + \sum_l \frac{\tilde{\beta}_l{}^2}{4\mathrm{c}\lambda_l}.
\end{aligned} \tag{B.17}$$

The integral is performed

$$\begin{aligned}
&\int \exp\left(-\mathrm{c}\mathbf{q}^T\mathbf{P}\mathbf{q} - \mathbf{q}^T\boldsymbol{\beta}\right) d^N\mathbf{q} \\
&= \exp\left(\sum_l \frac{\tilde{\beta}_l{}^2}{4\mathrm{c}\lambda_l}\right) \int \exp\left(-\sum_l \mathrm{c}\lambda_l \left(q_l' + \frac{\tilde{\beta}_l}{2\mathrm{c}\lambda_l}\right)^2\right) d^N\mathbf{q}' \\
&= \exp\left(\sum_l \frac{\tilde{\beta}_l{}^2}{4\mathrm{c}\lambda_l}\right) \sqrt{\frac{\pi^N}{\mathrm{c}^N \prod_l \lambda_l}} \\
&= \exp\left(\frac{\boldsymbol{\beta}^T\mathbf{P}^{-1}\boldsymbol{\beta}}{4\mathrm{c}}\right) \frac{\pi^{N/2}}{\mathrm{c}^{N/2}\sqrt{\det\left(\mathbf{P}\right)}}.
\end{aligned} \tag{B.18}$$

It has been shown that

$$\begin{aligned}
&\int \exp\left(-\mathrm{c}\mathbf{q}^T\mathbf{P}\mathbf{q} - \mathbf{q}^T\boldsymbol{\beta}\right) d^N\mathbf{q} \\
&= \exp\left(\frac{\boldsymbol{\beta}^T\mathbf{P}^{-1}\boldsymbol{\beta}}{4\mathrm{c}}\right) \frac{\pi^{N/2}}{\mathrm{c}^{N/2}\sqrt{\det\left(\mathbf{P}\right)}}.
\end{aligned} \tag{B.19}$$

In analogy to the functional integral over α, the case where the dimension is $N = \Omega = \mathrm{tr}(\mathbb{1})$ is considered, and the inclusion of kernels instead of symmetric matrices. The functional integral over a real field, q is obtained

$$\begin{aligned}
&\int \exp\left(-\mathrm{c}q \diamond P \diamond q - q \diamond \beta\right) \mathcal{D}[q] \\
&= \exp\left(\frac{\beta \diamond P^{-1} \diamond \beta}{4\mathrm{c}}\right) \frac{\pi^{\Omega/2}}{\mathrm{c}^{\Omega/2}\sqrt{\det\left(P\right)}}.
\end{aligned} \tag{B.20}$$

Appendix C

The delta functional

This proof was done independently. The functional integration of the Wigner functional leading to delta functionals are now performed

$$
\begin{aligned}
&\int W_{\hat{\rho}}\left[\alpha-\alpha_2,\beta\right]\exp\Bigg(\left(-2\alpha_2^*-\mu_2^*\right)\diamond\alpha_1-\alpha_1^*\diamond\left(\mu_1-2\alpha_2\right)\Bigg)\mathcal{D}^\circ[\alpha_1]\mathcal{D}^\circ[\alpha_2]\\
&=\int W_{\hat{\rho}}\left[p-p_2,q-q_2,\beta\right]\exp\Bigg(\Bigg(-\left(q_2-ip_2\right)-\frac{1}{\sqrt{2}}\mu_2^*\Bigg)\diamond\left(q_1+ip_1\right)\\
&-\left(q_1-ip_1\right)\diamond\Bigg(\frac{1}{\sqrt{2}}\mu_1-\left(q_2+ip_2\right)\Bigg)\Bigg)\mathcal{D}^\circ[p_1,q_1]\mathcal{D}^\circ[p_2,q_2]\\
&=\int W_{\hat{\rho}}\left[p-p_2,q-q_2,\beta\right]\exp\Bigg(-q_2\diamond q_1+ip_2\diamond q_1-\frac{1}{\sqrt{2}}\mu_2^*\diamond q_1-iq_2\diamond p_1\\
&-p_2\diamond p_1-\frac{i}{\sqrt{2}}\mu_2^*\diamond p_1-\frac{1}{\sqrt{2}}q_1\diamond\mu_1+q_1\diamond\left(q_2+ip_2\right)\\
&+\frac{i}{\sqrt{2}}p_1\diamond\mu_1-ip_1\diamond\left(q_2+ip_2\right)\Bigg)\mathcal{D}^\circ[p_1,q_1]\mathcal{D}^\circ[p_2,q_2]\\
&=\int W_{\hat{\rho}}\left[p-p_2,q-q_2,\beta\right]\exp\Bigg(2ip_2\diamond q_1-\frac{1}{\sqrt{2}}\mu_2^*\diamond q_1-2iq_2\diamond p_1\\
&-\frac{i}{\sqrt{2}}\mu_2^*\diamond p_1-\frac{1}{\sqrt{2}}q_1\diamond\mu_1+\frac{i}{\sqrt{2}}p_1\diamond\mu_1\Bigg)\mathcal{D}^\circ[p_1,q_1]\mathcal{D}^\circ[p_2,q_2].
\end{aligned}
\tag{C.1}
$$

The integral over p_1 is performed which produces a delta function. But just before this step, a change of variables is performed, $\tilde{p_1} = 2p_1$ and we obtain

$$\begin{aligned}
&\int W_{\hat{\rho}}\left[p-p_2, q-q_2, \beta\right] \exp\left(2ip_1 \diamond \left(-q_2 - \frac{1}{2\sqrt{2}}\mu_2^* + \frac{1}{2\sqrt{2}}\mu_1\right)\right. \\
&= \frac{1}{N_0}\int W_{\hat{\rho}}\left[p-p_2, q-q_2, \beta\right] \exp\left(i\tilde{p_1} \diamond \left(-q_2 - \frac{1}{2\sqrt{2}}\mu_2^* + \frac{1}{2\sqrt{2}}\mu_1\right)\right. \\
&\left. + 2ip_2 \diamond q_1 - \frac{1}{\sqrt{2}}\mu_2^* \diamond q_1 - \frac{1}{\sqrt{2}} q_1 \diamond \mu_1\right) \mathcal{D}^\circ[\tilde{p_1}, q_1]\mathcal{D}^\circ[p_2, q_2] \qquad \text{(C.2)} \\
&= \frac{1}{N_0}\int \delta\left[-q_2 + \frac{\mu_1 - \mu_2^*}{2\sqrt{2}}\right] W_{\hat{\rho}}\left[p-p_2, q-q_2, \beta\right] \exp\left(2ip_2 \diamond q_1\right. \\
&\left. - \frac{1}{\sqrt{2}}\mu_2^* \diamond q_1 - \frac{1}{\sqrt{2}} q_1 \diamond \mu_1\right) \mathcal{D}[q_1]\mathcal{D}^\circ[p_2, q_2].
\end{aligned}$$

The factor of $\frac{1}{N_0}$ is obtained by changing the integration measure to $\mathcal{D}^\circ[\frac{\tilde{p_1}}{2}]$, and pulling out the factor of $\frac{1}{2}$ from the integral measure. The field variable q_2 is now integrated over to give

$$\begin{aligned}
&\frac{1}{N_0}\int W_{\hat{\rho}}\left[p-p_2, q-\frac{\mu_1-\mu_2^*}{2\sqrt{2}}, \beta\right] \exp\left(2ip_2 \diamond q_1 - \frac{1}{\sqrt{2}}\mu_2^* \diamond q_1\right. \\
&\left. - \frac{1}{\sqrt{2}} q_1 \diamond \mu_1\right) \mathcal{D}[q_1]\mathcal{D}^\circ[p_2].
\end{aligned} \qquad \text{(C.3)}$$

Before q_1 is integrated over to produce another Dirac delta functional, a substitution similar to the method before is performed $\tilde{q_1} = 2q_1$. This gives

$$\begin{aligned}
&\frac{1}{N_0}\int W_{\hat{\rho}}\left[p-p_2, q-\frac{\mu_1-\mu_2^*}{2\sqrt{2}}, \beta\right] \exp\left(2iq_1 \diamond \left(p_2 + i\frac{1}{2\sqrt{2}}\mu_2^*\right.\right. \\
&\left.\left. + i\frac{1}{2\sqrt{2}}\mu_1\right)\right) \mathcal{D}[q_1]\mathcal{D}^\circ[p_2] \\
&= \frac{1}{N_0^2}\int W_{\hat{\rho}}\left[p-p_2, q-\frac{\mu_1-\mu_2^*}{2\sqrt{2}}, \beta\right] \exp\left(i\tilde{q_1} \diamond \left(p_2 + i\frac{1}{2\sqrt{2}}\mu_2^*\right.\right. \\
&\left.\left. + i\frac{1}{2\sqrt{2}}\mu_1\right)\right) \mathcal{D}[\tilde{q_1}]\mathcal{D}^\circ[p_2] \\
&= \frac{(2\pi)^\Omega}{N_0^2}\int W_{\hat{\rho}}\left[p-p_2, q-\frac{\mu_1-\mu_2^*}{2\sqrt{2}}, \beta\right] \delta\left[p_2 + i\frac{1}{2\sqrt{2}}\mu_2^* + i\frac{1}{2\sqrt{2}}\mu_1\right] \mathcal{D}^\circ[p_2].
\end{aligned} \qquad \text{(C.4)}$$

The delta functional with an imaginary component is justified by mentioning that the coefficients of i are generating parameter fields which will be set to 0 later in the calculations. Therefore, the expression above is used since the imaginary component will drop out later. This leads to

$$\begin{aligned}&\frac{1}{N_0^2}\int W_{\hat{\rho}}\left[p-p_2, q-\frac{\mu_1-\mu_2^*}{2\sqrt{2}}, \beta\right]\delta\left[p_2+i\frac{1}{2\sqrt{2}}\mu_2^*+i\frac{1}{2\sqrt{2}}\mu_1\right]\mathcal{D}[p_2]\\&=\frac{1}{N_0^2}W_{\hat{\rho}}\left[p+i\frac{\mu_2^*+\mu_1}{2\sqrt{2}}, q-\frac{\mu_1-\mu_2^*}{2\sqrt{2}}, \beta\right].\end{aligned}\tag{C.5}$$

The overall factor of $(2\pi)^\Omega$ cancels with the the factor of $\frac{1}{(2\pi)^\Omega}$ hidden in $\mathcal{D}^\circ[p_2]$. The dependence of $W_{\hat{\rho}}$ is written in terms of α and α^* instead of its p and q dependence. Consider the p, dependence

$$\begin{aligned}&p+i\frac{\mu_2^*+\mu_1}{2\sqrt{2}}\\&=i\left(\frac{\alpha^*-\alpha}{\sqrt{2}}+\frac{\mu_2^*+\mu_1}{2\sqrt{2}}\right)\\&=i\frac{1}{\sqrt{2}}\left(\alpha^*+\frac{\mu_2^*}{2}-\left(\alpha-\frac{\mu_1}{2}\right)\right).\end{aligned}\tag{C.6}$$

Doing exactly the same procedure for $q-\frac{\mu_1-\mu_2^*}{2\sqrt{2}}$ produces

$$\begin{aligned}&q-\frac{\mu_1-\mu_2^*}{2\sqrt{2}}\\&=\frac{1}{\sqrt{2}}\left(\alpha^*+\frac{\mu_2^*}{2}+\alpha-\frac{\mu_1}{2}\right).\end{aligned}\tag{C.7}$$

Therefore, Eq. (C.1) can be written as

$$\begin{aligned}&\int W_{\hat{\rho}}\left[\alpha-\alpha_2, \beta\right]\exp\left(\left(-2\alpha_2^*-\mu_2^*\right)\diamond\alpha_1-\alpha_1^*\diamond\left(\mu_1-2\alpha_2\right)\right)\mathcal{D}^\circ[\alpha_1]\mathcal{D}^\circ[\alpha_2]\\&=\frac{1}{N_0^2}W_{\hat{\rho}}\left[\alpha^*+\frac{\mu_2^*}{2}, \alpha-\frac{\mu_1}{2}, \beta\right].\end{aligned}\tag{C.8}$$

Appendix D

The Magnus expansion

The starting point for the Magnus expansion is the evolution equation [17]

$$\frac{\partial W_{\hat{\sigma}}}{\partial z} = \frac{1}{2}\frac{\delta W_{\hat{\sigma}}}{\delta \alpha^*} \diamond H \diamond \alpha + \frac{1}{2}\alpha^* \diamond H^* \diamond \frac{\delta W_{\hat{\sigma}}}{\delta \alpha}, \tag{D.1}$$

and the ansatz [17]

$$W_{\hat{\sigma}} = N_0 \exp(-2\alpha^* \diamond A(z) \diamond \alpha - \alpha \diamond B(z) \diamond \alpha - \alpha^* \diamond B^*(z) \diamond \alpha^*). \tag{D.2}$$

The aim is to solve for $W_{\hat{\sigma}}$ which means that the kernels $A(z)$ and $B(z)$ have to be found, and in order to obtain a solution for the kernels, the ansatz is substituted into the evolution equation

$$\begin{aligned}
&\left(-2\alpha^* \diamond \frac{\partial A(z)}{\partial z} \diamond \alpha - \alpha \diamond \frac{\partial B(z)}{\partial z} \diamond \alpha - \alpha^* \diamond \frac{\partial B^*(z)}{\partial z} \diamond \alpha^*\right) W_{\hat{\sigma}} \\
&= \frac{W_{\hat{\sigma}}}{2}\left(-2\alpha \diamond A^T(z) - \alpha^* \diamond B^\dagger(z) - \alpha^* \diamond B^*(z)\right) \diamond H \diamond \alpha \\
&+ \frac{W_{\hat{\sigma}}}{2}\alpha^* \diamond H^* \diamond \left(-2A^T(z) \diamond \alpha^* - B(z) \diamond \alpha - B^T(z) \diamond \alpha\right).
\end{aligned} \tag{D.3}$$

The above equation is divided by $W_{\hat{\sigma}}$, and the fact that $B(z)$ is symmetric is used in order to simplify the equation

$$\begin{aligned}
&2\alpha^* \diamond \frac{\partial A(z)}{\partial z} \diamond \alpha + \alpha \diamond \frac{\partial B(z)}{\partial z} \diamond \alpha + \alpha^* \diamond \frac{\partial B^*(z)}{\partial z} \diamond \alpha^* \\
&= \alpha \diamond A^T(z) \diamond H \diamond \alpha + \alpha^* \diamond B^*(z) \diamond H \diamond \alpha \\
&+ \alpha^* \diamond H^* \diamond A^T(z) \diamond \alpha^* + \alpha^* \diamond H^* \diamond B(z) \diamond \alpha.
\end{aligned} \tag{D.4}$$

The kernel derivatives, $\frac{\partial A(z)}{\partial z}$ and $\frac{\partial B(z)}{\partial z}$, are solved for. In order to solve for $\frac{\partial A(z)}{\partial z}$, the functional derivatives with respect to α^* and α is performed since $\frac{\partial A(z)}{\partial z}$ is diamond contracted with these complex field variables. Starting with the functional derivative with respect to α^*

$$\begin{aligned} &2\frac{\partial A(z)}{\partial z} \diamond \alpha + \frac{\partial B^*(z)}{\partial z} \diamond \alpha^* + \frac{\partial B^\dagger(z)}{\partial z} \diamond \alpha^* \\ &= B^*(z) \diamond H \diamond \alpha + H^* \diamond A^T(z) \diamond \alpha^* \\ &+ A(z) \diamond H^* \diamond \alpha^* + H^* \diamond B(z) \diamond \alpha, \end{aligned} \tag{D.5}$$

and now for the functional derivative with respect to α

$$\frac{\partial A(z)}{\partial z} = \frac{1}{2} B^*(z) \diamond H + \frac{1}{2} H^* \diamond B(z). \tag{D.6}$$

The same procedure is followed for $\frac{\partial B(z)}{\partial z}$ and $\frac{\partial B^*(z)}{\partial z}$, and produces the following system of kernel differential equations, where the dependence on the propagation distance for the kernels, H, is explicitly written [17]

$$\begin{aligned} \frac{\partial A(z)}{\partial z} &= \frac{1}{2} H^*(z) \diamond B(z) + \frac{1}{2} B^*(z) \diamond H(z), \\ \frac{\partial B(z)}{\partial z} &= \frac{1}{2} H(z) \diamond A(z) + \frac{1}{2} A^T(z) \diamond H(z), \\ \frac{\partial B^*(z)}{\partial z} &= \frac{1}{2} A(z) \diamond H^*(z) + \frac{1}{2} H^*(z) \diamond A^T(z). \end{aligned} \tag{D.7}$$

The reader is reminded that the diamond products act on the transverse wave vectors, the dependence on transverse wave vectors will not be explicitly written here for the sake of simplicity. The system of kernel differential equations above are solved by integrating with respect to z and back-substituting. The result will be solutions for A, B, and B^* in the form of an expansion, and is done below

$$\begin{aligned} &\int_0^z \frac{\partial A(z_1)}{\partial z_1} dz_1 = A(z) - A(0) \\ &= \frac{1}{2} \int_0^z H^*(z_1) \diamond B(z_1) dz_1 + \frac{1}{2} \int_0^z B^*(z_1) \diamond H(z_1) dz_1 \\ \implies &A(z) = \mathbb{1} + \frac{1}{2} \int_0^z H^*(z_1) \diamond B(z_1) dz_1 + \frac{1}{2} \int_0^z B^*(z_1) \diamond H(z_1) dz_1. \end{aligned} \tag{D.8}$$

Applying a similar procedure to B produces

$$\begin{aligned} B(z) &= \frac{1}{2}\int_0^z H(z_1)\diamond A(z_1)dz_1 + \frac{1}{2}\int_0^z A^T(z_1)\diamond H(z_1)dz_1, \\ B^*(z) &= \frac{1}{2}\int_0^z A(z_1)\diamond H^*(z_1)dz_1 + \frac{1}{2}\int_0^z H^*(z_1)\diamond A^T(z_1)dz_1. \end{aligned} \tag{D.9}$$

An expression for B^* is written above for convenience when back-substituting. Focusing on solving the differential equation for A, the SPDC kernels B and B^* is substituted into Eq. (D.8), which produces

$$\begin{aligned} A(z) &= \mathbb{1} + \frac{1}{2}\int_0^z H^*(z_1)\diamond \left(\frac{1}{2}\int_0^z H(z_1)\diamond A(z_1)dz_1\right. \\ &\left. +\frac{1}{2}\int_0^z A^T(z_1)\diamond H(z_1)dz_1\right)dz_1 \\ &+ \frac{1}{2}\int_0^z \left(\frac{1}{2}\int_0^z A(z_1)\diamond H^*(z_1)dz_1 + \frac{1}{2}\int_0^z H^*(z_1)\diamond A^T(z_1)dz_1\right)\diamond H(z_1)dz_1 \\ &= \mathbb{1} + \frac{1}{2^2}\int_0^z\int_0^{z_1} \big(H^*(z_1)\diamond H(z_2)\diamond A(z_2) + H^*(z_1)\diamond A^T(z_2)\diamond H(z_2) \\ &A(z_2)\diamond H^*(z_2)\diamond H(z_1) + H^*(z_2)\diamond A^T(z_2)\diamond H(z_1)\big)\, dz_2 dz_1. \end{aligned} \tag{D.10}$$

The above expression can get incredibly messy, therefore only the first order of A is considered for now, the second order will be considered afterwards. The first order of A comprises of diamond products of the form $H_1 \diamond H_2$, which is obtained by substituting A and A^T into itself once, and is given by

$$\begin{aligned} A^{(1)}(z) &= \frac{1}{2}\int_0^z\int_0^{z_1} \left(H^*(z_1)\diamond H(z_2) + H^*(z_2)\diamond H(z_1)\right) dz_2 dz_1 \\ &= \int_0^z\int_0^{z_1} \mathcal{Z}\left\{H^*(z_1)\diamond H(z_2)\right\} dz_2 dz_1, \end{aligned} \tag{D.11}$$

where [17]

$$\begin{aligned} &\mathcal{Z}\left\{H_1(z_1)\diamond\cdots\diamond H_n(z_n)\right\} \\ &= \frac{1}{2}\left[H_1(z_1)\diamond \mathcal{Z}\left\{H_2(z_2)\diamond\cdots\diamond H_n(z_n)\right\}\right. \\ &\left. +\mathcal{Z}\left\{H_1(z_2)\diamond\cdots\diamond H_{n-1}(z_n)\right\}\diamond H_n(z_1)\right], \end{aligned} \tag{D.12}$$

and $\mathcal{Z}\left\{H_1(z_1)\right\} = H_1(z_1)$. The second order term of A is now of interest and is obtained by substituting A and A^T into A (itself) twice and gathering the

terms which have the form $H_1 \diamond H_2 \diamond H_3 \diamond H_4$

$$\begin{aligned}
A^{(2)}(z) &= \frac{1}{2^3}\int_0^z \int_0^{z_1} \int_0^{z_2} \int_0^{z_3} (H^*(z_1)\diamond H(z_2)\diamond H^*(z_3)\diamond H(z_4) \\
&+ H^*(z_1)\diamond H(z_2)\diamond H^*(z_4)\diamond H(z_3) + H^*(z_1)\diamond H(z_4)\diamond H^*(z_3)\diamond H(z_2) \\
&+ H^*(z_1)\diamond H(z_3)\diamond H^*(z_4)\diamond H(z_2) + H^*(z_3)\diamond H(z_4)\diamond H^*(z_2)\diamond H(z_1) \\
&+ H^*(z_4)\diamond H(z_3)\diamond H^*(z_2)\diamond H(z_1) + H^*(z_2)\diamond H(z_4)\diamond H^*(z_3)\diamond H(z_1) \\
&+ H^*(z_2)\diamond H(z_3)\diamond H^*(z_4)\diamond H(z_1))\, dz_4 dz_3 dz_2 dz_1 \\
&= \int_0^z \int_0^{z_1} \int_0^{z_2} \int_0^{z_3} \mathcal{Z}\left\{H^*(z_1)\diamond H(z_2)\diamond H^*(z_3)\diamond H(z_4)\right\} dz_4 dz_3 dz_2 dz_1.
\end{aligned} \tag{D.13}$$

Note that the kernel, A, does not contain diamond products of an odd number of H kernels, it will be found in B. Finally, the Magnus expansion for A is obtained [17]

$$\begin{aligned}
A(z) &= \mathbb{1} + \int_0^z \int_0^{z_1} \mathcal{Z}\{H^*(z_1)\diamond H(z_2)\} dz_2 dz_1 \\
&+ \int_0^z \int_0^{z_1} \int_0^{z_2} \int_0^{z_3} \mathcal{Z}\{H^*(z_1)\diamond H(z_2)\diamond H^*(z_3)\diamond H(z_4)\} dz_4 dz_3 dz_2 dz_1 + \ldots.
\end{aligned} \tag{D.14}$$

The SPDC kernel, B, is much easier to obtain since an expression for A is calculated, and is done by simply substituting A and A^T into B, resulting in [17]

$$\begin{aligned}
B(z) &= \int_0^z H(z_1) dz_1 \\
&+ \int_0^z \int_0^{z_1} \int_0^{z_2} \mathcal{Z}\{H(z_1)\diamond H^*(z_2)\diamond H(z_3)\} dz_3 dz_2 dz_1 + \ldots.
\end{aligned} \tag{D.15}$$

The Magnus expansion for B^* is obtained by taking the complex conjugate of B.

A system of kernel differential equations were solved, and the solutions for the kernels were found for A and B in terms of an expansion. The expansion is called the "Magnus expansion" since it has a similar form of an expansion developed by W. Magnus called the Magnus expansion [10].

Appendix E

Derivation of the evolved SPDC state

A derivation on the evolution of the SPDC state is provided here. Firstly, the signal beam is chosen to interact with the object, therefore the star product of the object operators is made to attach to the signal beam. Following the definition of the star product

$$\begin{aligned} W_{\hat{S}\hat{\rho}\hat{S}^\dagger}[\alpha,\beta] &= W_{\hat{S}}[\beta] \star W_{\hat{\rho}}[\alpha,\beta] \star W_{\hat{S}^\dagger}[\beta] \\ &= N^2 \int \exp\Bigg[-\frac{1}{2}\left(\alpha_a+\alpha_b+\beta\right)^* \diamond H \diamond \left(\alpha_a+\alpha_b+\beta\right) \\ &- \frac{1}{2}\left(\alpha_a-\alpha_b+\beta\right)^* \diamond H^\dagger \diamond \left(\alpha_a-\alpha_b+\beta\right) + \left(\beta^*-\alpha_a^*\right) \diamond \alpha_b \\ &- \alpha_b^* \diamond \left(\beta-\alpha_a\right)\Bigg] W_{\hat{\rho}}[\alpha,\alpha_a]\mathcal{D}^\circ[\alpha_a,\alpha_b]. \end{aligned} \tag{E.1}$$

The next step is to bring the above equation into a form which can be integrated. The integration with respect to α_b is first considered, and the integral over α_a will be done later for convenience. The following is obtained

$$\begin{aligned} W_{\hat{S}\hat{\rho}\hat{S}^\dagger}[\alpha,\beta] = N^2 \int \exp\big[&-\alpha_b^* \diamond H_h \diamond \alpha_b - \alpha_b^* \diamond \left[H_a \diamond \left(\alpha_a+\beta\right)+\beta-\alpha_a\right] \\ &- \left[\left(\alpha_a^*+\beta^*\right) \diamond H_a - \beta^* + \alpha_a^*\right] \diamond \alpha_b - \left(\alpha_a^*+\beta^*\right) \diamond H_h \diamond \left(\alpha_a+\beta\right)\big] \\ &W_{\hat{\rho}}[\alpha,\alpha_a]\mathcal{D}^\circ[\alpha_a,\alpha_b], \end{aligned} \tag{E.2}$$

where $H_a = \frac{1}{2}\left(H - H^\dagger\right)$ and $H_h = \frac{1}{2}\left(H + H^\dagger\right)$. The functional integration is now performed over α_b, since it is in the form of Eq. (3.39), and simplifies

to

$$W_{\hat{S}\hat{\rho}\hat{S}^\dagger}[\alpha,\beta] = \frac{N^2 N_0}{\det\left(H+H^\dagger\right)} \int \exp\left[-2\alpha_a^* \diamond H_p \diamond \alpha_a - 2\beta^* \diamond H_p \diamond \beta \right. \\ \left. +2\alpha_a^* \diamond H_n \diamond \beta + 2\beta^* \diamond H_n^\dagger \diamond \alpha_a\right] W_{\hat{\rho}}[\alpha,\alpha_a]\mathcal{D}^\circ[\alpha_a], \tag{E.3}$$

where $H_p = \left(\mathbb{1} + H \diamond H^\dagger\right) \diamond \left(H+H^\dagger\right)^{-1}$ and $H_n = (\mathbb{1}+H) \diamond \left(\mathbb{1} - H^\dagger\right) \diamond \left(H+H^\dagger\right)^{-1}$.

Appendix F

Functional integration of the trace

The trace of interest is given below

$$\mathrm{tr}\left(W_{\hat{S}\hat{\rho}\hat{S}^\dagger}\mathcal{W}_B\mathcal{W}_A\right) = \int W_{\hat{S}\hat{\rho}\hat{S}^\dagger}[\alpha,\beta]\mathcal{W}_B[\beta]\mathcal{D}^\circ[\beta]\mathcal{W}_A[\alpha]\mathcal{D}^\circ[\alpha]. \tag{F.1}$$

The functional integral over β is now studied, and is performed by substituting Eqs. (5.3) and (5.12) for the bucket detector and evolved SPDC state respectively. Thereafter manipulating the equation in order to resemble the functional integral of an isotropic Gaussian in Eq. (3.39), and performing the functional integral over β yields

$$\begin{aligned}&\int W_{\hat{S}\hat{\rho}\hat{S}^\dagger}[\alpha,\beta]\mathcal{W}_B[\beta]\mathcal{D}^\circ[\beta]\\ &= N_E\int \exp\left(-2\alpha_a^*\diamond D_E\diamond\alpha_a\right)W_{\hat{\rho}}[\alpha,\alpha_a]\mathcal{D}^\circ[\alpha_a],\end{aligned} \tag{F.2}$$

where

$$D_E = H_p - H_n\diamond\left(H_p+\frac{1-J}{1+J}\mathbb{1}\right)^{-1}\diamond H_n = (\mathbb{1}-JE\diamond E)\diamond(\mathbb{1}+JE\diamond E)^{-1}, \tag{F.3}$$

and

$$N_E = \frac{N_0}{\det\left(\mathbb{1}+JE\diamond E\right)}. \tag{F.4}$$

The three equations above had been obtained from notes and discussions from my co-supervisor, FS Roux. The remaining integral measure originates

from the evolved SPDC state. This result is taken and substituted into the trace to obtain

$$
\begin{aligned}
&= \frac{2N_E}{1+K} \int W_{\hat{\rho}} \exp\Bigg(-2\alpha_a^* \diamond D_E \diamond \alpha_a \\
&-2\left(\frac{1-K}{1+K}\right) \alpha^* \diamond MM^* \diamond \alpha \Bigg) D^\circ[\alpha_a] D^\circ[\alpha] \\
&= \frac{2N_0^2 N_E}{1+K} \int \exp\Bigg(-2\alpha_a^* \diamond D_E \diamond \alpha_a - 2\left(\frac{1-K}{1+K}\right) \alpha^* \diamond MM^* \diamond \alpha \\
&- 2\alpha^* \diamond A \diamond \alpha - 2\alpha_a^* \diamond A \diamond \alpha_a - 2\alpha^* \diamond B \diamond \alpha_a^* - 2\alpha_a \diamond B^* \diamond \alpha \Bigg) D^\circ[\alpha_a, \alpha] \\
&= \frac{2N_0^2 N_E}{1+K} \int \exp\Bigg(-\alpha^* \diamond \left(2\left(\frac{1-K}{1+K}\right) MM^* + 2A \right) \diamond \alpha - \alpha^* \diamond (2B \diamond \alpha_a^*) \\
&- (2\alpha_a \diamond B^*) \diamond \alpha - 2\alpha_a^* \diamond D_E \diamond \alpha_a - 2\alpha_a^* \diamond A \diamond \alpha_a \Bigg) D^\circ[\alpha_a, \alpha] \\
&= \frac{2N_0 N_E}{(1+K) \det\left(\left(\frac{1-K}{1+K}\right) MM^* + A \right)} \\
\implies & \int \exp\Bigg(2\alpha_a^* \diamond B^* \diamond \left[\left(\frac{1-K}{1+K}\right) MM^* + A \right]^{-1} \diamond B \diamond \alpha_a^* \\
&- 2\alpha_a^* \diamond D_E \diamond \alpha_a - 2\alpha_a^* \diamond A \diamond \alpha_a \Bigg) D^\circ[\alpha_a] \\
&= \frac{2N_0}{(1+K) \det\left[\mathbb{1} + JE \diamond E\right] \det\left[A + (\frac{1-K}{1+K}) MM^*\right]} \\
&\times \frac{1}{\det\left[D_E + A - B \diamond (A^T + (\frac{1-K}{1+K}) M^* M)^{-1} \diamond B^*\right]}.
\end{aligned}
\tag{F.5}
$$

Appendix G

Taking the derivatives and simplifying the trace

This proof was done independently. The start point is to simplify the determinants of the trace which was derived in appendix F

$$\begin{aligned}&\frac{2N_0}{(1+K)\det\left[\mathbb{1}+JE\diamond E\right]\det\left[A+(\frac{1-K}{1+K})MM^*\right]}\\&\times\frac{1}{\det\left[D_E+A-B\diamond(A^T+(\frac{1-K}{1+K})M^*M)^{-1}\diamond B^*\right]},\end{aligned}\tag{G.1}$$

where

$$D_E=H_p-H_n\diamond\left(H_p+\frac{1-J}{1+J}\mathbb{1}\right)^{-1}\diamond H_n=(\mathbb{1}-JE\diamond E)\diamond(\mathbb{1}+JE\diamond E)^{-1}.\tag{G.2}$$

Simplifying the first determinant

$$\det\left[A+\left(\frac{1-K}{1+K}\right)MM^*\right]=\det(A)\det\left[\mathbb{1}+\gamma MM^*\diamond A^{-1}\right],\tag{G.3}$$

where

$$\gamma=\frac{1-K}{1+K}.\tag{G.4}$$

The second determinant can be rewritten as

$$\det\left[\mathbb{1}+\gamma MM^*\diamond A^{-1}\right]=\exp\left[\mathrm{tr}\left(\ln_\diamond\left(\mathbb{1}+\gamma MM^*\diamond A^{-1}\right)\right)\right].\tag{G.5}$$

The natural logarithm can be expanded as follows

$$\begin{aligned}
&\ln_\diamond\left(\mathbb{1}+\gamma MM^*\diamond A^{-1}\right)=\sum_{n=1}^{\infty}\frac{(-1)^{n+1}}{n}\left(\gamma MM^*\diamond A^{-1}\right)^{n_\diamond},\\
\implies &\operatorname{tr}\left(\ln_\diamond\left(\mathbb{1}+\gamma MM^*\diamond A^{-1}\right)\right)=\sum_{n=1}^{\infty}\frac{(-1)^{n+1}}{n}\operatorname{tr}\left[\left(\gamma MM^*\diamond A^{-1}\right)^{n_\diamond}\right]\\
&=-\gamma\int M(\mathbf{k})M^*(\mathbf{k}_2)\diamond A^{-1}(\mathbf{k}_2,\mathbf{k})\eth\mathbf{k}\\
&+\frac{1}{2}\operatorname{tr}\left[\gamma MM^*\diamond A^{-1}\diamond\gamma MM^*\diamond A^{-1}\right]+\cdots\\
&=-\gamma M^*\diamond A^{-1}\diamond M+\frac{\gamma^2}{2}\operatorname{tr}\left[M\eta M^*\diamond A^{-1}\right]+\cdots\\
&=-\gamma\eta+\frac{\gamma^2\eta^2}{2}+\cdots=\sum_{n=1}^{\infty}\frac{(-1)^{n+1}}{n}(\gamma\eta)^n\\
&=\ln(1+\gamma\eta),
\end{aligned}\tag{G.6}$$

where $\eta=M^*\diamond A^{-1}\diamond M$ is a constant. Finally, Eq. (G.5) reduces to

$$\det\left[\mathbb{1}+\gamma MM^*\diamond A^{-1}\right]=1+\gamma\eta,\tag{G.7}$$

and therefore,

$$\det\left[A+\left(\frac{1-K}{1+K}\right)MM^*\right]=(1+\gamma\eta)\det(A).\tag{G.8}$$

Consider the remaining determinant in Eq. (G.1)

$$\det\left[D_E+A-B\diamond\left(\mathbb{1}+\left(\frac{1-K}{1+K}\right)M^*M\diamond(A^{-1})^T\right)^{-1}\diamond(A^{-1})^T\diamond B^*\right].\tag{G.9}$$

To simplify the above equation, the inverse kernel needs to be simplified, and is done by assuming

$$\left(\mathbb{1}+\gamma M^*M\diamond(A^{-1})^T\right)^{-1}=\mathbb{1}-c\gamma M^*M\diamond(A^{-1})^T,\tag{G.10}$$

where c is a constant, it follows that

$$\left(\mathbb{1}+\gamma M^*M\diamond(A^{-1})^T\right)\diamond\left(\mathbb{1}-c\gamma M^*M\diamond(A^{-1})^T\right)=\mathbb{1}.\tag{G.11}$$

The constant, c, is now solved for

$$-c\gamma M^*M\diamond(A^{-1})^T+\gamma M^*M\diamond(A^{-1})^T-c\gamma^2 M^*M\diamond(A^{-1})^T\diamond M^*M\diamond(A^{-1})^T=0. \tag{G.12}$$

The above equation can be divided by γM^*, since it is not contracted to anything, and the right-hand side of the equation is diamond contracted by M^*

$$\begin{aligned} & -cM\diamond(A^{-1})^T\diamond M^*+M\diamond(A^{-1})^T\diamond M^* \\ \implies & -c\gamma M\diamond(A^{-1})^T\diamond M^*M\diamond(A^{-1})^T\diamond M^*=0 \\ \implies & -c\mu+\mu-c\gamma\mu^2=0, \\ \implies & c=\frac{1}{1+\gamma\mu}. \end{aligned} \tag{G.13}$$

The inverse kernel becomes

$$\left(\mathbb{1}+\gamma M^*M\diamond(A^{-1})^T\right)^{-1}=\mathbb{1}-\frac{\gamma M^*M\diamond(A^{-1})^T}{1+\gamma\mu}, \tag{G.14}$$

and is substituted into the determinant

$$\begin{aligned} &\det\left[D_E+A-B\diamond\left(A^T+\left(\frac{1-K}{1+K}\right)M^*M\right)^{-1}\diamond B^*\right] \\ &=\det\left[D_E+A-B\diamond\left(A^{-1}\right)^T\diamond B^*+\frac{\gamma B\diamond M^*M\diamond\left(A^{-2}\right)^T\diamond B^*}{1+\gamma\eta}\right]. \end{aligned} \tag{G.15}$$

Since A is Hermitian, it follows that $A^*=A^T$. Using the identity $A-B\diamond(A^*)^{-1}\diamond B^*=A^{-1}$ which was shown in chapter 4 as a normalization condition

$$\begin{aligned} &\det\left[D_E+A^{-1}+\frac{\gamma B\diamond M^*M\diamond\left(A^*\right)^{-2_\diamond}\diamond B^*}{1+\gamma\eta}\right] \\ &=\det\left(A^{-1}\right)\det\left[\mathbb{1}+D_E\diamond A+\frac{\gamma B\diamond M^*M\diamond\left(A^*\right)^{-2\diamond}\diamond B^*\diamond A}{1+\gamma\eta}\right]. \end{aligned} \tag{G.16}$$

Consider the determinant

$$\begin{aligned} &\det\left[\mathbb{1}+D_E\diamond A+\frac{\gamma B\diamond M^*M\diamond\left(A^*\right)^{-2\diamond}\diamond B^*\diamond A}{1+\gamma\eta}\right] \\ &=\det[\mathbb{1}+D_E\diamond A]\det\left[\mathbb{1}+\frac{\gamma B\diamond M^*M\diamond\left(A^*\right)^{-2\diamond}\diamond B^*\diamond A}{1+\gamma\eta}\right. \\ &\left.\diamond(\mathbb{1}+D_E\diamond A)^{-1}\right]. \end{aligned} \tag{G.17}$$

The first term of the Magnus expansion for A is considered, $A = \mathbb{1}$. Let $p = \left(\frac{1-J}{1+J}\right)$ and $F = \mathbb{1} + D_E$, which simplifies the second determinant to

$$\begin{aligned} &\det\left[\mathbb{1} + \frac{\gamma B \diamond M^* M \diamond B^* \diamond F^{-1}}{1+\gamma\eta}\right] \\ &= \exp\left[\mathrm{tr}\left(\ln_\diamond\left(\mathbb{1} + \frac{\gamma B \diamond M^* M \diamond B^* \diamond F^{-1}}{1+\gamma\eta}\right)\right)\right]. \end{aligned} \tag{G.18}$$

The natural logarithm produces

$$\begin{aligned} &\ln_\diamond\left(\mathbb{1} + \frac{\gamma B \diamond M^* M \diamond B^* \diamond F^{-1}}{1+\gamma\eta}\right) \\ &= \sum_{n=1}^{\infty} \frac{(-1)^{n+1}}{n}\left(\frac{\gamma B \diamond M^* M \diamond B^* \diamond F^{-1}}{1+\gamma\eta}\right)^{n_\diamond}. \end{aligned} \tag{G.19}$$

Taking the trace yields

$$\sum_{n=1}^{\infty} \frac{(-1)^{n+1}}{n}\,\mathrm{tr}\left[\left(\frac{\gamma B \diamond M^* M \diamond B^* \diamond F^{-1}}{1+\gamma\eta}\right)^{n_\diamond}\right]. \tag{G.20}$$

Evaluating the trace and setting $M \diamond B^* \diamond F^{-1} \diamond B \diamond M^* = \zeta$ simplifies the expression to

$$\begin{aligned} &\sum_{n=1}^{\infty} \frac{(-1)^{n+1}}{n}\left(\frac{\gamma\zeta}{1+\gamma\eta}\right)^n = \ln\left(1 + \frac{\gamma\zeta}{1+\gamma\eta}\right) \\ &\implies \det\left[\mathbb{1} + \frac{\gamma B \diamond M^* M \diamond B^* \diamond F^{-1}}{1+\gamma\eta}\right] \\ &= 1 + \frac{\gamma\zeta}{1+\gamma\eta}. \end{aligned} \tag{G.21}$$

The determinants in Eq. (G.1) reduces to

$$\begin{aligned} &\det\left[A + \left(\frac{1-K}{1+K}\right) MM^*\right] \det\left[D_E + A\right. \\ &\left. - B \diamond \left(A^T + \left(\frac{1-K}{1+K}\right) M^* M\right)^{-1} \diamond B^*\right] \det\left[\mathbb{1} + JE \diamond E\right] \\ &= (1+\gamma\eta)\left(1 + \frac{\gamma\zeta}{1+\gamma\eta}\right) \det[\mathbb{1} + D_E] \det\left[\mathbb{1} + JE \diamond E\right] \\ &= (1 + \gamma\eta + \gamma\zeta) \det[\mathbb{1} + D_E] \det\left[\mathbb{1} + JE \diamond E\right]. \end{aligned} \tag{G.22}$$

This simplifies equation (G.1) to

$$\frac{2N_0}{(1+K)\,(1+\gamma\eta+\gamma\zeta)\det[\mathbb{1}+D_E]\det\left[\mathbb{1}+JE\diamond E\right]}. \tag{G.23}$$

Simplifying the following determinant

$$\det\left(\mathbb{1}+JE\diamond E\right)=\exp[\mathrm{tr}\left(\ln_\diamond\left(\mathbb{1}+JE\diamond E\right)\right)]. \tag{G.24}$$

Simplifying the trace of the natural logarithm and noting that $JE\diamond E=E_2$

$$\begin{aligned}&\mathrm{tr}\left(\ln_\diamond\left(\mathbb{1}+JE\diamond E\right)\right)\\&=\sum_{n=1}^{\infty}\frac{(-1)^{n+1}}{n}\,\mathrm{tr}\left[\left(E_2\right)^{n_\diamond}\right].\end{aligned} \tag{G.25}$$

Looking at $(E_2)^{n_\diamond}$

$$\begin{aligned}\left(E_2\right)^{n_\diamond}&=\left[2\pi\delta\left(\omega_1-\omega_2\right)\int Jt^2\exp\left(i\mathbf{X}\cdot\left(\mathbf{k}_1-\mathbf{k}_2\right)\right)d^2\mathbf{X}\right]^{n_\diamond}\\&=2\pi\delta\left(\omega_1-\omega_2\right)\int J^nt^{2n}\exp\left(i\mathbf{X}\cdot\left(\mathbf{k}_1-\mathbf{k}_2\right)\right)d^2\mathbf{X},\\\implies\mathrm{tr}\left[\left(E_2\right)^{n_\diamond}\right]&=2\pi J^n\int t^{2n}\,\mathrm{tr}\left[\delta\left(\omega_1-\omega_2\right)\exp\left(i\mathbf{X}\cdot\left(\mathbf{k}_1-\mathbf{k}_2\right)\right)\right]d^2\mathbf{X}\\&=2\pi\delta(0)J^n\int t^{2n}d^2\mathbf{X}\int đ\mathbf{k}.\end{aligned} \tag{G.26}$$

The following is defined

$$\int t^{2n}d^2\mathbf{X}=\tau. \tag{G.27}$$

Eq. (G.26) then reduces to

$$\mathrm{tr}\left[\left(E_2\right)^{n_\diamond}\right]=2\pi\delta(0)J^n\tau\int đ\mathbf{k} \tag{G.28}$$

$$=\frac{J^n\tau\delta(0)\delta_{\mathbf{X}}(0)\int d^2\mathbf{k}d\omega}{(2\pi)^2\delta_{\mathbf{X}}(0)} \tag{G.29}$$

$$=\frac{J^n\tau}{(2\pi)^2\delta_{\mathbf{X}}(0)}\Omega, \tag{G.30}$$

where $\Omega = \mathrm{tr}(\mathbb{1})$. Eq. (G.25) then becomes

$$\mathrm{tr}\left(\ln_{\diamond}\left(\mathbb{1} + E_2\right)\right) \tag{G.31}$$

$$= \frac{\tau\Omega}{(2\pi)^2\delta_{\mathbf{X}}(0)} \sum_{n=1}^{\infty} \frac{(-1)^{n+1}}{n} J^n \tag{G.32}$$

$$= \frac{\tau\Omega}{(2\pi)^2\delta_{\mathbf{X}}(0)} \ln(1+J) \tag{G.33}$$

$$\implies \det\left(\mathbb{1} + E_2\right) = (1+J)^{\frac{\tau\Omega}{(2\pi)^2\delta_{\mathbf{X}}(0)}}. \tag{G.34}$$

With the methods shown above, it is possible to calculate $\det[\mathbb{1} + D_E] = N_0(1+J)^{-\frac{\tau\Omega}{(2\pi)^2\delta_{\mathbf{X}}(0)}}$, which brings Eq. (G.1) to

$$\frac{2}{(1+K)\left(1+\gamma\eta+\gamma\zeta\right)}. \tag{G.35}$$

Starting off with taking the derivative with respect to J and thereafter setting $J = 0$, where $\zeta_0 = \zeta|_{J=0}$, the above expression becomes

$$-\frac{\gamma M \diamond B^* \diamond E \diamond E \diamond B \diamond M^*}{(1+K)\left(1+\gamma\eta+\gamma\zeta_0\right)^2}. \tag{G.36}$$

Recall that $A = \mathbb{1}$, as a consequence, $\eta = M^* \diamond A^{-1} \diamond M = 1$. After taking the derivative with respect to K and setting $K = 0$

$$\frac{M \diamond B^* \diamond E \diamond E \diamond B \diamond M^* \left(2-\zeta_0\right)}{\left(2+\zeta_0\right)^3}. \tag{G.37}$$

Observe $\zeta_0 = M \diamond B^* \diamond F^{-1} \diamond B \diamond M^*|_{J=0}$. Each of the B kernels have a factor called the SPDC efficiency [19], which is an inefficient process. Therefore, it is possible to use the following approximation

$$2 \pm \zeta_0 \approx 2, \tag{G.38}$$

and simplifies $\mathcal{R}$ to

$$\mathcal{R} \approx \frac{M \diamond B^* \diamond E \diamond E \diamond B \diamond M^*}{4}. \tag{G.39}$$

Appendix H

Simplification of diamond products

This proof was done independently. The aim here is to simplify $M \diamond B^* \diamond E \diamond E \diamond B \diamond M^*$, and is done by calculating $M \diamond B^*$ first, thereafter, $M \diamond B^* \diamond E$. And finally since E is Hermitian and B is symmetric, the diamond product of $M \diamond B^* \diamond E$ with its Hermitian conjugate is taken in order to obtain $M \diamond B^* \diamond E \diamond E \diamond B \diamond M^*$. The reader is reminded that the SPDC kernel, B is given by

$$\begin{aligned} B^* &\approx \int_0^L H(z_1) dz_1 \\ &= \int_0^L \frac{4i\sqrt{2\pi\omega_p}\zeta_0^* \sigma_{ooe} w_p}{c^2} \sqrt{\omega_1 \omega_2} h(\omega_1 + \omega_2 - \omega_p, \delta_p) \\ &\exp\left(-\frac{1}{4} w_p^2 |\mathbf{k}_1 + \mathbf{k}_2|^2 - i\Delta k_z z_1\right) dz_1, \end{aligned} \tag{H.1}$$

where the first nonzero term of the Magnus expansion was used. Since the extreme thin crystal limit is considered, $z_1 \approx 0$ is set. The SPDC kernel becomes

$$B^* \approx \frac{4iL\sqrt{2\pi\omega_p}\zeta_0^* \sigma_{ooe} w_p}{c^2} \sqrt{\omega_1 \omega_2} h(\omega_1 + \omega_2 - \omega_p, \delta_p) \exp\left(-\frac{1}{4} w_p^2 |\mathbf{k}_1 + \mathbf{k}_2|^2\right). \tag{H.2}$$

The calculation for the diamond product of M with B^* is now performed

$$\begin{aligned} M \diamond B^* =& \frac{4\sqrt{2\pi\omega_p} i w_p L \sigma_{ooe} |\zeta_0| N_M}{c^2} \int \sqrt{\omega_1(\omega_p - \omega_1)} h(\omega_1 - \omega_d, \delta_d) \\ & \times h(\omega_p - \omega_1 - \omega_2, \delta_p) \\ & \times \exp\left(-\frac{w_p^2}{4} |\mathbf{k}_1 + \mathbf{k}_2|^2 - \frac{1}{4} w_0^2 |\mathbf{k}_1|^2 + i \mathbf{X}_0 \cdot \mathbf{k}_1 \right) đ\mathbf{k}_1. \end{aligned} \tag{H.3}$$

After integrating over $\mathbf{k}_1$ by using Eq. (I.10)

$$\begin{aligned} M \diamond B^* =& \frac{2\sqrt{2\pi\omega_p} i w_p L \sigma_{ooe} |\zeta_0| N_M}{c^2 \pi^2 (w_p^2 + w_0^2)} \\ & \exp\left(-\frac{w_p^2}{4} |\mathbf{k}_2|^2 - \frac{4|\mathbf{X}_0|^2 + 4 i w_p^2 \mathbf{X}_0 \cdot \mathbf{k}_2 - w_p^4 |\mathbf{k}_2|^2}{4(w_p^2 + w_0^2)} \right) \\ & \int \sqrt{\omega_1(\omega_p - \omega_1)} h(\omega_1 - \omega_d, \delta_d) h(\omega_p - \omega_1 - \omega_2, \delta_p) d\omega_1. \end{aligned} \tag{H.4}$$

Taking the diamond product of the above equation with E produces

$$\begin{aligned} M \diamond B^* \diamond E =& \frac{\sqrt{2\pi\omega_p} i w_p L \sigma_{ooe} |\zeta_0| N_M}{2 c^2 \pi^4 (w_p^2 + w_0^2)} \int \sqrt{\omega_1(\omega_p - \omega_1)} h(\omega_1 - \omega_d, \delta_d) \\ & h(\omega_p - \omega_1 - \omega_3, \delta_p) d\omega_1 \int t \exp\left(-\frac{w_p^2}{4} |\mathbf{k}_2|^2 \right. \\ & \left. - \frac{4|\mathbf{X}_0|^2 + 4 i w_p^2 \mathbf{X}_0 \cdot \mathbf{k}_2 - w_p^4 |\mathbf{k}_2|^2}{4(w_p^2 + w_0^2)} + i(\mathbf{k}_2 - \mathbf{k}_3) \cdot \mathbf{X} \right) d^2\mathbf{X} d^2\mathbf{k}_2 \\ =& \frac{\sqrt{2\pi\omega_p} i w_p L \sigma_{ooe} |\zeta_0| N_M}{2 c^2 \pi^4 (w_p^2 + w_0^2)} \int \sqrt{\omega_1(\omega_p - \omega_1)} h(\omega_1 - \omega_d, \delta_d) \\ & h(\omega_p - \omega_1 - \omega_3, \delta_p) d\omega_1 \int t \exp\left(\left(-\frac{w_p^2}{4} + \frac{w_p^4}{4(w_p^2 + w_0^2)} \right) |\mathbf{k}_2|^2 \right. \\ & \left. + \left(-\frac{i w_p^2 \mathbf{X}_0}{w_p^2 + w_0^2} + i\mathbf{X} \right) \cdot \mathbf{k}_2 - \frac{|\mathbf{X}_0|^2}{w_p^2 + w_0^2} - i \mathbf{k}_3 \cdot \mathbf{X} \right) d^2\mathbf{X} d^2\mathbf{k}_2. \end{aligned} \tag{H.5}$$

The above integral is evaluated by using Eq. (I.10) to obtain

$$M \diamond B^* \diamond E = \frac{2\sqrt{2\pi\omega_p} i L \sigma_{ooe} |\zeta_0| N_M}{c^2 \pi^3 w_p w_0^2} \int \sqrt{\omega_1(\omega_p - \omega_1)} h(\omega_1 - \omega_d, \delta_d)$$
$$h(\omega_p - \omega_1 - \omega_3, \delta_p) d\omega_1 \int t \exp\left(-\frac{|\mathbf{X}_0|^2}{w_p^2 + w_0^2} \right.$$
$$\left. -i\mathbf{k}_3 \cdot \mathbf{X} - \frac{1}{4(w_p^2 + w_0^2)} \left(\frac{\left|2w_p^2 \mathbf{X}_0 - 2(w_p^2 + w_0^2)\mathbf{X}\right|^2}{w_p^2 w_0^2} \right) \right) d^2\mathbf{X}. \tag{H.6}$$

Finally, calculating $M \diamond B^* \diamond E \diamond E \diamond B \diamond M^*$

$$\begin{aligned}
&M \diamond B^* \diamond E \diamond E \diamond B \diamond M^* \\
&= \frac{\omega_p L^2 |\sigma_{ooe} \zeta_0 N_M|^2}{c^4 \pi^8 w_p^2 w_0^4} \int \sqrt{\omega_1(\omega_p - \omega_1)\omega_1'(\omega_p - \omega_1')} h(\omega_1 - \omega_d, \delta_d) \\
&h(\omega_p - \omega_1 - \omega_3, \delta_p) d\omega_1 h^*(\omega_1' - \omega_d, \delta_d) h^*(\omega_p - \omega_1' - \omega_3, \delta_p) d\omega_1' d\omega_3 \\
&\int t(\mathbf{X}) t(\mathbf{X}') \exp\left(-\frac{1}{4(w_p^2 + w_0^2)} \left(\frac{\left|2w_p^2 \mathbf{X}_0 - 2(w_p^2 + w_0^2)\mathbf{X}\right|^2}{w_p^2 w_0^2} \right) \right. \\
&- \frac{1}{4(w_p^2 + w_0^2)} \left(\frac{\left|2w_p^2 \mathbf{X}_0 - 2(w_p^2 + w_0^2)\mathbf{X}'\right|^2}{w_p^2 w_0^2} \right) - \frac{2|\mathbf{X}_0|^2}{w_p^2 + w_0^2} \\
&\left. + i\mathbf{k}_3 \cdot (\mathbf{X}' - \mathbf{X}) \right) d^2\mathbf{X} d^2\mathbf{X}' d^2\mathbf{k}_3.
\end{aligned} \tag{H.7}$$

The integral over ω_1, ω_1' and ω_3 will produce a constant which will be labeled as Q along with the other constants

$$\begin{aligned}
Q = &\frac{4\omega_p L^2 |\sigma_{ooe} \zeta_0 N_M|^2}{c^4 \pi^6 w_p^2 w_0^4} \int \sqrt{\omega_1(\omega_p - \omega_1)\omega_1'(\omega_p - \omega_1')} h(\omega_1 - \omega_d, \delta_d) \\
&h(\omega_p - \omega_1 - \omega_3, \delta_p) d\omega_1 h^*(\omega_1' - \omega_d, \delta_d) h^*(\omega_p - \omega_1' - \omega_3, \delta_p) d\omega_1' d\omega_3.
\end{aligned} \tag{H.8}$$

Since the narrow spectral function is narrow, the replacements $\omega_1 = \omega_d$, and $\omega_1' = \omega_d$ can be performed, which produces

$$\begin{aligned}
Q = &\frac{4L^2 |\sigma_{ooe} \zeta_0 N_M|^2 \omega_p \omega_d (\omega_p - \omega_d)}{c^4 \pi^6 w_p^2 w_0^4} \int h(\omega_1 - \omega_d, \delta_d) \\
&h(\omega_p - \omega_1 - \omega_3, \delta_p) h^*(\omega_1' - \omega_d, \delta_d) h^*(\omega_p - \omega_1' - \omega_3, \delta_p) d\omega_1 d\omega_1' d\omega_3.
\end{aligned} \tag{H.9}$$

The narrow spectral functions, h, can be modeled as Gaussians i.e. $h(\omega,\delta) = \sqrt{\frac{\sqrt{2}}{\sqrt{\pi}\delta}}\exp\left(-\frac{\omega^2}{\delta^2}\right)$ where δ is proportional to the width of h. A similar integration of the narrow spectral functions have been done in appendix K, which brings Q to

$$Q = \frac{8\sqrt{2\pi}L^2|\sigma_{ooe}\zeta_0 N_M|^2\omega_p\omega_d(\omega_p-\omega_d)\delta_d\delta_p}{c^4\pi^5 w_p^2 w_0^4}. \tag{H.10}$$

Setting $N_M = \sqrt{2\pi}w_0$, as seen in Eq. (3.85), and considering the frequency phase matching condition for the degenerate case, i.e. $\omega_p = 2\omega_d$

$$Q = \frac{32\sqrt{2\pi}L^2\sigma_{ooe}^2|\zeta_0|^2\omega_d^3\delta_d\delta_p}{c^4\pi^4 w_p^2 w_0^2}. \tag{H.11}$$

Upon observation, Eq. (H.7) contains a two-dimensional delta function due to the diamond product with $\mathbf{k}_3$

$$\begin{aligned}
&M\diamond B^*\diamond E\diamond E\diamond B\diamond M^*\\
&= Q\int \delta(\mathbf{X}'-\mathbf{X})t(\mathbf{X})t(\mathbf{X}')\exp\left(-\frac{1}{4(w_p^2+w_0^2)}\left(\frac{\left|2w_p^2\mathbf{X}_0-2(w_p^2+w_0^2)\mathbf{X}\right|^2}{w_p^2w_0^2}\right)\right.\\
&\left.-\frac{1}{4(w_p^2+w_0^2)}\left(\frac{\left|2w_p^2\mathbf{X}_0-2(w_p^2+w_0^2)\mathbf{X}'\right|^2}{w_p^2w_0^2}\right)-\frac{2|\mathbf{X}_0|^2}{w_p^2+w_0^2}\right)d^2\mathbf{X}d^2\mathbf{X}'\\
&= Q\int t^2(\mathbf{X})\exp\left(-\frac{2|\mathbf{X}_0-\mathbf{X}|^2}{w_0^2}-\frac{2|\mathbf{X}|^2}{w_p^2}\right)d^2\mathbf{X}.
\end{aligned} \tag{H.12}$$

Therefore

$$\mathcal{R} = \frac{8\sqrt{2\pi}L^2\sigma_{ooe}^2|\zeta_0|^2\omega_d^3\delta_d\delta_p}{c^4\pi^4 w_p^2 w_0^2}\int t^2(\mathbf{X})\exp\left(-\frac{2|\mathbf{X}_0-\mathbf{X}|^2}{w_0^2}-\frac{2|\mathbf{X}|^2}{w_p^2}\right)d^2\mathbf{X}. \tag{H.13}$$

Appendix I

The point spread function for the rational thin crystal limit

This proof was done independently. The SPDC kernels, A and B, are approximated by taking the first term of its Magnus expansion. Keep in mind that B and H are kernels and therefore have dependencies on two transverse wave vector variables. In the calculation below, the dependence is not explicitly written since the z variable is currently of interest. The simplification for the approximation of B starts with writing

$$\begin{aligned} B^* &\approx \int_0^L H(z_1)dz_1 \\ &= \int_0^L i\Omega_0\sqrt{\omega_1\omega_2}h(\omega_1+\omega_2-\omega_p,\delta_p)\exp\left(-\frac{1}{4}w_p^2|\mathbf{k}_1+\mathbf{k}_2|^2-i\Delta k_z z_1\right)dz_1, \end{aligned} \tag{I.1}$$

where

$$\Omega_0 = 4\sqrt{2\pi\omega_p}\frac{\zeta_0^*\sigma_{ooe}w_p}{c^2}. \tag{I.2}$$

The diamond product of M with B^* is considered below

$$\begin{aligned} &M\diamond B^* \\ &= \int_0^L\int N_M h(\omega_1-\omega_d,\delta_d)i\Omega_0\sqrt{\omega_1\omega_2}h(\omega_1+\omega_2-\omega_p,\delta_p) \\ &\times\exp\left(-\frac{1}{4}w_0^2|\mathbf{k}_1|^2+i\mathbf{X}_0\cdot\mathbf{k}_1-\frac{1}{4}w_p^2|\mathbf{k}_1+\mathbf{k}_2|^2-i\Delta k_z z_1\right)đ\mathbf{k}_1dz_1. \end{aligned} \tag{I.3}$$

The phase mismatch is given by [20]

$$\begin{aligned}
&\Delta k_z \\
&= \frac{1}{2}\frac{k_z(\omega_1)k_z(\omega_2)}{k_z(\omega_1)+k_z(\omega_2)}\left|\frac{\mathbf{k}_1}{k_z(\omega_1)}-\frac{\mathbf{k}_2}{k_z(\omega_2)}\right|^2-\frac{k^2(\omega_1)}{2k_z(\omega_1)} \\
&+\frac{1}{2}k_z(\omega_1)-\frac{k^2(\omega_2)}{2k_z(\omega_2)}+\frac{1}{2}k_z(\omega_2),
\end{aligned} \tag{I.4}$$

where

$$k_z(\omega)=\frac{\omega\cos(\theta(\omega))}{v(\omega)}, \tag{I.5}$$

and

$$k(\omega)=\frac{\omega}{v(\omega)}. \tag{I.6}$$

Essentially when the diamond product is taken, ω is only affected in $k(\omega)$ and $k_z(\omega)$. The wave numbers, $k(\omega)$ and $k_z(\omega)$, will not be interfered with when integrating over $\mathbf{k}_1$ or $\mathbf{k}_2$ in the diamond product. Returning to the diamond product with M and B^*, substitution of the phase mismatch condition yields

$$\begin{aligned}
&M\diamond B^* \\
&=\int_0^L\int N_M h(\omega_1-\omega_d,\delta_d)i\Omega_0\sqrt{\omega_1\omega_2}h(\omega_1+\omega_2-\omega_p,\delta_p) \\
&\times\exp\left(-\frac{1}{4}w_0^2|\mathbf{k}_1|^2+i\mathbf{X}_0\cdot\mathbf{k}_1-\frac{1}{4}w_p^2|\mathbf{k}_1+\mathbf{k}_2|^2\right. \\
&-i\left(\frac{1}{2}\frac{k_z(\omega_1)k_z(\omega_2)}{k_z(\omega_1)+k_z(\omega_2)}\left|\frac{\mathbf{k}_1}{k_z(\omega_1)}-\frac{\mathbf{k}_2}{k_z(\omega_2)}\right|^2-\frac{k^2(\omega_1)}{2k_z(\omega_1)}+\frac{1}{2}k_z(\omega_1)-\frac{k^2(\omega_2)}{2k_z(\omega_2)}\right. \\
&\left.\left.+\frac{1}{2}k_z(\omega_2)\right)z_1\right)d\mathbf{k}_1dz_1.
\end{aligned} \tag{I.7}$$

It is argued that δ_d is very small, leading to a very narrow spectral function, $h(\omega_1-\omega_d,\delta_d)$. It is therefore possible to set $\omega_1=\omega_d$ in the exponent and its coefficient excluding $h(\omega_1+\omega_2-\omega_p,\delta_p)$. Similarly, the replacement $\omega_2=$

$\omega_p - \omega_d$ is performed

$$
\begin{aligned}
&M \diamond B^* \\
&= \int_0^L \exp\left(-i\left(-\frac{k^2(\omega_d)}{2k_z(\omega_d)} + \frac{1}{2}k_z(\omega_d) - \frac{k^2(\omega_p-\omega_d)}{2k_z(\omega_p-\omega_d)} + \frac{1}{2}k_z(\omega_p-\omega_d)\right)z_1\right) \\
&\int N_M i\Omega_0 \sqrt{\omega_d\,(\omega_p-\omega_d)}h(\omega_1-\omega_d,\delta_d)h(\omega_1+\omega_2-\omega_p,\delta_p)\exp\left(-\frac{1}{4}w_0^2|\mathbf{k}_1|^2\right. \\
&+ i\mathbf{X}_0\cdot\mathbf{k}_1 - \frac{1}{4}w_p^2|\mathbf{k}_1+\mathbf{k}_2|^2 \\
&\left.-\frac{i}{2}\frac{k_z(\omega_d)k_z(\omega_p-\omega_d)}{k_z(\omega_d)+k_z(\omega_p-\omega_d)}\left|\frac{\mathbf{k}_1}{k_z(\omega_d)} - \frac{\mathbf{k}_2}{k_z(\omega_p-\omega_d)}\right|^2 z_1\right)\frac{d^2\mathbf{k}_1}{(2\pi)^3}dz_1 d\omega_1.
\end{aligned}
\tag{I.8}
$$

Consider the degenerate case for SPDC, i.e. the signal and idler beams have the same frequency, so $\omega_p = 2\omega_d$, which will simplify the terms with $k_z(\omega)$, so $k_z(\omega_p - \omega_d) = k_z(\omega_d)$. The phase matching condition $k(\omega_p) = k_z(\omega_d) + k_z(\omega_p - \omega_d) = 2k_z(\omega_d)$ can also be used. The implication is that the beam axis of the pump beam is the z axis which means that $\theta = 0$. The expression, $M \diamond B^*$, reduces to

$$
\begin{aligned}
&M \diamond B^* \\
&= \int_0^L \exp\left(\left(i\frac{k^2(\omega_d)}{k_z(\omega_d)} - ik_z(\omega_d)\right)z_1\right) \\
&\int N_M i\Omega_0\omega_d h(\omega_1-\omega_d,\delta_d)h(\omega_1+\omega_2-\omega_p,\delta_p)\exp\left(-\frac{1}{4}w_0^2|\mathbf{k}_1|^2\right. \\
&\left.+i\mathbf{X}_0\cdot\mathbf{k}_1 - \frac{1}{4}w_p^2|\mathbf{k}_1+\mathbf{k}_2|^2 - \frac{iz_1}{4k_z(\omega_d)}|\mathbf{k}_1-\mathbf{k}_2|^2\right)\frac{d^2\mathbf{k}_1}{(2\pi)^3}dz_1 d\omega_1.
\end{aligned}
\tag{I.9}
$$

Consider the following identity to aid in the above integration

$$
\begin{aligned}
&\int \exp\left(a|\mathbf{k}_1|^2 + \mathbf{V}\cdot\mathbf{k}_1 + b|\mathbf{k}_1+\mathbf{k}_2|^2 + c\left|\frac{\mathbf{k}_1}{d} - \frac{\mathbf{k}_2}{e}\right|^2\right)d^2\mathbf{k}_1 \\
&= -\frac{\pi}{a+b+\frac{c}{d^2}}\exp\left(\frac{-|\mathbf{V}|^2 - (4b-\frac{4c}{de})\mathbf{V}\cdot\mathbf{k}_2}{4(a+b+\frac{c}{d^2})}\right. \\
&\left.+\left(b+\frac{c}{e^2} - \frac{b^2 - \frac{2cb}{de} + \frac{c^2}{d^2e^2}}{a+b+\frac{c}{d^2}}\right)|\mathbf{k}_2|^2\right),
\end{aligned}
\tag{I.10}
$$

where a, b, c, d, and e are constants with respect to the integration, $\mathbf{V}$ is a vector, and the absolute value is defined as the vector absolute value. A proof of equation (I.10) can be seen in appendix J. The integration of Eq. (I.9) is now performed by noting that the integration parameters are

$$\begin{aligned} a &= -\frac{1}{4}w_0^2, \\ b &= -\frac{1}{4}w_p^2, \\ c &= -\frac{iz_1}{4k_z(\omega_d)}, \\ d &= e = 1, \\ \mathbf{V} &= i\mathbf{X}_0. \end{aligned} \tag{I.11}$$

The exponent after integration becomes

$$\begin{aligned} &\frac{|\mathbf{X}_0|^2 - i\left(-w_p^2 + \frac{iz_1}{k_z(\omega_d)}\right)\mathbf{X}_0 \cdot \mathbf{k}_2}{-w_0^2 - w_p^2 - \frac{iz_1}{k_z(\omega_d)}} \\ &+ \left(-\frac{1}{4}w_p^2 + \frac{-iz_1}{4k_z(\omega_d)} - \frac{\frac{1}{16}w_p^4 - \frac{iz_1w_p^2}{8k_z(\omega_d)} - \frac{z_1^2}{16k_z^2(\omega_d)}}{-\frac{1}{4}w_0^2 - \frac{1}{4}w_p^2 - \frac{iz_1}{4k_z(\omega_d)}}\right)|\mathbf{k}_2|^2. \end{aligned} \tag{I.12}$$

Define $\chi = \frac{k^2(\omega_d)}{k_z(\omega_d)} - k_z(\omega_d) = k(\omega_d)\left(\frac{1}{\cos(\theta(\omega_d))} - \cos(\theta(\omega_d))\right)$ for convenience. Clearly χ depends on the down-conversion angle, $\theta(\omega_d)$. The smaller the

down-conversion angle, the smaller the value of χ, which brings $M \diamond B^*$ to

$$
\begin{aligned}
& M \diamond B^* \\
& = \int_0^L \exp\left(i\chi z_1\right) \\
& \int \frac{\pi N_M i\Omega_0 \omega_d h(\omega_1-\omega_d,\delta_d)h(\omega_1+\omega_2-\omega_p,\delta_p)}{\frac{1}{4}w_0^2+\frac{1}{4}w_p^2+\frac{iz_1}{4k_z(\omega_d)}} \\
& \exp\left(\frac{\left|\mathbf{X}_0\right|^2 - i\left(-w_p^2+\frac{iz_1}{k_z(\omega_d)}\right)\mathbf{X}_0\cdot\mathbf{k}_2}{-w_0^2-w_p^2-\frac{iz_1}{k_z(\omega_d)}}\right. \\
& \left.+\left(-\frac{1}{4}w_p^2+\frac{-iz_1}{4}\frac{1}{k_z(\omega_d)}-\frac{\frac{1}{16}w_p^4-\frac{1}{8}\frac{iz_1w_p^2}{k_z(\omega_d)}-\frac{1}{16}\frac{z_1^2}{k_z^2(\omega_d)}}{-\frac{1}{4}w_0^2-\frac{1}{4}w_p^2-\frac{iz_1}{4}\frac{1}{k_z(\omega_d)}}\right)\left|\mathbf{k}_2\right|^2\right)\frac{1}{(2\pi)^3}dz_1d\omega_1 \\
& = \int\int_0^L \frac{\pi N_M i\Omega_0 \omega_d h(\omega_1-\omega_d,\delta_d)h(\omega_1+\omega_2-\omega_p,\delta_p)}{\frac{1}{4}w_0^2+\frac{1}{4}w_p^2+\frac{iz_1}{4k_z(\omega_d)}} \\
& \exp\left(i\chi z_1-\frac{\left|\mathbf{X}_0\right|^2}{w_0^2+w_p^2+\frac{iz_1}{k_z(\omega_d)}}\right) \\
& \exp\left(\frac{i\left(-w_p^2+\frac{iz_1}{k_z(\omega_d)}\right)\mathbf{X}_0\cdot\mathbf{k}_2}{w_0^2+w_p^2+\frac{iz_1}{k_z(\omega_d)}}+\left(-\frac{1}{4}w_p^2-\frac{iz_1}{4k_z(\omega_d)}\right.\right. \\
& \left.\left.+\frac{\frac{1}{16}w_p^4-\frac{iz_1w_p^2}{8k_z(\omega_d)}-\frac{z_1^2}{16k_z^2(\omega_d)}}{\frac{1}{4}w_0^2+\frac{1}{4}w_p^2+\frac{iz_1}{4k_z(\omega_d)}}\right)\left|\mathbf{k}_2\right|^2\right)\frac{1}{(2\pi)^3}dz_1d\omega_1.
\end{aligned}
\tag{I.13}
$$

The following is defined

$$
\begin{aligned}
c_1 &= -\frac{1}{4}w_p^2-\frac{iz_1}{4k_z(\omega_d)}+\frac{\frac{1}{16}w_p^4-\frac{iz_1w_p^2}{8k_z(\omega_d)}-\frac{z_1^2}{16k_z(\omega_d)^2}}{\frac{1}{4}w_0^2+\frac{1}{4}w_p^2+\frac{iz_1}{4k_z(\omega_d)}}, \\
g &= \frac{i\left(-w_p^2+\frac{iz_1}{k_z(\omega_d)}\right)}{w_0^2+w_p^2+\frac{iz_1}{k_z(\omega_d)}}, \\
\Theta &= \frac{\pi N_M i\Omega_0\omega_d}{(2\pi)^3\left(\frac{1}{4}w_0^2+\frac{1}{4}w_p^2+\frac{iz_1}{4k_z(\omega_d)}\right)}\exp\left(i\chi z_1-\frac{\left|\mathbf{X}_0\right|^2}{w_0^2+w_p^2+\frac{iz_1}{k_z(\omega_d)}}\right),
\end{aligned}
\tag{I.14}
$$

which brings $M \diamond B^*$ to

$$\begin{aligned} M \diamond B^* = \int \int_0^L & h(\omega_1 - \omega_d, \delta_d) h(\omega_1 + \omega_2 - \omega_p, \delta_p) \Theta \\ & \times \exp\left(g\mathbf{X}_0 \cdot \mathbf{k}_2 + c_1 |\mathbf{k}_2|^2\right) dz_1 d\omega_1, \end{aligned} \tag{I.15}$$

$h(\omega_1 - \omega_d, \delta_d) h(\omega_1 + \omega_2 - \omega_p, \delta_p)$ is kept outside of the defined variables in Eq. (I.22) so that a delta function is conveniently formed when calculating $M \diamond B^* \diamond E \diamond E \diamond B \diamond M^*$. Proceeding with the diamond product $M \diamond B^* \diamond E$

$$\begin{aligned} & M \diamond B^* \diamond E \\ & = 2\pi \int \int_0^L t(\mathbf{X}) h(\omega_1 - \omega_d, \delta_d) h(\omega_1 + \omega_2 - \omega_p, \delta_p) \Theta \\ & \exp\left(g\mathbf{X}_0 \cdot \mathbf{k}_2 + c_1 |\mathbf{k}_2|^2 + i\left(\mathbf{k}_2 - \mathbf{k}_3\right) \cdot \mathbf{X}\right) dz_1 d^2\mathbf{X} d\mathbf{k}_2 d\omega_1 \\ & = \frac{1}{(2\pi)^2} \int \int_0^L t(\mathbf{X}) h(\omega_1 - \omega_d, \delta_d) h(\omega_1 + \omega_3 - \omega_p, \delta_p) \Theta \exp\left(g\mathbf{X}_0 \cdot \mathbf{k}_2\right. \\ & \left. + c_1 |\mathbf{k}_2|^2 + i\left(\mathbf{k}_2 - \mathbf{k}_3\right) \cdot \mathbf{X}\right) dz_1 d^2\mathbf{X} d^2\mathbf{k}_2 d\omega_1 \\ & = \frac{1}{(2\pi)^2} \int \int_0^L \exp\left(-i\mathbf{k}_3 \cdot \mathbf{X}\right) t(\mathbf{X}) h(\omega_1 - \omega_d, \delta_d) h(\omega_1 + \omega_3 - \omega_p, \delta_p) \Theta \\ & \exp\left(c_1 |\mathbf{k}_2|^2 + (i\mathbf{X} + g\mathbf{X}_0) \cdot \mathbf{k}_2\right) dz_1 d^2\mathbf{X} d^2\mathbf{k}_2 d\omega_1. \end{aligned} \tag{I.16}$$

Using the functional integral of a Gaussian in Eq. (I.10), the integral of the above expression is performed over $\mathbf{k}_2$ by setting

$$\begin{aligned} & a = c_1, \\ & b = c = 0, \\ & \mathbf{V} = i\mathbf{X} + g\mathbf{X}_0, \\ & d, e \neq 0, \end{aligned} \tag{I.17}$$

which simplifies the expression to

$$\begin{aligned} M \diamond B^* \diamond E = & -\frac{1}{(2\pi)^2} \int \int_0^L \frac{\pi}{c_1} \exp\left(-i\mathbf{k}_3 \cdot \mathbf{X}\right) t(\mathbf{X}) h(\omega_1 - \omega_d, \delta_d) \\ & h(\omega_1 + \omega_3 - \omega_p, \delta_p) \Theta \exp\left(-\frac{|i\mathbf{X} + g\mathbf{X}_0|^2}{4c_1}\right) dz_1 d^2\mathbf{X} d\omega_1. \end{aligned} \tag{I.18}$$

The reader is reminded that the absolute value is the components of a vector squared. This is not equal to the complex absolute value. The diamond product of Eq. (I.18) is taken with its Hermitian conjugate to obtain $M \diamond B^* \diamond E \diamond E \diamond B \diamond M^*$ which follows because E is Hermitian and B is symmetric. However, since $M \diamond B^* \diamond E$ only depends on one transverse wave vector, $\mathbf{k}_3$, it is symmetric and therefore the diamond product of Eq. (I.18) with its complex conjugate is taken i.e. $M \diamond B^* \diamond E \diamond E \diamond B \diamond M^* = \|M \diamond B^* \diamond E\|^2$. The z dependencies is now introduced and the evaluation of the diamond product is attempted

$$\begin{aligned}
&M \diamond B^* \diamond E \diamond E \diamond B \diamond M^* \\
&= \frac{\pi^2}{(2\pi)^7} \int \int_0^L \int_0^L \frac{h(\omega_1 - \omega_d, \delta_d) h(\omega_1 + \omega_3 - \omega_p, \delta_p) h(\omega_1' + \omega_3 - \omega_p, \delta_p)}{c_1(z_1) c_1^*(z_2)} \\
&h(\omega_1' - \omega_d, \delta_d) \exp\left(-i\mathbf{k}_3 \cdot (\mathbf{X} - \mathbf{X}')\right) t(\mathbf{X}) t(\mathbf{X}') \Theta(z_1) \Theta^*(z_2) \\
&\exp\left(-\frac{|i\mathbf{X} + g\mathbf{X}_0|^2}{4c_1(z_1)} - \frac{|-i\mathbf{X} + g^*\mathbf{X}_0|^2}{4c_1^*(z_2)} \right) dz_1 d^2\mathbf{X} dz_2 d^2\mathbf{X}' d^2\mathbf{k}_3 d\omega_1 d\omega_1' d\omega_3.
\end{aligned} \tag{I.19}$$

The value of the integral over the narrow spectral functions is now substituted, which is calculated in appendix K. The integral over $\mathbf{k}_3$ forms a two-dimensional Dirac delta function, $\delta(\mathbf{X} - \mathbf{X}')$

$$\begin{aligned}
&M \diamond B^* \diamond E \diamond E \diamond B \diamond M^* \\
&= \frac{\pi^2 \sqrt{2\pi} \delta_d \delta_p}{(2\pi)^4} \int \int_0^L \int_0^L \frac{t(\mathbf{X})^2 \Theta(z_1) \Theta^*(z_2)}{c_1(z_1) c_1^*(z_2)} \\
&\exp\left(-\frac{|i\mathbf{X} + g\mathbf{X}_0|^2}{4c_1(z_1)} - \frac{|-i\mathbf{X} + g^*\mathbf{X}_0|^2}{4c_1^*(z_2)} \right) dz_1 d^2\mathbf{X} dz_2.
\end{aligned} \tag{I.20}$$

The above expression can be simplified a little further by realizing that the integral over z_1 and z_2 are very similar. The integral over z_2 is equal to the complex conjugate of the integral over z_1. It is then possible to write the

following

$$
\begin{aligned}
&M \diamond B^* \diamond E \diamond E \diamond B \diamond M^* \\
&= \frac{\pi^2\sqrt{2\pi}\delta_d\delta_p}{(2\pi)^4} \int t(\mathbf{X})^2 \\
&\int_0^L \frac{\Theta(z_1)}{c_1(z_1)} \exp\left(-\frac{|i\mathbf{X} + g\mathbf{X}_0|^2}{4c_1(z_1)}\right) dz_1 \\
&\int_0^L \frac{\Theta^*(z_2)}{c_1^*(z_2)} \exp\left(-\frac{|-i\mathbf{X} + g^*\mathbf{X}_0|^2}{4c_1^*(z_2)}\right) dz_2 d^2\mathbf{X} \\
&= \frac{\pi^2\sqrt{2\pi}\delta_d\delta_p}{(2\pi)^4} \int t(\mathbf{X})^2 \\
&\left|\int_0^L \frac{\Theta(z_1)}{c_1(z_1)} \exp\left(-\frac{|i\mathbf{X} + g\mathbf{X}_0|^2}{4c_1(z_1)}\right) dz_1\right|^2 d^2\mathbf{X},
\end{aligned}
\tag{I.21}
$$

the variables g, c_1, and Θ are rewritten for convenience

$$
\begin{aligned}
c_1 &= -\frac{1}{4}w_p^2 - \frac{iz_1}{4k_z(\omega_d)} + \frac{\frac{1}{16}w_p^4 - \frac{iz_1 w_p^2}{8k_z(\omega_d)} - \frac{z_1^2}{16k_z(\omega_d)^2}}{\frac{1}{4}w_0^2 + \frac{1}{4}w_p^2 + \frac{iz_1}{4k_z(\omega_d)}}, \\
g &= \frac{i\left(-w_p^2 + \frac{iz_1}{k_z(\omega_d)}\right)}{w_0^2 + w_p^2 + \frac{iz_1}{k_z(\omega_d)}}, \\
\Theta &= \frac{\pi N_M i\Omega_0\omega_d}{(2\pi)^3\left(\frac{1}{4}w_0^2 + \frac{1}{4}w_p^2 + \frac{iz_1}{4k_z(\omega_d)}\right)} \\
&\times \exp\left(i\chi z_1 - \frac{|\mathbf{X}_0|^2}{w_0^2 + w_p^2 + \frac{iz_1}{k_z(\omega_d)}}\right).
\end{aligned}
\tag{I.22}
$$

The current aim is to simplify the integral over z_1. For this purpose, the Taylor expansion is considered. The defined variables above are substituted into $M \diamond B^* \diamond E \diamond E \diamond B \diamond M^*$ and the expression outside of the exponential is Taylor expanded to the 0th order. Afterwards, the argument of the exponential is Taylor expanded to first order, which will be called the coefficient, and then integrated over z_1. The expression outside of the exponent is now focused on. The integral over z_1 contains the factor $\frac{\Theta(z_1)}{c_1(z_1)}$. The variable $\Theta(z_1)$ contains an exponential, so only the expression outside the exponential along

with $c_1(z_1)$ is considered

$$\text{coefficient} = \frac{\pi N_M i\Omega_0\omega_d}{c_1(z_1)(2\pi)^3\left(\frac{1}{4}w_0^2+\frac{1}{4}w_p^2+\frac{iz_1}{4k_z(\omega_d)}\right)}. \tag{I.23}$$

In order to Taylor expand Eq. (I.23), a small parameter which can be used to Taylor expand is needed. The thin crystal length is defined to be L and a small dimensionless parameter is defined as

$$\mathcal{P} = \frac{L}{w_p^2 k_z(\omega_p)} = \frac{L}{2w_p^2 k_z(\omega_d)}, \tag{I.24}$$

and was also shown in section 2.3. The parameter $\mathcal{P}$ will be used as an expansion parameter. The substitution $z_1 = t_1 L$ is made, where $0 \leq t \leq 1$. Rewriting Eq. (I.23) in terms of $\mathcal{P}$ and the new definition of z_1, then expanding to the 0th order

$$\begin{aligned}\text{coefficient} &= \frac{\pi N_M i\Omega_0\omega_d}{-\frac{1}{4}w_p^2-\frac{iw_p^2t_1\mathcal{P}}{2}+\frac{\frac{1}{16}w_p^4-\frac{it_1w_p^4\mathcal{P}}{4}-\frac{w_p^4t_1^2\mathcal{P}^2}{4}}{\frac{1}{4}w_0^2+\frac{1}{4}w_p^2+\frac{iw_p^2t_1\mathcal{P}}{2}}} \\ &\times \frac{1}{(2\pi)^3\left(\frac{1}{4}w_0^2+\frac{1}{4}w_p^2+\frac{iw_p^2t_1\mathcal{P}}{2}\right)} \\ &\approx -\frac{16\pi N_M i\Omega_0\omega_d}{(2\pi)^3 w_p^2 w_0^2}.\end{aligned} \tag{I.25}$$

The simplification of the exponent under the integral of z_1 is considered. A piece of the exponential is found in $\Theta(z_1)$, which produces

$$\begin{aligned}&\text{exponential} \\ &= \exp\left(i\chi z_1 - \frac{|\mathbf{X}_0|^2}{w_0^2+w_p^2+\frac{iz_1}{k_z(\omega_d)}} - \frac{|i\mathbf{X}+g\mathbf{X}_0|^2}{4c_1(z_1)}\right).\end{aligned} \tag{I.26}$$

The goal is to make this expression linear with t_1. Since the first term is linear in z_1, it will be linear in t_1, so the second term is simplified by writing it in terms of $\mathcal{P}$ and the new definition of z_1, then Taylor expanding to 1st

order. Writing in terms of $\mathcal{P}$

$$
\begin{aligned}
&- \frac{|\mathbf{X}_0|^2}{w_0^2 + w_p^2 + \frac{iz_1}{k_z(\omega_d)}} - \frac{-|\mathbf{X}|^2 + 2gi\mathbf{X}\cdot\mathbf{X}_0 + |g\mathbf{X}_0|^2}{4c_1(z_1)} \\
&= -\frac{|\mathbf{X}_0|^2}{w_0^2 + w_p^2 + 2iw_p^2 t_1 \mathcal{P}} \\
&- \frac{\left(w_0^2 + w_p^2 + 2it_1 w_p^2 \mathcal{P}\right)|\mathbf{X}|^2 + 2i\mathbf{X}\cdot\mathbf{X}_0\left(iw_p^2 + 2t_1\mathcal{P}w_p^2\right)}{w_p^2 w_0^2 + 2it_1 w_p^2 \mathcal{P} w_0^2 + 8it_1\mathcal{P}w_p^4} \\
&+ \frac{\frac{\left(iw_p^2 + 2t_1\mathcal{P}w_p^2\right)^2}{w_0^2 + w_p^2 + 2it_1\mathcal{P}w_p^2}|\mathbf{X}_0|^2}{w_p^2 w_0^2 + 2it_1 w_p^2 \mathcal{P} w_0^2 + 8it_1\mathcal{P}w_p^4}.
\end{aligned}
\tag{I.27}
$$

Taylor expanding to first order

$$
\begin{aligned}
&- \frac{|\mathbf{X}_0|^2}{w_0^2+w_p^2+\frac{iz_1}{k_z(\omega_d)}} - \frac{-|\mathbf{X}|^2+2gi\mathbf{X}\cdot\mathbf{X}_0+|g\mathbf{X}_0|^2}{4c_1(z_1)} \\
&\approx -\frac{|\mathbf{X}_0|^2}{w_0^2+w_p^2} + \frac{|\mathbf{X}_0|^2\left(2iw_p^2t_1\right)}{\left(w_0^2+w_p^2\right)^2}\mathcal{P} \\
&- \frac{(w_0^2+w_p^2)|\mathbf{X}|^2 - 2w_p^2\mathbf{X}\cdot\mathbf{X}_0 + \frac{w_p^4}{w_0^2+w_p^2}|\mathbf{X}_0|^2}{w_p^2w_0^2} \\
&- \frac{\left(w_p^2w_0^2\right)\left(2it_1w_p^2|\mathbf{X}|^2 + 2i\mathbf{X}\cdot\mathbf{X}_0\left(2t_1w_p^2\right) - \left(\frac{4it_1w_p^4w_0^2+6it_1w_p^6}{\left(w_0^2+w_p^2\right)^2}\right)|\mathbf{X}_0|^2\right)}{\left(w_p^2w_0^2\right)^2}\mathcal{P} \\
&+ \frac{(2it_1w_p^2w_0^2+8it_1w_p^4)\left(\left(w_0^2+w_p^2\right)|\mathbf{X}|^2 + 2i\mathbf{X}\cdot\mathbf{X}_0\left(iw_p^2\right)\right)}{\left(w_p^2w_0^2\right)^2}\mathcal{P} \\
&- \frac{(2it_1w_p^2w_0^2+8it_1w_p^4)\left(\frac{\left(iw_p^2\right)^2}{w_0^2+w_p^2}|\mathbf{X}_0|^2\right)}{\left(w_p^2w_0^2\right)^2}\mathcal{P} \\
&= -\frac{|\mathbf{X}_0|^2}{w_0^2+w_p^2} + \frac{(w_0^2+w_p^2)\left|\mathbf{X}-\frac{w_p^2}{w_0^2+w_p^2}\mathbf{X}_0\right|^2}{w_p^2w_0^2}\left(\frac{(2it_1w_0^2+8it_1w_p^2)}{w_0^2}\mathcal{P}-1\right) \\
&- \frac{2it_1w_p^2\left(|\mathbf{X}|^2+2\mathbf{X}\cdot\mathbf{X}_0 - \frac{3w_p^2w_0^2+3w_p^4}{\left(w_0^2+w_p^2\right)^2}|\mathbf{X}_0|^2\right)}{w_p^2w_0^2}\mathcal{P} \\
&= -\frac{|\mathbf{X}_0|^2}{w_0^2+w_p^2} + \frac{(w_0^2+w_p^2)\left|\mathbf{X}-\frac{w_p^2}{w_0^2+w_p^2}\mathbf{X}_0\right|^2}{w_p^2w_0^2}\left(\frac{(2it_1w_0^2+8it_1w_p^2)}{w_0^2}\mathcal{P}-1\right) \\
&- \frac{2it_1\left(|\mathbf{X}+\mathbf{X}_0|^2 - \frac{5w_p^2w_0^2+4w_p^4+w_0^4}{\left(w_0^2+w_p^2\right)^2}|\mathbf{X}_0|^2\right)}{w_0^2}\mathcal{P},
\end{aligned}
\tag{I.28}
$$

which brings the exponent in Eq. (I.26) to

$$
\begin{aligned}
&\text{exponential} \\
&= \exp\left(\left[i\chi L - \frac{2i\left(|\mathbf{X}+\mathbf{X}_0|^2 - \frac{5w_p^2w_0^2+4w_p^4+w_0^4}{\left(w_0^2+w_p^2\right)^2}|\mathbf{X}_0|^2\right)}{w_0^2}\mathcal{P}\right.\right. \\
&\left.\left. + \frac{(w_0^2+w_p^2)(2iw_0^2+8iw_p^2)\mathcal{P}\left|\mathbf{X}-\frac{w_p^2}{w_0^2+w_p^2}\mathbf{X}_0\right|^2}{w_p^2w_0^4}\right]t_1 - \frac{|\mathbf{X}_0|^2}{w_0^2+w_p^2}\right. \\
&\left. - \frac{(w_0^2+w_p^2)\left|\mathbf{X}-\frac{w_p^2}{w_0^2+w_p^2}\mathbf{X}_0\right|^2}{w_p^2w_0^2}\right),
\end{aligned}
\tag{I.29}
$$

which is linear in t_1. The exponent of $M \diamond B^* \diamond E \diamond E \diamond B \diamond M^*$ is the only expression which depends on t_1, and is easier to integrate than without the Taylor expansions. The expression, $M \diamond B^* \diamond E \diamond E \diamond B \diamond M^*$, becomes

$$
\begin{aligned}
&M \diamond B^* \diamond E \diamond E \diamond B \diamond M^* \\
&= \frac{2^4\sqrt{2\pi}N_M^2|\Omega_0|^2\omega_d^2L^2\delta_d\delta_p}{(2\pi)^6w_p^4w_0^4}\int t(\mathbf{X})^2 \\
&\times \exp\left(-\frac{2|\mathbf{X}_0|^2}{w_0^2+w_p^2} - \frac{2(w_0^2+w_p^2)\left|\mathbf{X}-\frac{w_p^2}{w_0^2+w_p^2}\mathbf{X}_0\right|^2}{w_p^2w_0^2}\right) \\
&\times \left|\int_0^1 \exp\left(\left[i\chi L + i\frac{2\mathcal{P}\left|\left(w_0^2+2w_p^2\right)\mathbf{X}' - 2w_p^2\mathbf{X}_0\right|^2}{w_p^2w_0^4}\right]t_1\right)dt_1\right|^2 d^2\mathbf{X}.
\end{aligned}
\tag{I.30}
$$

Integrating over t_1

$$
\begin{aligned}
&M \diamond B^* \diamond E \diamond E \diamond B \diamond M^* \\
&= \frac{2^4\sqrt{2\pi}N_M^2|\Omega_0|^2\omega_d^2L^2\delta_d\delta_p}{(2\pi)^6 w_p^4 w_0^4} \int t(\mathbf{X})^2 \\
&\times \exp\left(-\frac{2|\mathbf{X}_0|^2}{w_0^2+w_p^2} - \frac{2(w_0^2+w_p^2)\left|\mathbf{X} - \frac{w_p^2}{w_0^2+w_p^2}\mathbf{X}_0\right|^2}{w_p^2 w_0^2}\right) \\
&\times \left[\chi L + \frac{2\mathcal{P}\left|\left(w_0^2+2w_p^2\right)\mathbf{X}' - 2w_p^2\mathbf{X}_0\right|^2}{w_p^2 w_0^4}\right]^{-2} \\
&\times \left(2 - \exp\left(i\chi L + i\frac{2\mathcal{P}\left|\left(w_0^2+2w_p^2\right)\mathbf{X}' - 2w_p^2\mathbf{X}_0\right|^2}{w_p^2 w_0^4}\right)\right. \\
&\left. - \exp\left(-i\chi L - i\frac{2\mathcal{P}\left|\left(w_0^2+2w_p^2\right)\mathbf{X}' - 2w_p^2\mathbf{X}_0\right|^2}{w_p^2 w_0^4}\right)\right) d^2\mathbf{X}.
\end{aligned}
\tag{I.31}
$$

The last exponential can be simplified into a cosine function

$$
\begin{aligned}
&M \diamond B^* \diamond E \diamond E \diamond B \diamond M^* \\
&= \frac{2^4\sqrt{2\pi}N_M^2|\Omega_0|^2\omega_d^2L^2\delta_d\delta_p}{(2\pi)^6 w_p^4 w_0^4} \int t(\mathbf{X})^2 \\
&\times \exp\left(-\frac{2|\mathbf{X}_0|^2}{w_0^2+w_p^2} - \frac{2(w_0^2+w_p^2)\left|\mathbf{X} - \frac{w_p^2}{w_0^2+w_p^2}\mathbf{X}_0\right|^2}{w_p^2 w_0^2}\right) \\
&\times \left[\chi L + \frac{2\mathcal{P}\left|\left(w_0^2+2w_p^2\right)\mathbf{X}' - 2w_p^2\mathbf{X}_0\right|^2}{w_p^2 w_0^4}\right]^{-2} \\
&\times \left(1 - \cos\left(\chi L + \frac{2\mathcal{P}\left|\left(w_0^2+2w_p^2\right)\mathbf{X}' - 2w_p^2\mathbf{X}_0\right|^2}{w_p^2 w_0^4}\right)\right) d^2\mathbf{X}.
\end{aligned}
\tag{I.32}
$$

Considering the last factor

$$
\frac{1-\cos(\epsilon)}{\epsilon^2}, \tag{I.33}
$$

where

$$
\epsilon = \chi L + \frac{2\mathcal{P}\left|\left(w_0^2+2w_p^2\right)\mathbf{X}' - 2w_p^2\mathbf{X}_0\right|^2}{w_p^2 w_0^4}. \tag{I.34}
$$

Collinear light is considered, i.e. a small down-conversion angle, $\theta \approx 0$ which implies $\chi \approx 0$. Therefore, the value of ϵ is small since $\mathcal{P}$ is also small and is shown in section 2.3. It is possible to use L'Hôpital's rule twice in order to simplify the result

$$\begin{aligned}
&\lim_{\epsilon\to 0}\left(\frac{1-\cos(\epsilon)}{\epsilon^2}\right)\\
&=\lim_{\epsilon\to 0}\left(\frac{\sin(\epsilon)}{2\epsilon}\right)\\
&=\lim_{\epsilon\to 0}\left(\frac{\cos(\epsilon)}{2}\right)\\
&=\frac{1}{2}.
\end{aligned} \tag{I.35}$$

Eq (I.32) conveniently simplifies to

$$\begin{aligned}
&M\diamond B^*\diamond E\diamond E\diamond B\diamond M^*\\
&=\frac{2^3\sqrt{2\pi}N_M^2|\Omega_0|^2\omega_d^2L^2\delta_d\delta_p}{(2\pi)^6w_p^4w_0^4}\int t(\mathbf{X})^2\\
&\exp\left(-\frac{2|\mathbf{X}_0|^2}{w_0^2+w_p^2}-\frac{2(w_0^2+w_p^2)\left|\mathbf{X}-\frac{w_p^2}{w_0^2+w_p^2}\mathbf{X}_0\right|^2}{w_p^2w_0^2}\right)d^2\mathbf{X}.
\end{aligned} \tag{I.36}$$

Noting that $N_M=\sqrt{2\pi}w_0$, and rearranging the above equation reduces $\mathcal{R}$ to

$$\begin{aligned}
\mathcal{R}&\approx\frac{M\diamond B^*\diamond E\diamond E\diamond B\diamond M^*}{4}\\
&=\frac{2\sqrt{2\pi}|\Omega_0|^2\omega_d^2L^2\delta_d\delta_p}{(2\pi)^5w_p^4w_0^2}\int t(\mathbf{X})^2\exp\left(-\frac{2|\mathbf{X}_0-\mathbf{X}|^2}{w_0^2}-\frac{2|\mathbf{X}|^2}{w_p^2}\right)d^2\mathbf{X}.
\end{aligned} \tag{I.37}$$

Substituting Ω_0

$$\mathcal{R}\approx\frac{4\sqrt{2\pi}|\zeta_0|^2\sigma_{ooe}^2\omega_d^3L^2\delta_d\delta_p}{\pi^4w_p^2w_0^2c^4}\int t(\mathbf{X})^2\exp\left(-\frac{2|\mathbf{X}_0-\mathbf{X}|^2}{w_0^2}-\frac{2|\mathbf{X}|^2}{w_p^2}\right)d^2\mathbf{X}. \tag{I.38}$$

Extracting the image from $\mathcal{R}$

$$\begin{aligned} T(\mathbf{X}_0) &= \int t(\mathbf{X})^2 \exp\left(-\frac{2|\mathbf{X}_0 - \mathbf{X}|^2}{w_0^2} - \frac{2|\mathbf{X}|^2}{w_p^2}\right) d^2\mathbf{X} \\ &= \int t(\mathbf{X})^2 h\left(\mathbf{X}_0, \mathbf{X}\right) d^2\mathbf{X}, \end{aligned} \tag{I.39}$$

where the $h\left(\mathbf{X}_0, \mathbf{X}\right)$ is the PSF. The above image is the same as for the case with the extreme thin crystal limit, and a similar interpretation applies.

Appendix J

Derivation of the diamond product integral

This proof was done independently. The following integral, which arises numerous times during calculations in slightly different forms, is proved

$$\begin{aligned}
&\int \exp\left(a|\mathbf{k}_1|^2 + \mathbf{V}\cdot\mathbf{k}_1 + b|\mathbf{k}_1+\mathbf{k}_2|^2 + c\left|\frac{\mathbf{k}_1}{d} - \frac{\mathbf{k}_2}{e}\right|^2\right) d^2\mathbf{k}_1 \\
&= -\frac{\pi}{a+b+\frac{c}{d^2}} \exp\left(\frac{-|\mathbf{V}|^2 - (4b - \frac{4c}{de})\mathbf{V}\cdot\mathbf{k}_2}{4(a+b+\frac{c}{d^2})}\right. \\
&\left. + \left(b + \frac{c}{e^2} - \frac{b^2 - \frac{2cb}{de} + \frac{c^2}{d^2e^2}}{a+b+\frac{c}{d^2}}\right)|\mathbf{k}_2|^2\right),
\end{aligned} \tag{J.1}$$

where a, b, c, d, and e are constants with respect to the integration, and $\mathbf{V}$ is a vector which is also constant with respect to the integration. The absolute value is defined as the vector absolute value. The exponent is rearranged and

completing the square yields

$$
\begin{aligned}
&a|\mathbf{k}_1|^2 + \mathbf{V}\cdot\mathbf{k}_1 + b|\mathbf{k}_1+\mathbf{k}_2|^2 + c\left|\frac{\mathbf{k}_1}{d} - \frac{\mathbf{k}_2}{e}\right|^2 \\
&= \left(a+b+\frac{c}{d^2}\right)\left(|\mathbf{k}_1|^2 + \frac{\left(\mathbf{V}+2\mathbf{k}_2 b - \frac{2c\mathbf{k}_2}{de}\right)\cdot\mathbf{k}_1}{a+b+\frac{c}{d^2}}\right) + b|\mathbf{k}_2|^2 + \frac{c}{e^2}|\mathbf{k}_2|^2 \\
&= \left(a+b+\frac{c}{d^2}\right)\left[\left(k_{1x}+\frac{1}{2}\sigma_x\right)^2 + \left(k_{1y}+\frac{1}{2}\sigma_y\right)^2\right] \\
&- \frac{1}{4}\left(a+b+\frac{c}{d^2}\right)\left(\sigma_x^2+\sigma_y^2\right) + b|\mathbf{k}_2|^2 + \frac{c}{e^2}|\mathbf{k}_2|^2,
\end{aligned}
\tag{J.2}
$$

where $\boldsymbol{\sigma}$ is a vector with components σ_x and σ_y and is defined as $\boldsymbol{\sigma} = \frac{\left(\mathbf{V}+2\mathbf{k}_2 b - \frac{2c\mathbf{k}_2}{de}\right)}{a+b+\frac{c}{d^2}}$. The integral becomes

$$
\begin{aligned}
&\int \exp\left(a|\mathbf{k}_1|^2 + \mathbf{V}\cdot\mathbf{k}_1 + b|\mathbf{k}_1+\mathbf{k}_2|^2 + c\left|\frac{\mathbf{k}_1}{d} - \frac{\mathbf{k}_2}{e}\right|^2\right) d^2\mathbf{k}_1 \\
&= \int \exp\left(\left(a+b+\frac{c}{d^2}\right)\left[\left(k_{1x}+\frac{1}{2}\sigma_x\right)^2 + \left(k_{1y}+\frac{1}{2}\sigma_y\right)^2\right]\right. \\
&\left. -\frac{1}{4}\left(a+b+\frac{c}{d^2}\right)\left(\sigma_x^2+\sigma_y^2\right) + b|\mathbf{k}_2|^2 + \frac{c}{e^2}|\mathbf{k}_2|^2\right) d^2\mathbf{k}_1 \\
&= -\frac{\pi}{a+b+\frac{c}{d^2}}\exp\left(-\frac{1}{4}\left(a+b+\frac{c}{d^2}\right)\left(\sigma_x^2+\sigma_y^2\right) + b|\mathbf{k}_2|^2 + \frac{c}{e^2}|\mathbf{k}_2|^2\right).
\end{aligned}
\tag{J.3}
$$

The terms $\sigma_x^2+\sigma_y^2$ are simplified by using the definition of $\boldsymbol{\sigma}$, expanding, and then grouping up terms to finally obtain

$$
\begin{aligned}
&\int \exp\left(a|\mathbf{k}_1|^2 + \mathbf{V}\cdot\mathbf{k}_1 + b|\mathbf{k}_1+\mathbf{k}_2|^2 + c\left|\frac{\mathbf{k}_1}{d} - \frac{\mathbf{k}_2}{e}\right|^2\right) d^2\mathbf{k}_1 \\
&= -\frac{\pi}{a+b+\frac{c}{d^2}}\exp\left(\frac{-|\mathbf{V}|^2 - \left(4b - \frac{4c}{de}\right)\mathbf{V}\cdot\mathbf{k}_2}{4\left(a+b+\frac{c}{d^2}\right)}\right. \\
&\left. + \left(b + \frac{c}{e^2} - \frac{b^2 - \frac{2cb}{de} + \frac{c^2}{d^2e^2}}{a+b+\frac{c}{d^2}}\right)|\mathbf{k}_2|^2\right).
\end{aligned}
\tag{J.4}
$$

Appendix K

Narrow spectral function simplification

Consider firstly the integral over ω_1 and ω_1', and then, the integral over ω_3. Let $\omega_x = \omega_3 - \omega_p$

$$\begin{aligned} &\int h(\omega_1 - \omega_d, \delta_d) h(\omega_1 + \omega_3 - \omega_p, \delta_p) \\ &h(\omega_1' - \omega_d, \delta_d) h(\omega_1' + \omega_3 - \omega_p, \delta_p) d\omega_1 d\omega_1' \\ &= \left[\int h(\omega_1 - \omega_d, \delta_d) h(\omega_1 + \omega_3 - \omega_p, \delta_p) d\omega_1 \right]^2 \\ &= \left[\int h(\omega_1 - \omega_d, \delta_d) h(\omega_1 + \omega_x, \delta_p) d\omega_1 \right]^2 . \end{aligned} \tag{K.1}$$

The definition of the narrow spectral function in terms of a Gaussian is now substituted

$$
\begin{aligned}
&\frac{2}{\pi\delta_d\delta_p}\left[\int \exp\left(-\frac{\left(\omega_1-\omega_d\right)^2}{\delta_d^2}-\frac{\left(\omega_1+\omega_x\right)^2}{\delta_p^2}\right)d\omega_1\right]^2 \\
&=\frac{2}{\pi\delta_d\delta_p}\left[\int \exp\left(-\frac{\delta_p^2\omega_1^2-2\delta_p^2\omega_d\omega_1+\delta_p^2\omega_d^2+\delta_d^2\omega_1^2+2\delta_d^2\omega_1\omega_x+\delta_d^2\omega_x^2}{\delta_d^2\delta_p^2}\right)d\omega_1\right]^2 \\
&=\frac{2}{\pi\delta_d\delta_p}\left[\int \exp\left(-\frac{\left(\delta_p^2+\delta_d^2\right)\left(\omega_1+\frac{\delta_d^2\omega_x-\delta_p^2\omega_d}{\delta_p^2+\delta_d^2}\right)^2}{\delta_d^2\delta_p^2}\right.\right. \\
&\left.\left.-\frac{\frac{-2\delta_d^2\delta_p^2\omega_d\omega_x-\delta_p^2\delta_d^2\omega_x^2-\delta_p^2\delta_d^2\omega_d^2}{\delta_p^2+\delta_d^2}}{\delta_d^2\delta_p^2}\right)d\omega_1\right]^2 \\
&=\frac{2\delta_d\delta_p}{\delta_p^2+\delta_d^2}\exp\left(-\frac{2\left(\omega_x+\omega_d\right)^2}{\delta_p^2+\delta_d^2}\right) \\
&=\sqrt{2\pi}\delta_d\delta_p h^2\left(\omega_x+\omega_d,\sqrt{\delta_p^2+\delta_d^2}\right).
\end{aligned}
\tag{K.2}
$$

The integral over ω_3 is now considered, and a change of integration variables is performed such that $\omega_x=\omega_3-\omega_p$ is integrate over

$$
\begin{aligned}
&\int h(\omega_1-\omega_d,\delta_d)h(\omega_1+\omega_3-\omega_p,\delta_p) \\
&h(\omega_1'-\omega_d,\delta_d)h(\omega_1'+\omega_3-\omega_p,\delta_p)d\omega_1 d\omega_1' d\omega_3 \\
&=2\pi\sqrt{2\pi}\delta_d\delta_p\int h^2\left(\omega_x+\omega_d,\sqrt{\delta_p^2+\delta_d^2}\right)\frac{d\omega_x}{2\pi} \\
&=2\pi\sqrt{2\pi}\delta_d\delta_p.
\end{aligned}
\tag{K.3}
$$